

KANSAS GEOLOGICAL SURVEY
OPEN-FILE REPORT 2000-28

Sequence Stratigraphy of the Bethany Falls Limestone
in Eastern Kansas and Western Missouri

by

Nathan Aaron Wilke

Disclaimer

The Kansas Geological Survey does not guarantee this document to be free from errors or inaccuracies and disclaims any responsibility or liability for interpretations based on data used in the production of this document or decisions based thereon. This report is intended to make results of research available at the earliest possible data, but is not intended to constitute final or formal publications.

KANSAS GEOLOGICAL SURVEY
1930 Constant Avenue
University of Kansas
Lawrence, KS 66047

Sequence Stratigraphy of the Bethany Falls Limestone
in Eastern Kansas and Western Missouri

by

Nathan Aaron Wilke
B.S., Lake Superior State University, 1997

Submitted to the Department of Geology
and the Faculty of the Graduate School of
the University of Kansas
in partial fulfillment of the requirements
for the degree of Master of Science

2000



Chairman



Committee Members



for the Department

ABSTRACT

This study of the depositional environments and the sequence stratigraphic framework of the Swope Formation (Missourian Series, Pennsylvanian System) in eastern Kansas and western Missouri contributes to understanding small-scale cyclicity and sequence stratigraphy of midcontinent carbonates. Subaerial exposure surfaces and associated features are common components of shallow-marine carbonate cycles in the Pennsylvanian of the midcontinent. Improved recognition of such surfaces is of economic importance because the distribution of reservoir facies may be closely associated with subaerial exposure.

Fourteen core and outcrop localities were studied in order to define lithofacies and to recognize vertical and lateral variability within the Bethany Falls Limestone of the Swope Formation. Eight distinct lithofacies were differentiated on the basis of polished slabs and thin section analysis. These facies are: 1) mottled skeletal wackestone; 2) phylloid algal packstone; 3) lime mudstone; 4) oolite; 5) skeletal packstone; 6) skeletal grainstone; 7) fenestral wackestone; and 8) paleosol lithofacies. Pedogenic features, both in paleosols and subtidal rocks, were documented.

Two cycles of eustatic sea-level change were recognized based on identification of exposure surfaces, correlation of lithofacies, and interpreted depositional environments. These eustatic sea level changes resulted in the formation of two sequences within the study area. Regional depositional patterns are affected by antecedent topography, and changes in relative and eustatic sealevels. This study also improved understanding of stratigraphic relationships within the Swope Formation and related units.

Acknowledgments

I would like to thank my committee for their invaluable help during my research and for their critiques and comments on this manuscript. Their suggestions have strengthened this paper. My adviser Tim Carr was a constant source of guidance, input, and knowledge. He has helped me become a better geologist, and has helped expose me to the fascinating world of petroleum exploration and development. Lake Superior State University provided an excellent undergraduate education.

Lynn Watney, Dave Newell, and Bill Guy, all of the Petroleum Research Section, were extremely helpful and provided many hours of discussion and observations on the myriad world of carbonates, sequence stratigraphy and oil. I would like to thank the entire non-technical staff of the Kansas Geological Survey, for not only putting up with me, but helping check out vehicles, make photocopies, and other numerous activities. The Petroleum Research Section of the Kansas Geological Survey gave me not only financial support, but also an incredible education into both the world of research and petroleum geology.

I would like to thank Joe Anderson for drilling two core holes for me (in nice weather), and Dave Young for generously donating his time to log those holes for me. A special thanks goes to both Rural Water District #2, Miami

County, and the Raines household for allowing me to drill two boreholes on their land, with a minimum of hassle.

I would like to thank Phillips Petroleum Company, and especially the now defunct Australia Exploration Group (which was not *my* fault), for giving me a chance in the petroleum business. Scott Irvine, Mary Tisdale, Doug Campbell and Chris Holien all provided guidance and support.

John Hopkins first introduced me to the Bethany Falls, and I will never forgive him for that. Scott Beatty and Alex Martinez provided valuable support, advice and friendship that was crucial to my development as a graduate student.

Jason Cansler and Niall Toomey might have delayed my stay at KU, but their friendship was worth it. They also provided invaluable advice and discussion (often over a beer at West). I would like to thank various downtown establishments, for helping me keep my sanity.

An inordinate amount of thanks is due my family. Without their support and understanding, finishing would have been much more difficult. They tolerated and accepted my wide range of moods, and didn't get too upset when I didn't talk to them for the past four months of my thesis.

And lastly, I would like to thank my baseball bat, because I definitely think better with it.

TABLE OF CONTENTS

LIST OF FIGURES	ix
LIST OF TABLES	xiii
Chapter 1: Introduction	14
Introduction	15
Study Area	20
Depositional sequence vs. cyclothem	20
Regional Geology	22
Previous Investigations	26
Methodology	27
Chapter 2: Facies of the Bethany Falls Limestone, Hushpuckney Shale, Middle Creek Limestone and Elm Branch Shale	30
Lithofacies & Depositional Environments of the Bethany Falls Limestone	31
Mottled Skeletal Wackestone Facies	31
Description	31
Paleoenvironmental Interpretation	34
Phylloid Algal Packstone Facies	36
Description	36
Paleoenvironmental Interpretation	40
Lime Mudstone Facies	41
Description	41
Paleoenvironmental Interpretation	44
Oolite Facies	45
Description	45
Paleoenvironmental Interpretation	55
Skeletal Packstone Facies	57
Description	57
Paleoenvironmental Interpretation	57
Skeletal Grainstone Facies	59
Description	59
Paleoenvironmental Interpretation	62
Fenestral Wackestone Facies	63
Description	63
Paleoenvironmental Interpretation	67
Paleosol Facies	69
Description	69
Paleoenvironmental Interpretation	72

Lithofacies & Depositional Environments of the Elm Branch Shale, the Hushpuckney Shale, and the Middle Creek Limestone	76
Elm Branch Shale – Blocky Mudstone Facies	77
Description	77
Paleoenvironmental Interpretation	77
Elm Branch Shale – Skeletal Wackestone Facies	79
Description	79
Paleoenvironmental Interpretation	79
Middle Creek Limestone – Phylloid Algal Wackestone/Packstone Facies	79
Description	79
Paleoenvironmental Interpretation	81
Middle Creek Limestone – Calcareous Shale Facies	81
Description	81
Paleoenvironmental Interpretation	81
Hushpuckney Shale – Fissile Black Shale Facies	83
Description	83
Paleoenvironmental Interpretation	83
Hushpuckney Shale – Gray Shale Facies	85
Description	85
Paleoenvironmental Interpretation	85
Chapter 3: Sequence Stratigraphy of the Bethany Falls Limestone	87
Sequence Stratigraphic Nomenclature	88
Identification of Sequences	90
Sequence A	90
Sequence B	92
Stratigraphic Datum	93
Sequence A – Elm Branch Shale Interval	96
Description	96
Interpretation	97
Sequence A – Lower Hushpuckney Shale Interval	97
Description	97
Interpretation	99
Sequence A – Bethany Falls Limestone Interval	100
Description	100
Interpretation	102
Sequence B – Upper Bethany Falls Limestone Interval	109
Description	109
Interpretation	110
Casual Mechanisms for Sequence Development	114
Chapter 4: Conclusions	115

References	120
Appendix 1: Measured Stratigraphic Sections	127
Outcrop and Core Locations	128
Symbols for Sections	130
Locality Farlinville	132
Locality LaCygne West	133
Locality LaCygne East	134
Locality LaCygne North	135
Locality Fontana	136
Locality 383 rd Street	137
Locality Ridgeview Road	139
Locality Raines #1 Core	141
Locality RWD-2 Well #1 Core	143
Locality Chestnut Drive	145
Locality Dodson	147
Locality Lake Jacomo South	148
Locality Lake Jacomo North	150
Locality Raytown Road	152
Appendix 2: Spectral Gamma Ray Logs Discussion and Interpretation	154
Logfacies of the Bethany Falls Limestone and Hushpuckney Shale	155
Logfacies A	155
Logfacies B	161
Logfacies C	163
Logfacies D	165
Logfacies E	165
Logfacies Interpretations	165
Symbols for Logs	170
Locality Farlinville	171
Locality LaCygne West	172
Locality LaCygne East	173
Locality LaCygne North	174
Locality Fontana	175
Locality 383 rd Street	176
Locality Ridgeview Road	177
Locality Raines #1 Core	178
Locality RWD-2 Well #1 Core	179
Locality Chestnut Drive	180
Locality Dodson	181

Locality Lake Jacomo South	182
Locality Lake Jacomo North	183
Locality Raytown Road	184

LIST OF FIGURES

Figure 1.1. Stratigraphic column for the Bronson Subgroup.	16
Figure 1.2. Typical four member “Kansas” cyclothem.	17
Figure 1.3. Cumulative oil production in Kansas.	19
Figure 1.4. Index map of study area.	21
Figure 1.5. Major structural features in Kansas.	23
Figure 2.1. Photograph of polished core section illustrating mottled skeletal wackestone facies appearance.	32
Figure 2.2. Photograph of polished slab illustrating mottled skeletal wackestone facies appearance.	33
Figure 2.3. Photomicrographs illustrating the mottled skeletal wackestone fabric and bioclast filled burrows.	33
Figure 2.4. Polished slab of mottled skeletal wackestone with <i>Chaetetes</i> in growth position.	35
Figure 2.5. Outcrop and polished slab photographs of the phylloid algal facies.	38
Figure 2.6. Photomicrographs of phylloid algal facies.	39
Figure 2.7. Polished slab and outcrop photo of autobrecciated lime mudstone facies.	42
Figure 2.8. Photomicrographs of lime mudstone lithofacies.	43
Figure 2.9. Outcrop photographs of cross-bedded oolitic grainstone in the upper portion of the Bethany Falls Limestone.	46
Figure 2.10. Photographs of polished slabs of ooid grainstone subfacies of the oolite facies.	48
Figure 2.11. Photomicrograph and photograph of ooid grainstone subfacies within the oolite facies.	49

Figure 2.12. Photograph and photomicrograph of the ooid packstone/wackestone subfacies of the oolite facies.	50
Figure 2.13. Outcrop photo of paleo-karst tube or rhizolith in ooid grainstone subfacies.	52
Figure 2.14. Vertical tube terminating coincident with radioactive anomaly at Farlinville Quarry.	53
Figure 2.15. Contact between low porosity and oomolodic porosity grainstone coincident with radioactive anomaly.	54
Figure 2.16. Polished slab photographs of skeletal packstone facies illustrating packed nature and lack of phylloid algal blades.	58
Figure 2.17. Outcrop photo of cross-bedded skeletal grainstone.	60
Figure 2.18. Polished slab photographs of skeletal packstone facies illustrating cross-bedding and incorporated lime mudstone clasts.	61
Figure 2.19. Photograph of fenestral wackestone facies.	65
Figure 2.20. Photomicrograph and photographs of birds eye vugs within the fenestral wackestone facies.	66
Figure 2.21. Polished slab photograph of autobrecciated lime mudstone subfacies of the paleosol facies.	70
Figure 2.22. Photographs and photomicrographs of autobrecciated lime mudstone subfacies.	71
Figure 2.23. Outcrop photo of autobrecciated lime mudstone coincident with radioactive anomaly.	73
Figure 2.24. Polished core section illustrating contact of autoclastically brecciated lime mudstone and lime mudstone coincident with radioactive anomaly.	74
Figure 2.25. Photograph and photomicrograph of surficial laminar calcrete subfacies of the paleosol facies.	75
Figure 2.26. Photographs of the Elm Branch Shale.	78

Figure 2.27. Polished slab photograph of limestone from within the upper Elm Branch Shale.	80
Figure 2.28. Polished slab photographs of typical Middle Creek Limestone.	82
Figure 2.29. Photographs of core sections of the Hushpuckney Shale.	84
Figure 3.1. South to north lithostratigraphic cross-section across field area datumed on the top of the Hushpuckney Shale.	In packet
Figure 3.2. South to north lithostratigraphic cross-section across field area datumed on the base of the phylloid algal lithofacies.	In packet
Figure 3.3. Generalized depositional model illustrating development of the Elm Branch Shale and lower Hushpuckney Shale intervals.	98
Figure 3.4. Generalized depositional model illustrating development of the early Bethany Falls Limestone Interval and the late Bethany Falls Limestone Interval.	105
Figure 3.5. Generalized depositional model illustrating development of the latest Bethany Falls Limestone Interval of sequence A and the early Upper Bethany Limestone Interval of sequence B.	106
Figure 3.6. Generalized depositional model illustrating development of the latest Upper Bethany Falls Limestone Interval of sequence B.	111
Figure 3.7. Diagrammatic south to north lithostratigraphic cross section from Missouri to Oklahoma illustrating inferred relationships of the Ladore Shale, Mound Valley Limestone, and the Bethany Falls Limestone.	113
Figure App 2.1. Spectral gamma ray profiles of 383 rd Street and Farlinville localities.	156
Figure App 2.2. Outcrop photograph of rhizolith terminating in a horizontal manner.	158
Figure App 2.3. Spectral gamma ray profile and polished slab photograph from the 300 cm height at LaCygne East.	159
Figure App 2.4. Photograph and photomicrographs of ooid grainstone, oomoldic porosity, and cements partially filling oomolds.	160

Figure App 2.5. Spectral gamma ray profiles of Raytown and Lake Jacomo South localities. **162**

Figure App 2.6. Photograph of polished core section with contact between autoclastically brecciated lime mudstone and lime mudstone. **164**

Figure App 2.7. Spectral gamma ray profiles of Raines #1 and Ridgeview Road localities. **166**

Figure App 2.8. Cross section of spectral gamma ray profiles across field area with interpreted zone of vadose influence. **In packet**

LIST OF TABLES

Table 2.1. Strike and dip directions of cross beds within oolite grainstone subfacies.	45
---	-----------

Chapter 1: Introduction

Chapter One

Introduction

The Swope Limestone (Figure 1.1) has been described as a typical "Kansas cyclothem" (Heckel, 1977, 1986; Nollsch, 1983). An ideal Kansas cyclothem consists of four lithofacies (Figure 1.2). At the base of an ideal cyclothem is a thin (0.3 to 1.5 m), transgressive limestone. The transgressive limestone is covered by a thin (0.3 to 2.0 m), offshore, black "core" shale. The core shale is overlain by a thicker (1.5 to 9.0 m), shoaling-upward regressive limestone capped with a subaerial exposure surface. Above the exposure surface, the upper member of a Kansas cyclothem is the nearshore to terrigenous "outside" shale. The "outside" shale is commonly poorly exposed and of widely varying thickness (0 to 30 m; Heckel, 1977).

All of the representative lithofacies of the "Kansas" cyclothem are present within the Swope Limestone in northeastern Kansas. However, in some eastern Kansas outcrops, French et al. (1989), French and Watney (1993), Stover (1992) and Carr et al. (1995) recognized an extra apparent subaerial exposure surface intrastratal the regressive Bethany Falls Limestone Member of the Swope Limestone.

Additional subaerial exposure surfaces within the Bethany Falls Limestone suggest departure from the ideal cyclothem model of Heckel

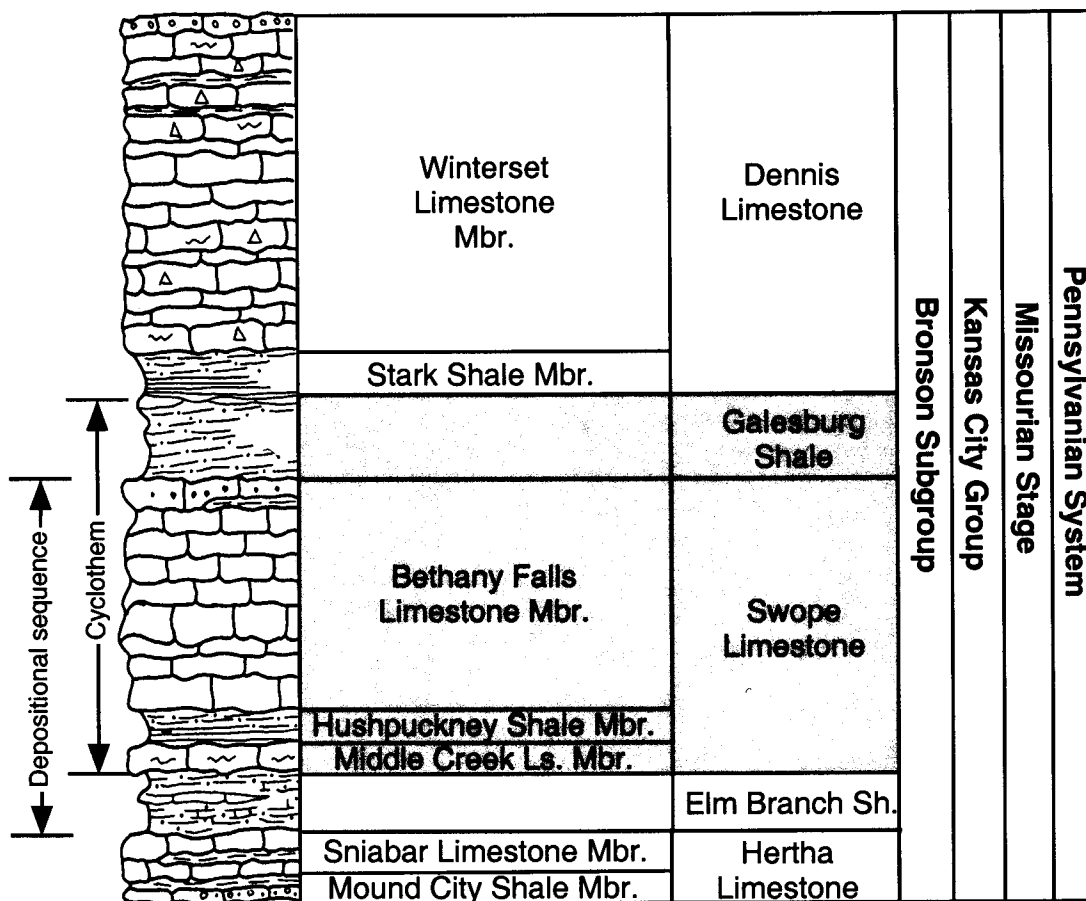


Figure 1.1. Stratigraphic column for the Bronson Subgroup showing the general relationships and lithologies of the units examined for this study. The Swope cyclothem is highlighted. The boundaries of a depositional sequence and a cyclothem are shown on the left. Modified from Miller (1966).

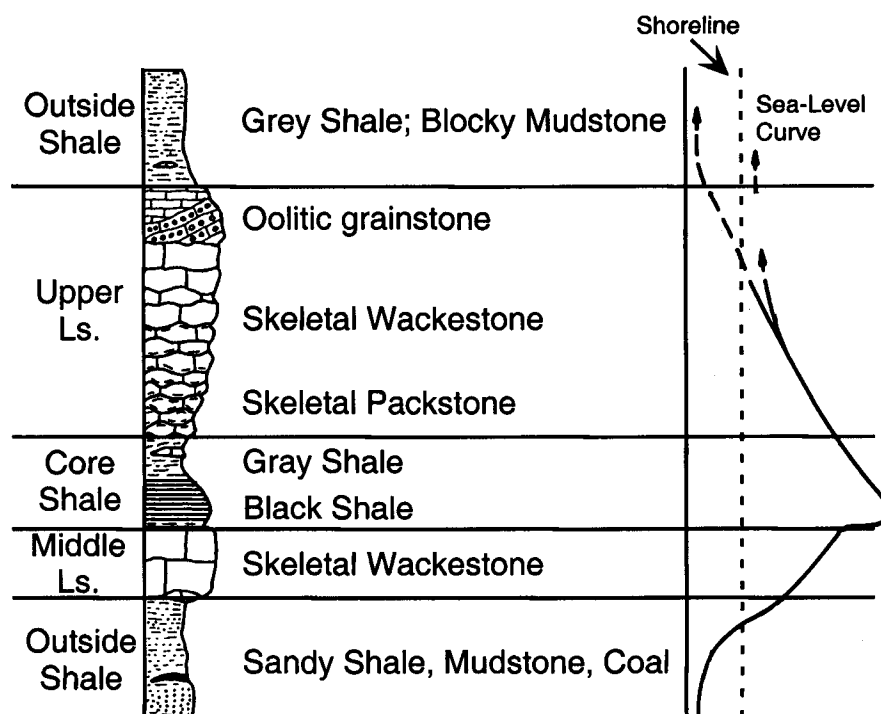


Figure 1.2. Ideal four-member "Kansas" cyclothem in Midcontinent Pennsylvanian with inferred paleobathymetry. Modified from Heckel (1986).

(1977). The sea level curve proposed by Heckel (1986) appears not to include small-scale cyclicity suggested by possible additional subaerial exposure surfaces (Figure 1.2). Various autocyclic processes, small-scale allocyclic processes, and local variations in shelf configuration might further increase the stratigraphic complexity within the Swope Limestone.

The Bethany Falls Limestone and other similar Missourian carbonates are important petroleum reservoirs in Kansas. Cumulative oil production out of the Pennsylvanian (Missourian) is over 1.5 billion barrels, representing 23 percent of total Kansas production (Figure 1.3). Localized stratigraphic and structural anomalies appear to be preferred sites for reservoir development in regressive limestones of the Lansing and Kansas City groups (Watney, 1984). The Swope Limestone is known in the subsurface of western Kansas as the K-zone, Kansas City Group (Merriam, 1963, p. 128). Isolated oolitic grainstones, typically with oomoldic porosity, provide potential reservoir zones within the Bethany Falls, which is the regressive “upper” limestone of the Swope Limestone (French and Watney, 1993).

In midcontinent Pennsylvanian carbonates, economic reservoir facies are often associated with subaerial exposure. Subaerial exposure and shallow water conditions occurring shortly after deposition of the regressive limestone can have a significant effect on reservoir properties (Budd et al., 1995). Recognition and mapping of such surfaces is of economic importance to maintain current petroleum production.

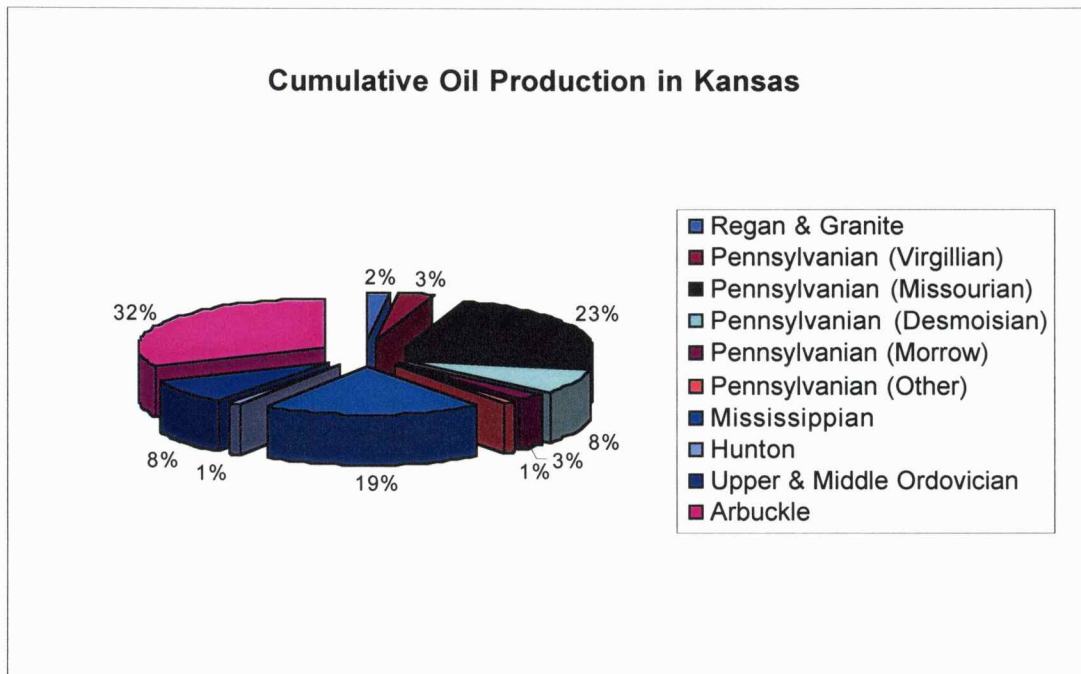


Figure 1.3. Cumulative oil production in Kansas. The Swope Formation is in the Kansas City Group, which is assigned to the Pennsylvanian (Missourian) section (shown in black) above. Cumulative oil production out of the Pennsylvanian (Missourian) section accounts for 23 percent of the oil produced in Kansas. Production data from Carr et al. (1995).

The goal of this study is the development of a high-resolution sequence stratigraphic model of the Bethany Falls Limestone, based upon a careful sedimentological study. Improved understanding of the interaction of factors that affect depositional and post-depositional processes in Missourian carbonates of the midcontinent will improve predictive capabilities for the petroleum reservoirs of the Bethany Falls Limestone and other similar Missourian limestone units. A new detailed relative sea-level curve was produced, and the internal geometries of the Bethany Falls Limestone are better delineated.

Study Area

The Swope Limestone crops out in a north-south belt in eastern Kansas and western Missouri (Figure 1.4). The field area for this study is Linn and Miami Counties in eastern Kansas and Jackson County in western Missouri. Careful examination of a combination of 14 roadcuts, quarry exposures, and shallow drill cores provide the data for this study. Legal descriptions of all field localities and measured section descriptions are provided in Appendix 1.

Depositional sequence vs. cyclothem

Mitchum et al. (1977) defined a depositional sequence as “a stratigraphic unit composed of a relatively conformable succession of genetically related strata and bounded at its top and base by unconformities

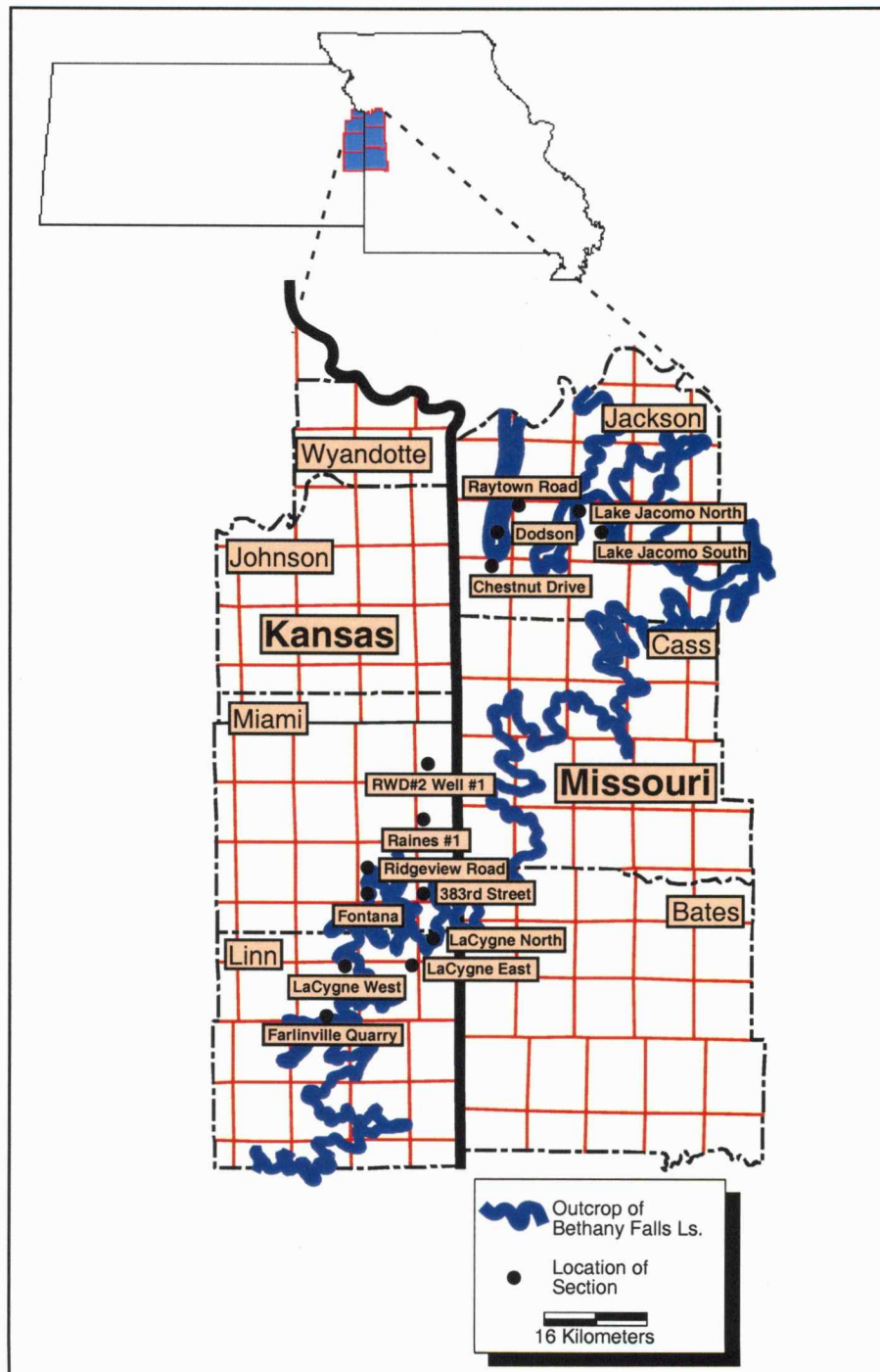


Figure 1.4. Map of study area showing Bethany Falls outcrop belt with locations of sections used in this study.

or their correlative conformities." The Swope Limestone has been defined as a portion of a cyclothem-scale depositional sequence (Watney et al., 1995). Sequence boundaries do not coincide with cyclothem boundaries as the top of the Elm Branch Shale is the base of the cyclothem and the top of the Galesburg Shale is the top of the cyclothem (Figure 1.1). Where sequence boundaries are also surfaces of subaerial exposure, sequence boundaries are important for creation, preservation, enhancement and destruction of porosity (French and Watney, 1993). For that reason, mapping units with sequence stratigraphic methods is more advantageous than with cyclothem stratigraphy, which uses "outside" non-marine shales as bounding units.

In addition to bounding surfaces, conceptual differences exist between correlations based upon cyclothem stratigraphy and depositional sequence stratigraphy. Cyclothem are defined based upon lithostratigraphic units that can be time transgressive. Depositional sequences are defined based upon chronostratigraphically significant surfaces that are independent of lithostratigraphy (Mitchum et al., 1977; Watney et al., 1995).

Regional Geology

The Swope Limestone represents a portion of a shallow marine shelf that extended from northeastern Oklahoma into Iowa (Mossler, 1971). The study area of eastern Kansas and western Missouri was in the Forest City Basin (Figure 1.5). During the Pennsylvanian, epeiric seas episodically

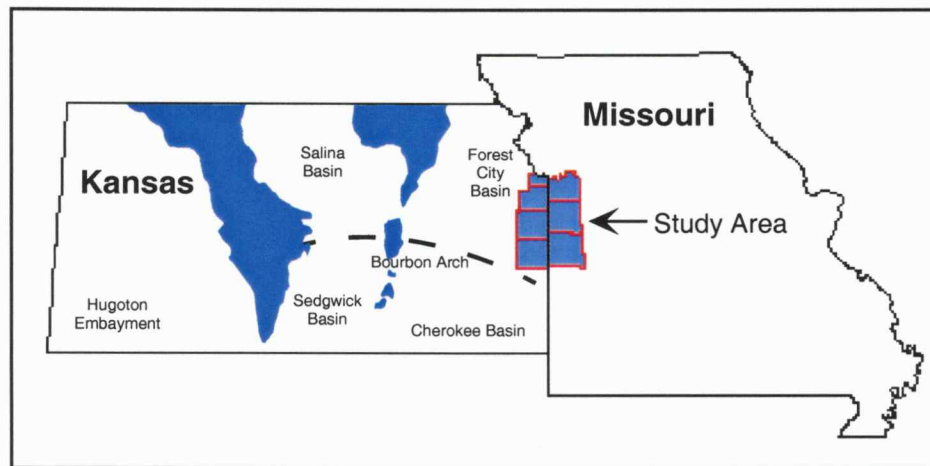


Figure 1.5. Major structural features in Kansas. The study area is located in the Forest City Basin. Modified from Merriam (1963).

covered the midcontinent. The apparent major control on the cyclicity observed in the upper Pennsylvanian was sea-level variations attributed to Gondwanan glaciation (Heckel, 1986). During periods of relative sea-level highstand, the shoreline was approximately in Iowa (Heckel, 1980). As relative sea level dropped, the shoreline migrated southward into Kansas. Southward along the outcrop belt of the Swope Limestone is essentially basinward.

The Swope Limestone, in ascending order, consists of 1) Middle Creek Limestone Member; 2) Hushpuckney Shale; and 3) Bethany Falls Limestone Member (Figure 1.1). The overlying Galesburg Shale is the “outside” shale of Heckel’s (1977) four member Kansas cyclothem.

The regressive Bethany Falls Limestone is composed of skeletal packstone-wackestone grading up into phylloid-algal and skeletal wackestone that changes upward to wackestone to lime mudstone (Watney et al., 1989). Locally, the Bethany Falls Limestone has a thick oolitic grainstone in its upper portion (French et al., 1989). The Bethany Falls Limestone reflects open marine to very shallow restricted marine conditions (Watney et al., 1989). The upper surface of the Bethany Falls displays evidence for subaerial exposure such as rhizoliths, paleosols and autoclastic brecciation (Watney et al., 1989; and French et al., 1989). At the Farlinville North Quarry, within the Bethany Falls, French et al. (1989) and Stover

(1992) recognized possible rhizoliths and fenestral fabrics in the wackestone immediately below the overlying oolitic grainstone, which might be evidence for subaerial exposure that could have predated deposition of the upper part of the Bethany Falls Limestone.

The lower portion of the Hushpuckney Shale is a fissile, black, phosphatic, highly radioactive shale, reflecting deposition in deep, anoxic marine conditions (Heckel, 1977; and Watney et al., 1989). The Hushpuckney Shale grades up into blocky gray shale, as conditions became dysoxic (Heckel, 1986; and Watney et al., 1989). The high natural gamma radiation of the Hushpuckney Shale serves as an easily recognized subsurface marker for correlation across the midcontinent (Watney et al., 1989).

The Middle Creek Limestone is a faunally diverse phylloid-algal wackestone that was deposited in a relatively shallow normal marine environment (Watney et al., 1989). The Galesburg Shale is a dark gray siltstone with coaly stringers, fossiliferous shale, and locally thin carbonates. The Galesburg Shale has been interpreted as forming in a variety of terrigenous environments, ranging from deltaic, to coal producing freshwater swamps, to sulfaquent, a soil type deposited in coastal marshes (Schutter, 1983).

Previous Investigations

Beds cropping out in the falls of Big Creek in Bethany, Missouri provided Broadhead (1866) with the type section for the Bethany Falls Limestone. The Bethany Falls Limestone was later included within the Swope Limestone, named after outcrops near Swope Park, Missouri (Moore, 1932).

Payton (1966) undertook detailed petrographic examinations of the Swope and Dennis formations in Missouri and Iowa. Payton examined localities along the outcrop belt from southern Kansas City into Iowa. He differentiated nine facies within the Bethany Falls Limestone, based on lithological and paleontological data gathered from point counts of thin sections. He also interpreted environmental conditions under which these lithofacies formed.

Mossler (1971) made a preliminary study of diagenesis and dolomitization of the Bethany Falls Limestone in southeastern Kansas. Mossler (1973) followed that up with a sedimentological study of the Swope Limestone from Farlinville Quarry (Figure 1.4) into southern Kansas. He divided the Bethany Falls Limestone into four distinct lithofacies.

Nollsch (1983) provided a detailed diagenetic study of the Swope Limestone from southern Kansas into southwestern Iowa. Watney (1980, 1984, 1985), Watney et al., (1989), Watney and French (1988) and French and Watney (1993) provided models for cyclic sedimentation, measured

sections, interpretations of depositional environments, and sequence stratigraphic models in western and eastern Kansas. Stover (1992) made a detailed stratigraphic and depositional study of Farlinville Quarry.

French et al. (1989), French and Watney (1993), and Stover's (1992) investigations recognized apparent subaerial exposure surfaces within the Bethany Falls Limestone in eastern Kansas. Carr et al. (1995), and Hoth et al. (1998) used these studies as a basis for geochemical and petrophysical examinations of the Bethany Falls Limestone in eastern Kansas.

Methodology

The basis of this study was the detailed measurement of seven outcrops and two cores of the Bethany Falls Limestone. Additionally, data from five previously studied outcrops were verified and incorporated (Carr et al., 1995).

Oolitic grainstones have been recognized in the upper portion of the Bethany Falls near Farlinville (Mossler, 1973). Lime mudstones are present in the upper Bethany Falls in the southern Kansas City area, with oolitic grainstones absent (Watney et al., 1989). To further delineate the contact between these two facies, additional outcrops were located and examined, and two shallow cores were drilled in Miami County (Figure 1.4).

Outcrops in Cass County are extremely poor, leading to a gap of about 30 kilometers between the RWD-2 #1 core and outcrops in southern Kansas

City, MO. However, lithologies in the RWD-2 #1 core and the southern Kansas City outcrops are remarkably similar.

Outcrops were selected from literature searches, from the measured section library at the Kansas Geological Survey, and by driving along the outcrop belt in eastern Kansas and western Missouri. Criteria for selection were location and completeness of section. Sections rarely encompassed the entire Swope Limestone. However, the sections examined provided a relatively complete section of the Bethany Falls Limestone.

The outcrops were measured both by conventional means as well as surface logging at 15-cm intervals with a handheld differential spectrometer/scintillometer (Scintrex GRS-500). Cores are NX size and were collected with the Kansas Geological Survey's rotary coring and drilling rig. Cores are housed in the Kansas Geological Survey. The wells were logged with a natural gamma and induction tool (Century 9511). Log data were examined in order to recognize radioactive anomalies that could possibly serve as markers for correlation.

Approximately 70 hand samples were slabbed and polished. 40 thin sections were examined. Additional hand samples and thin sections available from the Carr et al. (1995) study were examined. Thin sections were either polished or left at 600 grit, and left uncovered. Thin sections and polished slabs were examined using the naked eye, low-power

stereomicroscope, and a standard petrographic microscope. Thin sections and polished slabs are housed in the Kansas Geological Survey.

Examination of outcrops, cores, and samples provided detailed data about sedimentary structures, fauna, grain type, grain size, and lateral and vertical relationships. These data helped to establish the lithofacies and infer the depositional environments within the Bethany Falls Limestone.

**Chapter 2: Facies of the Bethany Falls Limestone, Hushpuckney Shale,
Middle Creek Limestone and Elm Branch Shale**

Chapter Two

Lithofacies & Depositional Environments of the Bethany Falls

Limestone

The Bethany Falls Limestone consists of eight discrete lithofacies. The subdivision into eight lithofacies is based upon attributes observed in outcrops, cores, polished slabs, and thin sections. Depositional environments range from relatively deep, low energy marine environments to shallow, restricted marine environments.

Mottled Skeletal Wackestone Facies

Description

Mottled skeletal wackestone is the most common facies in the Bethany Falls Limestone, and is present in all measured sections and cores. Bedding is thin to medium in scale (10 to 25 cm), wavy, and weathers a light brown (5YR 6/4) to grayish-orange (10YR 7/4). Fresh exposures are yellowish gray (5Y 8/1) to light gray (N7) with medium gray (N5) mottling. Stylolites are common (Figure 2.1).

The dominant depositional fabric observed in hand samples is wackestone (Figures 2.1, 2.2). However, isolated patches of packed skeletal material were observed in both thin section and hand samples (Figures 2.1, 2.3). The bulbous to cylindrical areas of packed skeletal material range in size from 3 to 5 mm in width and 2 to 4 cm in length, and are typically

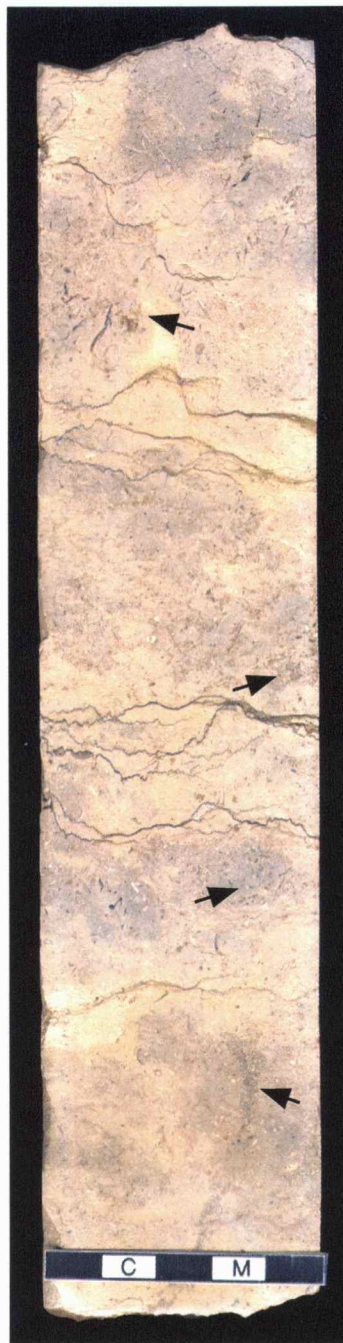


Figure 2.1. Polished core section showing mottled skeletal wackestone facies. Note the abundant stylolites. Arrows highlight packed skeletal material. The areas of packed skeletal material are interpreted as filling burrows (scale = 5 cm; sample RWD-2 BF#65).



Figure 2.2. Polished slab showing mottled skeletal wackestone facies. Skeletal material is typically fragmented and appears extensively bioturbated. Color mottling is related to later meteoric infiltration, with darker areas being microspar and lighter areas less-altered micrite (scale = 5 cm; sample Lacygne West BF#2).

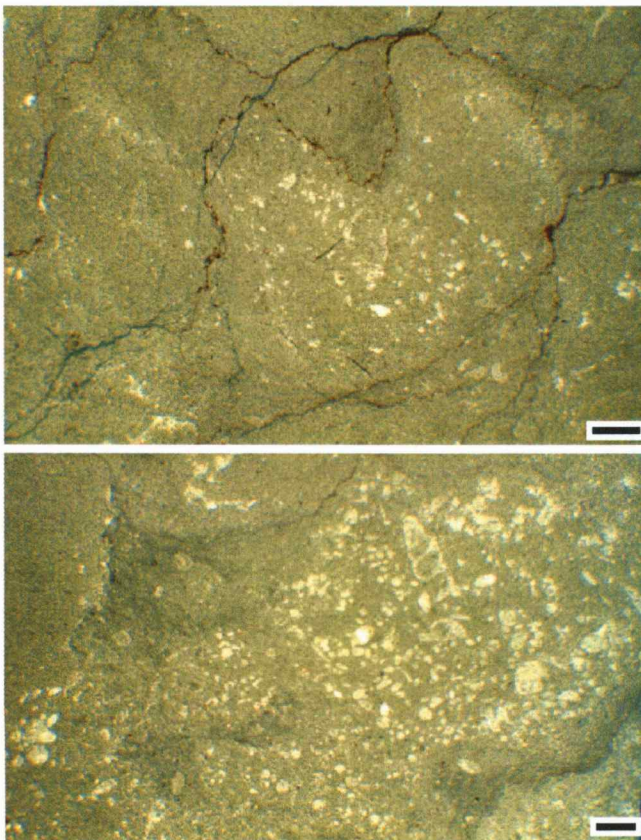


Figure 2.3. Photomicrographs illustrating the skeletal wackestone fabric. Both samples exhibit depositional micrite matrix with areas of packed skeletal fragments filling burrows (sample Chestnut Drive-11; transmitted light; scale bar = 1 mm).

oriented vertically (Figure 2.1). These patches of skeletal material typically have a swirled appearance.

Common identified skeletal components include brachiopods, fenestrate bryozoans, crinoids, bivalves, gastropods, foraminifera, phylloid algae, serpulid worm tubes, and tabulate and rugose corals. Corals rarely occur in growth position (Figure 2.4). Trilobites and ostracodes were rarely observed. Most bioclasts are disarticulated, but unabraded, and are typically less than 1 cm in length. Some bioclasts, especially worm tubes, appear coated with what appears to be algae. Phylloid algal fragments lack cellular preservation, and occur as molds filled with blocky calcite spar. Skeletal fragments comprise about 10 to 15 percent of the rock.

The fabric is predominantly micrite. In some places the micrite appears to have been recrystallized to microspar.

Paleoenvironmental Interpretation

The distinctive color mottling in the mottled skeletal wackestone has been interpreted as the result of preferential infiltration of meteoric water through more permeable zones during subsequent subaerial exposure. Nollsch (1983) determined that the dark mottles were microspar and the lighter areas were less-altered micrite. The dark microspar is isotopically more negative in both carbon and oxygen than the lighter micrite, and is related to meteoric diagenesis (Nollsch, 1983). Mottling appears to have

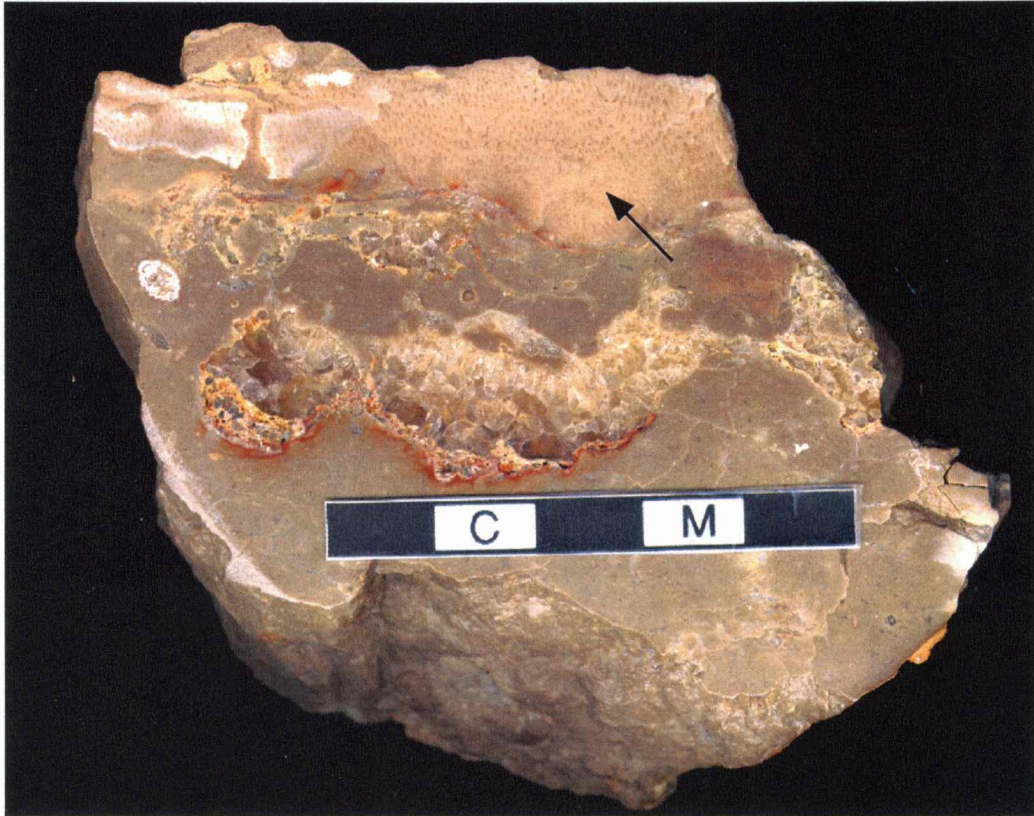


Figure 2.4. Polished slab of mottled skeletal wackestone with *Chaetetes* in growth position (arrow). White staining in upper left corner is a product of recent weathering (scale = 5 cm; sample Lake Jacomo North BF1).

been influenced by burrow systems and shale partings that controlled the permeability and provided pathways for diagenetic fluid flow.

Micrite is the dominant matrix of the mottled skeletal wackestone facies. Abundant framework organisms that would have trapped and bound carbonate mud were not observed.

The unabraded skeletal materials are the remains of organisms that lived within the mottled skeletal wackestone. The diverse fauna, including corals in growth position, is further evidence of a quiet, normal marine environment (Figure 2.4). Corals, bryozoans, crinoids, and brachiopods indicate a normal salinity marine environment (Heckel, 1972). The patchy, swirled nature of the skeletal grains, as well as the packed accumulations of skeletal material in burrows, is evidence of extensive bioturbation. In modern environments irregular patches of packed skeletal material can be produced by storm infilling of excavated burrow systems (Tedesco and Wanless, 1989). The combination of fauna and micrite indicates the mottled skeletal wackestone facies was deposited in a relatively normal-marine low-energy environment below wave base.

Phylloid Algal Packstone Facies

Description

The phylloid algal facies is recognized in all measured sections and cores in this study. Stratification is typically poorly developed, with thin to

medium bedding (10 to 50 cm). The packstone has a swirled texture that was observed in both outcrop and hand sample. Weathered exposures are typically a light brownish-gray (5YR 6/1), whereas fresh exposures are yellowish gray (5Y 8/1). Stylolites are present, but are less common than in the mottled skeletal wackestone facies.

The dominant depositional fabric observed in outcrop and samples is packstone (Figure 2.5). Skeletal material represents a diverse biota dominated by brachiopods and phylloid algal blades. The phylloid algal blades are completely replaced with coarse calcite spar, making specific identification difficult (Figure 2.6a, c). Associated fauna consist of bryozoans, foraminifera, serpulid worm tubes, crinoids, bivalves, gastropods, and corals. Trilobites and ostracodes are much less common. Skeletal material is commonly disarticulated, and comprises up to 30 to 40 percent of the rock. Skeletal material ranges in size from 1mm to 4 cm. Rare brachiopod fragments are up to 3 cm in length (Figure 2.5c). Phylloid algal blades are typically broken into pieces between 5 mm and 1 cm (Figures 2.5, 2.6a). Rare blades occur up to 4 cm in length. Corals in growth position were observed (Figure 2.6b). Serpulid worm tubes are disarticulated. Most worm tubes are filled with spar; however, some have a micrite filling (Figure 2.6c).

The matrix is a mixture of homogeneous micrite and micrite with a vaguely peloidal texture. In some patches, skeletal material is more concentrated, with hardly any micrite present. Geopetal fabrics are present,



Figure 2.5.

(A) Phylloid algal facies as seen in outcrop.

Arrows highlight wavy calcite veins which are phylloid algal blades (locality Raytown).

(B) Polished slab illustrating appearance of phylloid algal facies. Phylloid algal blades occur as coarse calcite spar. Note geopetal structures and packed nature of the facies (scale = 5 cm; sample Ridgeview Rd BF2 #4).

(C) Polished slab showing diverse biota in phylloid algal facies. Note the swirled texture of the fabric (scale = 5 cm; sample 383rd Street BF#2).

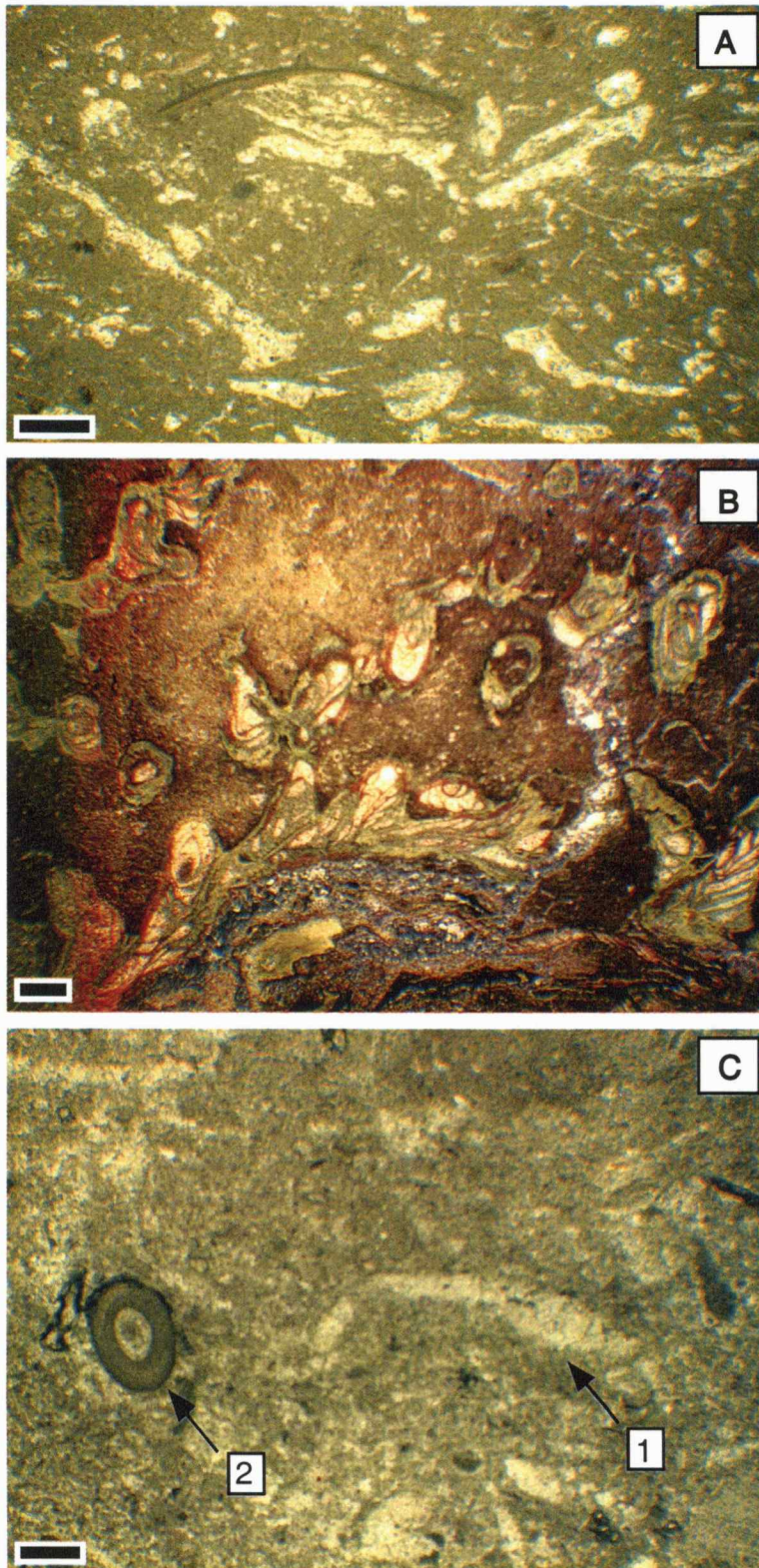


Figure 2.6.

(A) Photomicrograph of phylloid algal facies. Phylloid algal blades occur as coarse calcite spar. Note skeletal fragments (transmitted light; scale = 1 mm; sample RWD-2 BF#1).

(B) Photomicrograph of in-situ coral (transmitted light; scale = 1 mm; sample Farlinville 8/3 1A).

(C) Photomicrograph illustrating two common skeletal components in phylloid algal facies: 1) phylloid algal blades and 2) serpulid worm tubes. Note concentric laminae and spar filled void in worm tube (transmitted light; scale = 1 mm; sample Chestnut Drive #3).

with micrite lining the floors of articulated bivalves, and coarse spar infilling the remainder of the space.

Paleoenvironmental Interpretation

The abundant and diverse skeletal materials are interpreted to represent organisms that lived in the area. The phylloid algal blades are not in growth position and apparently did not act as baffles for the micrite.

Phylloid algae are dependent on sunlight for photosynthetic processes. Studies on modern photosynthetic algae, which serve as a analog to the phylloid algae found within the Bethany Falls Limestone, thrive in 20 to 30 m of water, but can grow to depths of 70 to 100 m (Phipps and Roberts, 1988). However, it should be noted that photosynthetic algae occur in greatest abundance in water depths less than 30 m.

The swirled nature observed in hand sample, and the regions with almost a skeletal grainstone fill, are related to extensive bioturbation. Burrowing organisms resulted in disarticulation of skeletal remains and the resulting burrow systems were subsequently filled during storms with skeletal material.

The diverse biota indicates a normal salinity marine environment. With the abundant, diverse biota, the abundance of algae, the packstone fabric, and the depositional micrite, the phylloid algal packstone was deposited in a relatively low-energy normal-marine environment below normal wave base. Photosynthetic algae can occur as deep as 100 m, but

the abundance of algae in the phylloid algal packstone facies suggests deposition in depths favorable to algal growth (typically less than 30 m).

Lime Mudstone Facies

Description

The lime mudstone facies is present in the northern portion of the study area, from the RWD-2 #1 core to the Raytown Road locality (Figure 1.4). Bedding is indistinct in the lime mudstone lithofacies, wavy, and with thickness from thin to medium (5 cm to 25 cm; Figure 2.7). Weathered exposures are medium light gray (N6), have a rubbly appearance and a distinct and pervasive medium dark gray (N4) color mottling. The mottling in the lime mudstone facies is similar to the mottling observed in the skeletal wackestone facies.

Grains of any sort are uncommon and account for less than 10 percent of the rock. The rare skeletal grains are relatively diverse. Bivalves, gastropods, brachiopods, bryozoans, crinoids and foraminifera were observed. Skeletal grains are typically disarticulated and more abraded than grains seen in the previous two lithofacies. However, the gastropods are relatively small in size (1-3 mm), and appear to be unabraded (Figure 2.8a, b). Grains are randomly scattered throughout the facies, with no beds, lenses, or accumulations of grains. Sizes range from 1 mm to 1 cm.



Figure 2.7.

(A) Polished slab showing fabric and pervasive color mottling of lime mudstone facies. Note stylolites and horizontal and vertical color mottling (scale = 5 cm; sample Raytown BF#6).

(B) Outcrop photo from Lake Jacomo South showing rubbly field appearance of the lime mudstone facies. Mottles are not dominantly horizontal as in A, appearing more random.

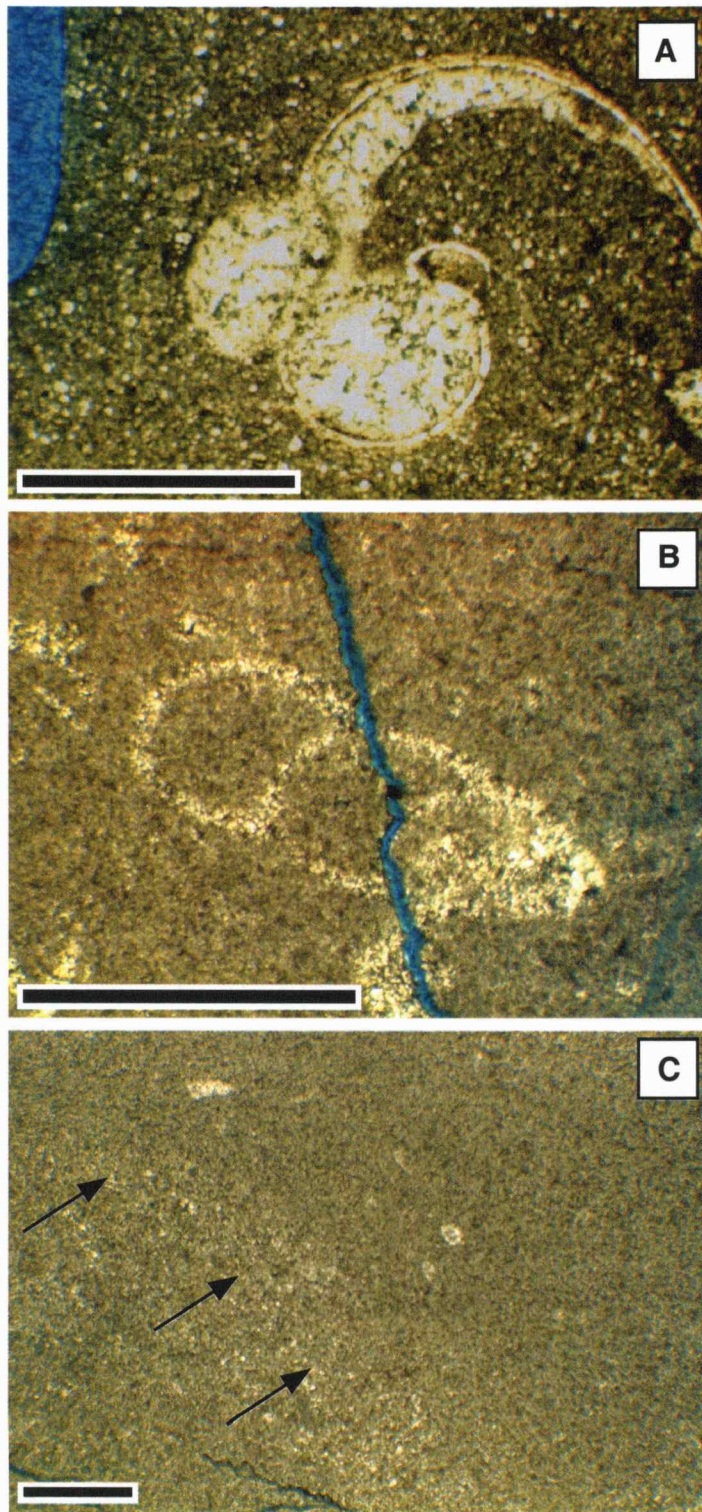


Figure 2.8.

(A) (B) Photomicrographs of gastropods in lime mudstone.

Fossil grains are rare and typically depauperate (transmitted light; scale = 1 mm; samples RWD-2 #1, Lake Jacomo North #3).

(C) Photomicrograph of lime mudstone facies illustrating color mottling. The microspar (left side) appears as dark gray mottles in hand sample. Note the arrows showing the textural differences between the micrite and microspar area (transmitted light; scale = 1 mm; sample Raytown #6).

Matrix is dominantly depositional micrite. The dark gray mottles, when petrographically examined, appear to be microspar (Figure 2.8c). Lighter gray areas are relatively homogenous micrite (Figure 2.8c).

Paleoenvironmental Interpretation

The skeletal grains, when present, are abraded. The few grains relatively unabraded are typically gastropods. Gastropods that are found in this facies are depauperate and not readily observable in hand-sample or outcrop (Figure 2.8a, b).

The lime mudstone lithofacies appears extensively bioturbated. The indistinct bedding and the color mottling, some of which appears to be burrow shaped, are evidence of bioturbation. Scavenging organisms likely reworked the sediment, resulting in the random distribution of skeletal grains.

The rare normal marine grains, such as brachiopods and crinoids, represent grains washed in by storms from adjacent normal marine environments. The abraded nature of these normal marine organisms suggests transport. Unabraded grains, such as the depauperate gastropods and bivalves, are interpreted as indigenous to the lime mudstone environment. The mottled appearance as well as the depauperate fauna are characteristic of restricted subtidal environments (Enos, 1983). Based upon quantity, depositional characteristics, and type and condition of the skeletal grains present, the lime mudstone lithofacies is interpreted to represent a restricted marine environment. Abnormal nutrient and salinity levels, and

possibly temperature fluctuations are possible results of decreased water circulation. Possible causes for restriction will be discussed in the sequence stratigraphy chapter.

Oolite facies

Description

The oolite facies is divided into two subfacies. The main subfacies is ooid grainstone. A second less common subfacies is composed of micrite-rich ooid packstone and oolitic peloidal wackestone. Both oolite subfacies are found in the southern portion of the field area, from Farlinville to the Raines #1 core (Figure 1.4).

The ooid grainstone subfacies is cross-bedded and weathers brownish gray (5YR 4/1) (Figure 2.9). Cross beds are centimeter scale, and are planar tabular (Figure 2.9). Bed thickness ranges from medium to thick (50 to 100 cm). Within single outcrops, dip directions of cross-beds are unidirectional (Table 1, Figure 2.9).

Locality	N	Dips	Strikes (azimuth)
Farlinville	5	15° - 22° SSE	30° - 35°
LaCygne East	4	17° - 20° N	90° - 95°
LaCygne West	5	20° - 23° NE	105° - 115°
Fontana	6	18° - 22° SSW	320° - 330°

Table 1. Dip directions and strikes of cross beds within the oolite grainstone subfacies.



Figure 2.9. Outcrop photographs of cross-bedded oolitic grainstone in the upper portion of the Bethany Falls Limestone at the (A) Farlinville Locality and (B) Fontana locality. Note the unidirectional dip direction of the planar tabular cross beds.

Table 1 illustrates the consistency of dip direction within singular locations, and the difference in dip direction observed from one locality to another. Dips are generally in the 18° to 22° range, and dip either basinward (south) or shoreward (north). Due to the consistent unidirectional dip direction of cross-beds within a single outcrop, numerous dip measurements were not collected for the construction of Rose diagrams.

In fresh exposure, the ooid grainstone subfacies is slightly yellowish gray (5Y 8/1) to medium light gray (N6) (Figure 2.10). The ooids range from 0.5 to 1.0 mm in diameter. Many individual ooids have been completely dissolved out, resulting in oomoldic porosity (Figure 2.10). Ooids have also been replaced with calcite spar, and some have been micritized (Figure 2.11a). In ooids with preserved original structure, micritic peloids are the dominant nuclei. Skeletal fragments are rare in the oolite grainstone subfacies. Observed skeletal grains are well-abraded brachiopods, bivalves, and gastropods (Figure 2.11b). At the contact between the ooid grainstone and underlying facies, centimeter scale erosion was observed.

The second subfacies is a micrite-rich ooid packstone and oolitic-peloidal wackestone that is less common than the ooid grainstone subfacies. (Figure 2.12a). The ooid packstone/wackestone subfacies is found at Farlinville, 383rd Street, and the Raines #1 core. At Farlinville, the ooid packstone/wackestone subfacies occurs as thin to medium (10 to 50 cm) lenses of ooid packstone. At both Raines #1 core and 383rd Street, oolitic-

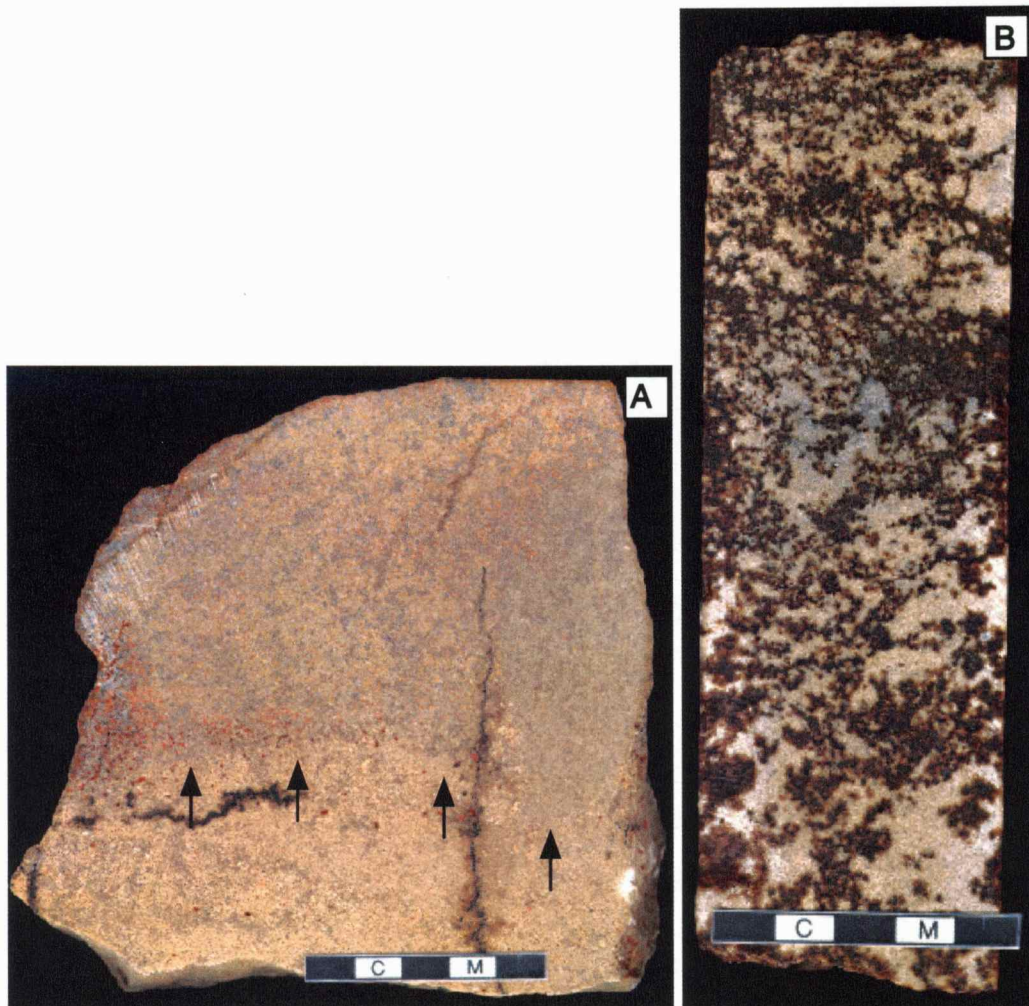


Figure 2.10. (A) Polished slab of ooid grainstone. Note the arrows showing the contact between the oomoldic portion (bottom) and the undissolved ooid section (upper; scale = 5 cm; sample LaCygne East BF#4).

(B) Polished core section of oomoldic ooid grainstone. Oil staining highlights oomoldic porosity (scale = 5 cm; sample Raines #1 BF#78).

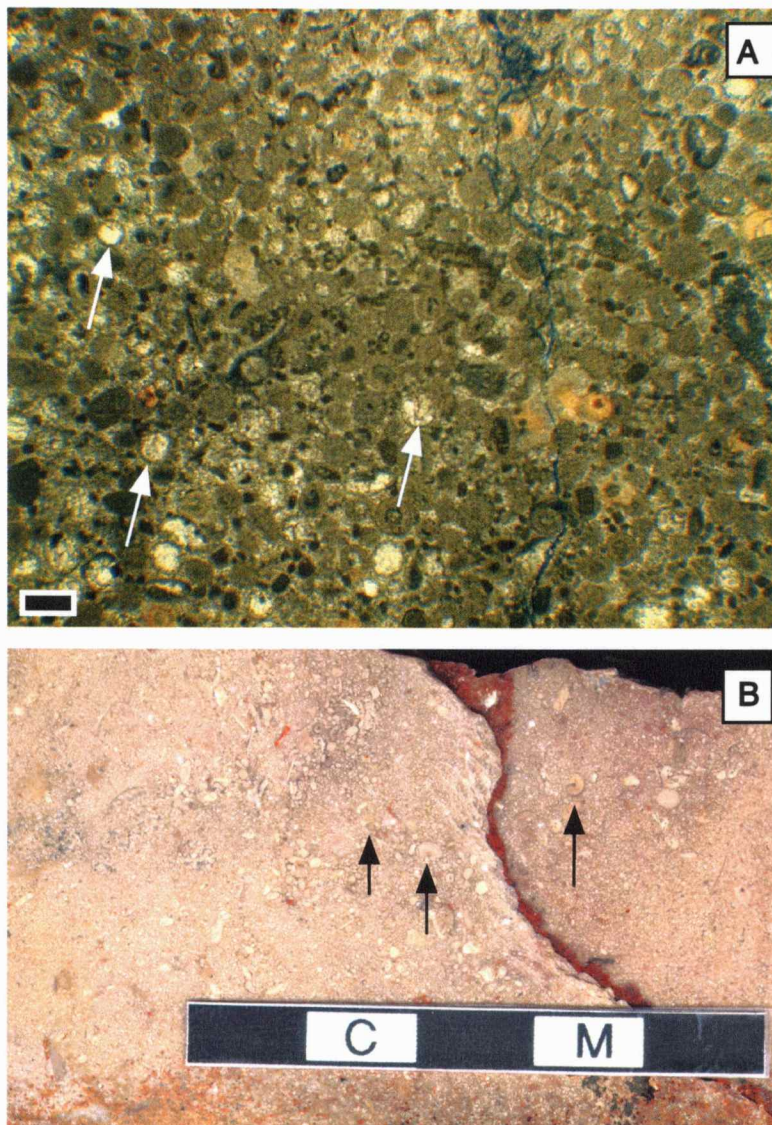


Figure 2.11.

(A) Photomicrograph of ooid grainstone. Note the arrows showing micrite envelopes around spar-replaced ooids. Some original internal structure of the ooids is preserved, however, ooids are commonly micritized (transmitted light; scale = 1 mm; sample Farlinville 5). (B) Polished slab of ooid grainstone. Arrows highlight gastropods within the fabric, possibly transported in (scale = 5 cm; sample 383rd Street BF#6).

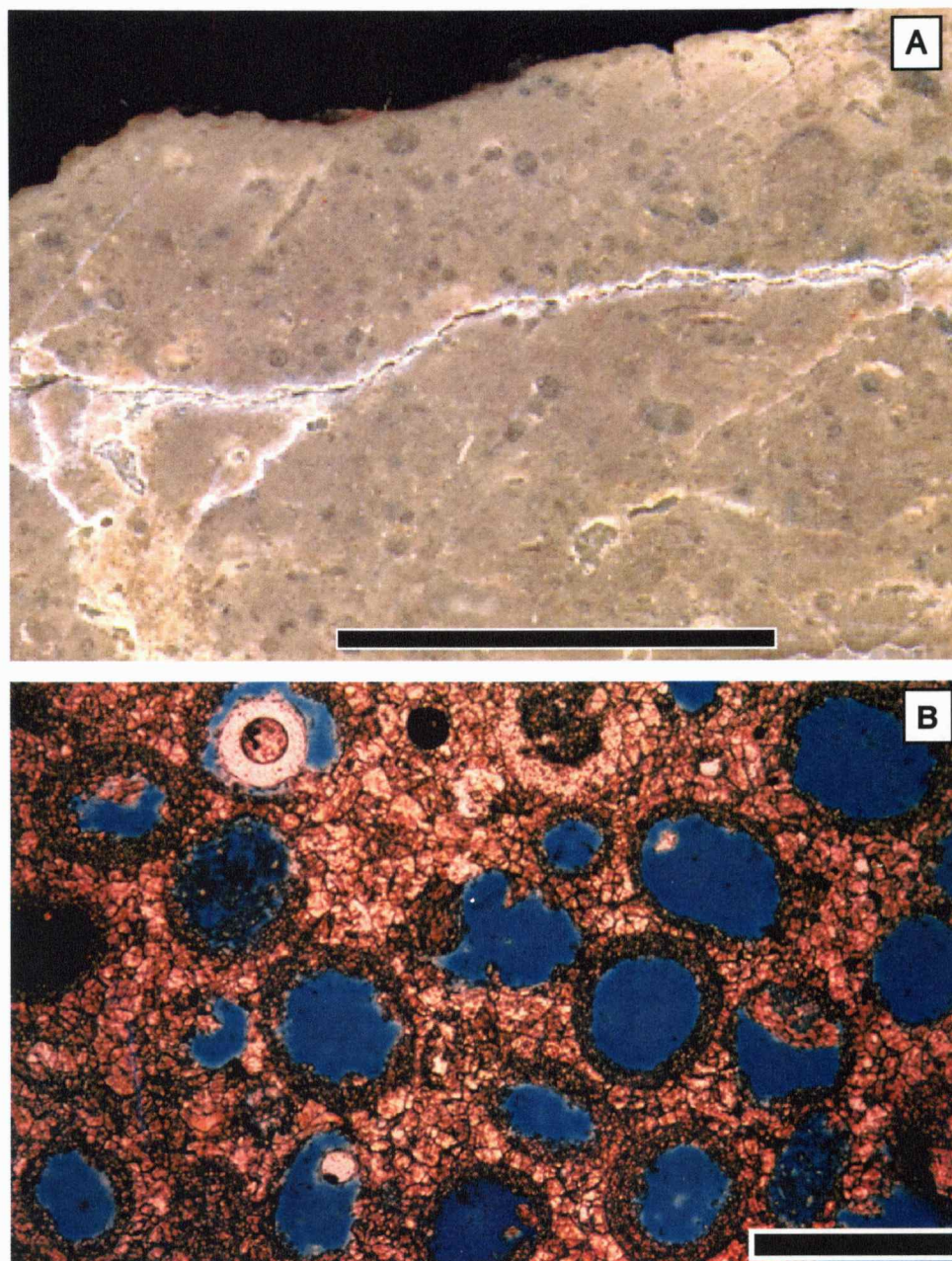


Figure 2.12. (A) Slab of oolitic wackestone. Ooids in this rock have been dissolved and replaced with calcite spar (scale = 1 cm, sample 383rd Street BF#18).

(B) Photomicrograph of oomoldic porosity within the ooid grainstone (transmitted light; scale = 1 mm; sample Farlinville #10).

peloidal wackestone caps the ooid grainstone. At 383rd Street, the capping wackestone is irregular in thickness, from non-existent to medium bedded (25 cm).

Ooids in the ooid packstone/wackestone subfacies range from 0.5 to 1.0 mm. Ooids have been micritized, dissolved, or replaced with spar (Figure 2.12). Original structure in the ooids was not observed. Weathered exposures are light brownish gray (5YR 6/1), while fresh surfaces are a yellowish gray (5Y 8/1). Homogenous micrite is present, along with peloidal textured micrite. Peloids are indistinct. Both the ooid grainstone and ooid packstone/wackestone subfacies were observed as being penetrated by numerous vertical tubes (Figure 2.13). Tubes are typically 1 to 8 cm in diameter, and up to 150 cm in length. Some tubes were observed to bifurcate downwards, decreasing diameter at bifurcation junctions, whereas other tubes have a relatively variable diameter, with cm scale differences observed (Figure 2.14). Within the oolite facies at the Farlinville locality, vertical tubes with a diameter of between 1 and 5 cm terminate in a horizontal manner (Figure 2.14). These features are also coincident with uranium and potassium anomalies observed on the spectral gamma ray log of the outcrop (Figure 2.14).

At the Raines #1 borehole, within the oolite facies, oolitic grainstone with oomoldic porosity is observed underlying oolitic grainstone with little porosity (Figure 2.15). The contact between the oomoldic porosity and the



Figure 2.13. Paleo-karst tube or rhizolith in ooid grainstone sub-facies. Tubes are found filled with calcite, ferroan dolomite, shaly material, or empty. This tube is hollow, but has a halo of cemented ooids surrounding it, preserving the original structure of the tube (locality LaCygne West).

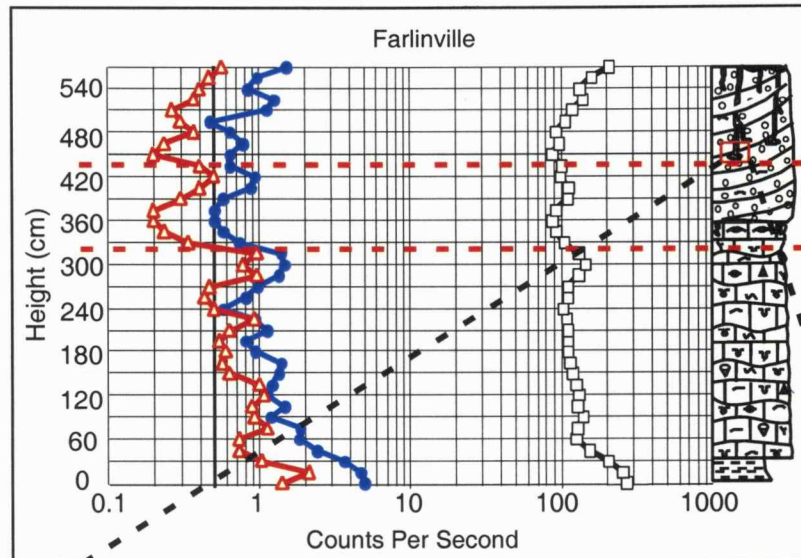


Figure 2.14. Vertical tube terminating in a horizontal manner coincident with uranium and potassium rich radioactive anomaly at Falinville. This structure is interpreted as being a rhizolith terminating at the vadose/phreatic zone boundary.

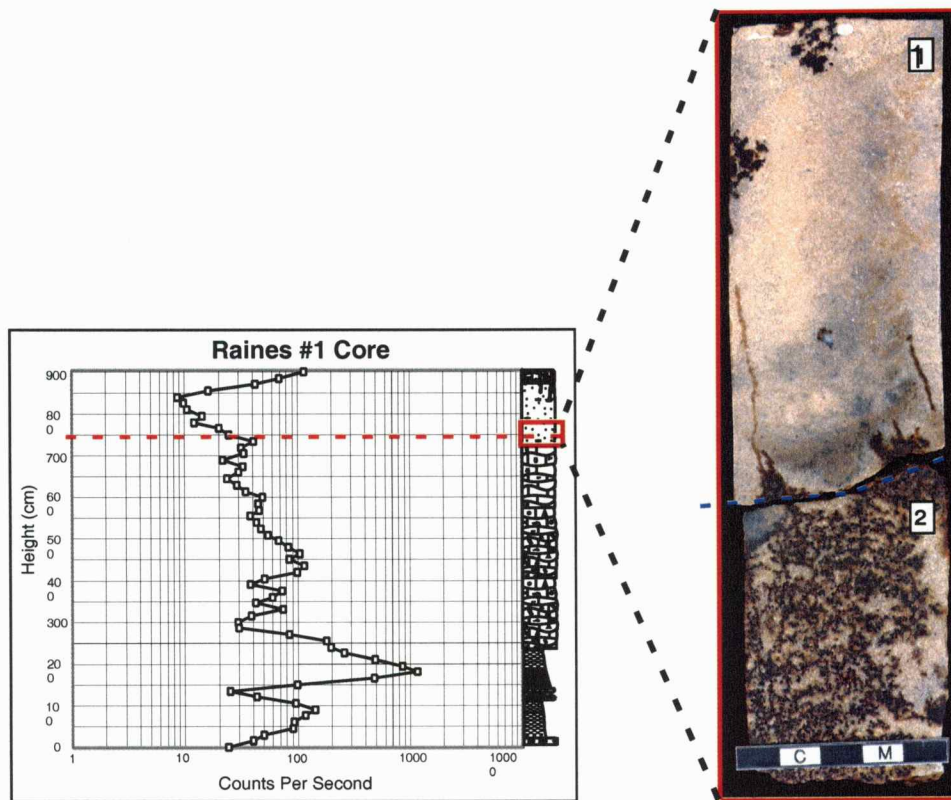


Figure 2.15. Contact between (1) low porosity ooid grainstone and (2) oomoldic porosity ooid grainstone. Oil staining highlights porosity differences. The contact between the low porosity zone and the oomoldic porosity zone is coincident with a radioactive anomaly.

low porosity grainstone is coincident with a radioactive anomaly observed on the gamma-ray log (Figure 2.15).

Paleoenvironmental Interpretation

Descriptions of Cenozoic sand accumulations in south Florida and the Bahamas provide an analog for the ooid grainstones and packstones observed in this study (e.g. Ball, 1967; Hine, 1977; Halley, et al., 1983; Evans, 1984; Harris, 1984). Ball (1967) classified modern sand accumulations of the Bahamas and south Florida into four groups: (1) tidal-bar belts; (2) storm dominated marine sand belts; (3) aeolian dunes; and (4) platform interior blankets. Modern oolitic sand bodies vary in size, and can be as little as 1.5 km wide (Ball, 1967). The four groups of carbonate sand accumulations are differentiated based upon setting, geometry, internal structure, composition, and texture (Ball, 1967). In this field area, outcrop data is limited; therefore, only the most basic interpretations can be made about the type and distribution of oolitic sand bodies.

The planar tabular cross-bedded oolitic grainstone lacks micrite, and within single outcrops, have unidirectional dip directions. Physical sedimentary features such as trough cross bedding, herringbone cross bedding or other types of bi-directional cross bedding were not observed, as would be expected in a tidal-bar belt. Also, location of these oolitic grainstones in a tidal energy damping epeiric sea, relatively far up on the shelf, discounts the possibility of the high tidal currents (>100 cm/sec)

needed to produce tidal-bar belts (Ball, 1967). Relatively coarse bioclasts were observed within the oolite grainstone facies (Figure 2.11b). This lack of sorting is evidence against an eolian origin. Keystone vugs were not observed, which further discounts an eolian origin. Eolian deposits commonly have a bimodal distribution, and possibly inversely graded bedding. Neither of these features were observed. I interpret the cross-bedded ooid grainstone subfacies as reflecting deposition in a storm dominated marine sand belt. Water depth was likely less than 10 m, but still in the subtidal range. The cross-bedded oolitic grainstone was likely formed in a storm dominated marine sand belt.

Cross-beds were not observed in the micrite-rich ooid packstone and oolitic-peloidal wackestone. The packstone and wackestone are similar to those described by Harris (1984) in the Joulters shoal. The presence of micrite and the absence of cross-beds suggest a lower energy environment than the oolitic grainstone deposited in a storm dominated marine sand belt. The presence of peloids and the absence of well-defined bedding suggest extensive burrowing and reworking by organisms. I interpret the ooid packstone and wackestone as being deposited landward of the active ooid sands, on stabilized and burrowed sand and possibly relict sand bars.

Skeletal Packstone Facies

Description

The skeletal packstone lithofacies is found in the southern portion of the study area, from Farlinville to 383rd Street (Figure 1.4). Bedding is indistinct and wavy, ranging in thickness from thin to medium (10 to 25 cm). Fresh exposures are light gray (N7) in color whereas weathered exposures are pale yellowish orange (10YR 8/6).

The skeletal packstone lithofacies is similar to the phylloid algal packstone facies except for the complete absence of phylloid algal blades. Common identifiable skeletal components are brachiopods, bryozoans, crinoids, foraminifera, bivalves, and gastropods. Worm tubes and ostracodes were rarely observed. Skeletal grain size ranges from 1mm up to 1 cm. Most bioclasts are disarticulated, with the exception of rare bivalves and ostracodes (Figure 2.16).

The dominant fabric is packstone (Figure 2.16a, b). The fabric has a swirled appearance, with no preferred orientation of grains. The matrix is a homogenous micrite. Color mottling was not observed in the skeletal packstone lithofacies.

Paleoenvironmental Interpretation

The abundant diverse biota represented by the skeletal material is interpreted to have lived in this facies. Grains are not abraded, only disarticulated. Disarticulation and the swirled nature of the fabric probably

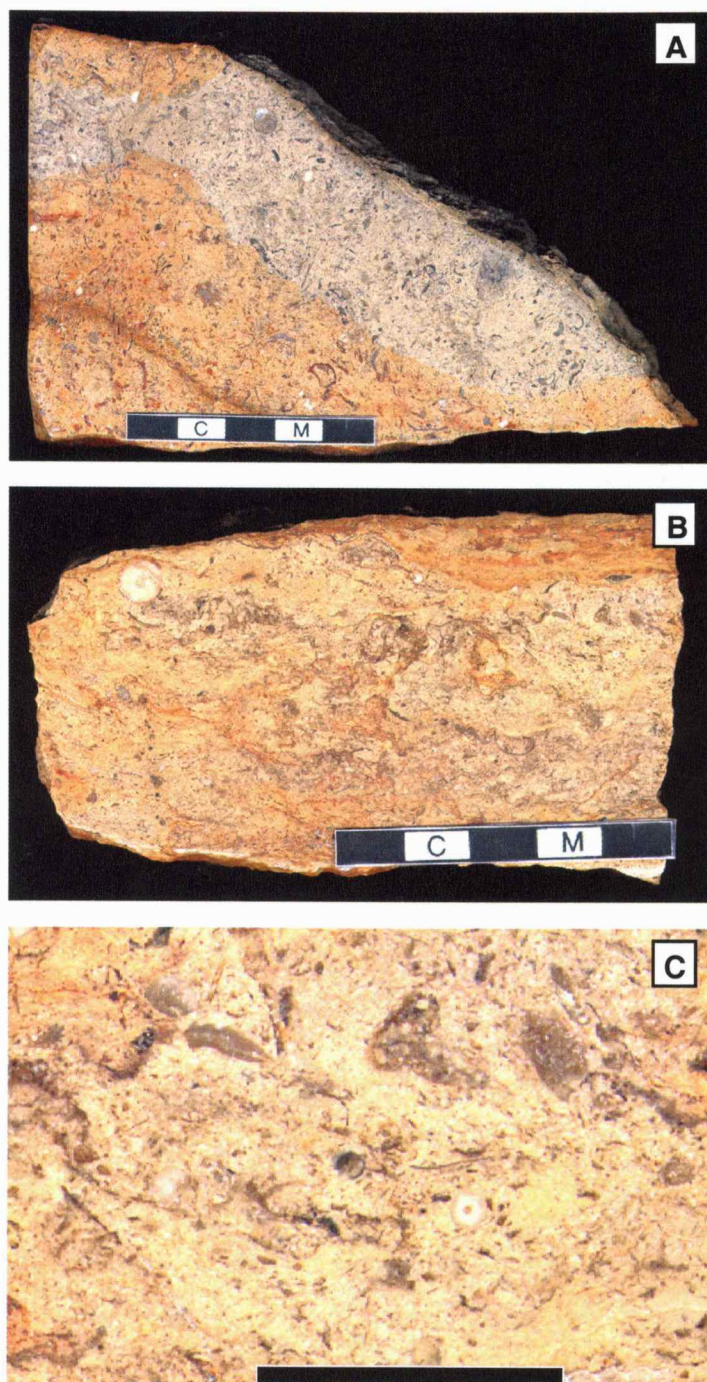


Figure 2.16.

(A) Polished slab of skeletal packstone facies. Note lack of algal blades and packed nature of sample. The brown color is the result of recent weathering processes (scale = 5 cm; sample Ridgeview Road BF1 #3).

(B) Polished slab showing swirled texture of the skeletal packstone facies. The diverse, packed biota and absence of algal blades characterizes the skeletal packstone lithofacies (scale = 5 cm; sample 383rd Street BF #1).

(C) Closeup picture of polished slab pictured above. Disarticulation of the various skeletal fragments is illustrated (scale = 1 cm; sample 383 BF #1).

resulted from extensive bioturbation. The bryozoans, crinoids, and brachiopods indicate a normal salinity marine environment (Heckel, 1972).

The presence of micrite matrix is evidence of a low energy environment. The absence of phylloid algal blades might indicate that this facies was deposited in deeper water than the phylloid algal facies. Relatively deep water might have precluded effective sunlight illumination, making algal growth difficult. The combination of fauna present and depositional characteristics suggests that the skeletal packstone lithofacies was deposited in a relatively normal-marine deeper-water environment below wave base.

Skeletal Grainstone Facies

Description

The skeletal grainstone lithofacies is only recognized at the Lake Jacomo North and Lake Jacomo South localities. The skeletal grainstone is cross-bedded at both localities (faintly at Lake Jacomo South), and is composed of a single bed ranging from 80 to 100 cm thick. Dips on the planar tabular cross beds range from 15° to 18° towards the northeast, and strike 125° to 135° (Figure 2.17). Fresh surfaces show alternating light gray (N7) and light brownish gray beds (5YR 4/1), with weathered surfaces a light gray (Figure 2.18a).

The fabric is grainstone at Lake Jacomo North, and a mix of grainstone/packstone at Lake Jacomo South. Skeletal grains make up the

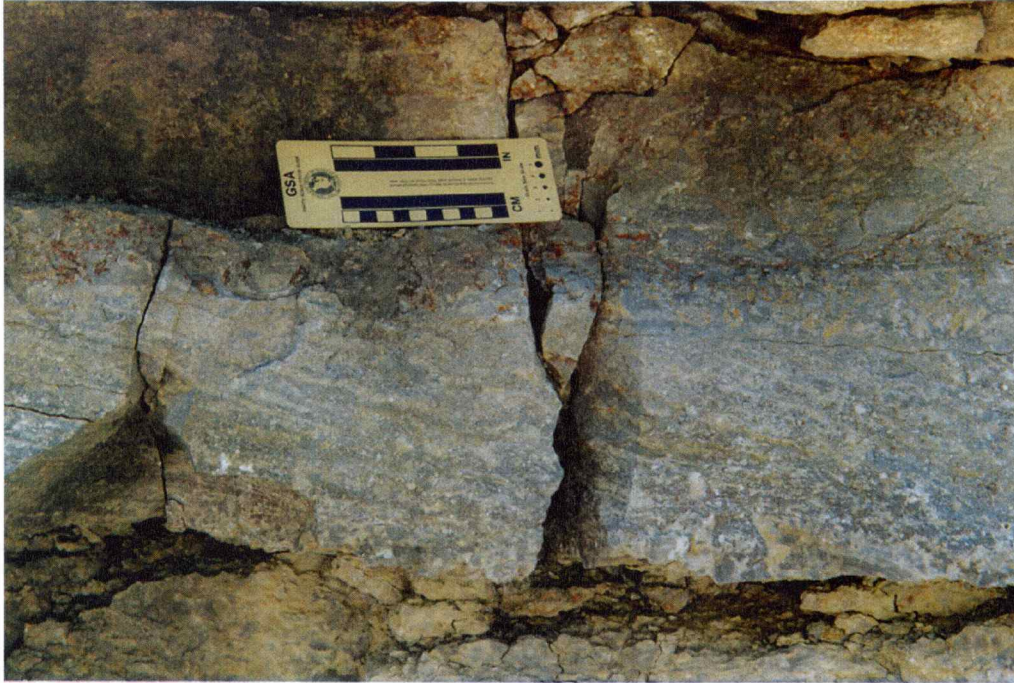


Figure 2.17. Outcrop of cross-bedded skeletal grainstone at Lake Jacomo North. Cross-beds are centimeter scale, with unidirectional dip of about 15-18 degrees.

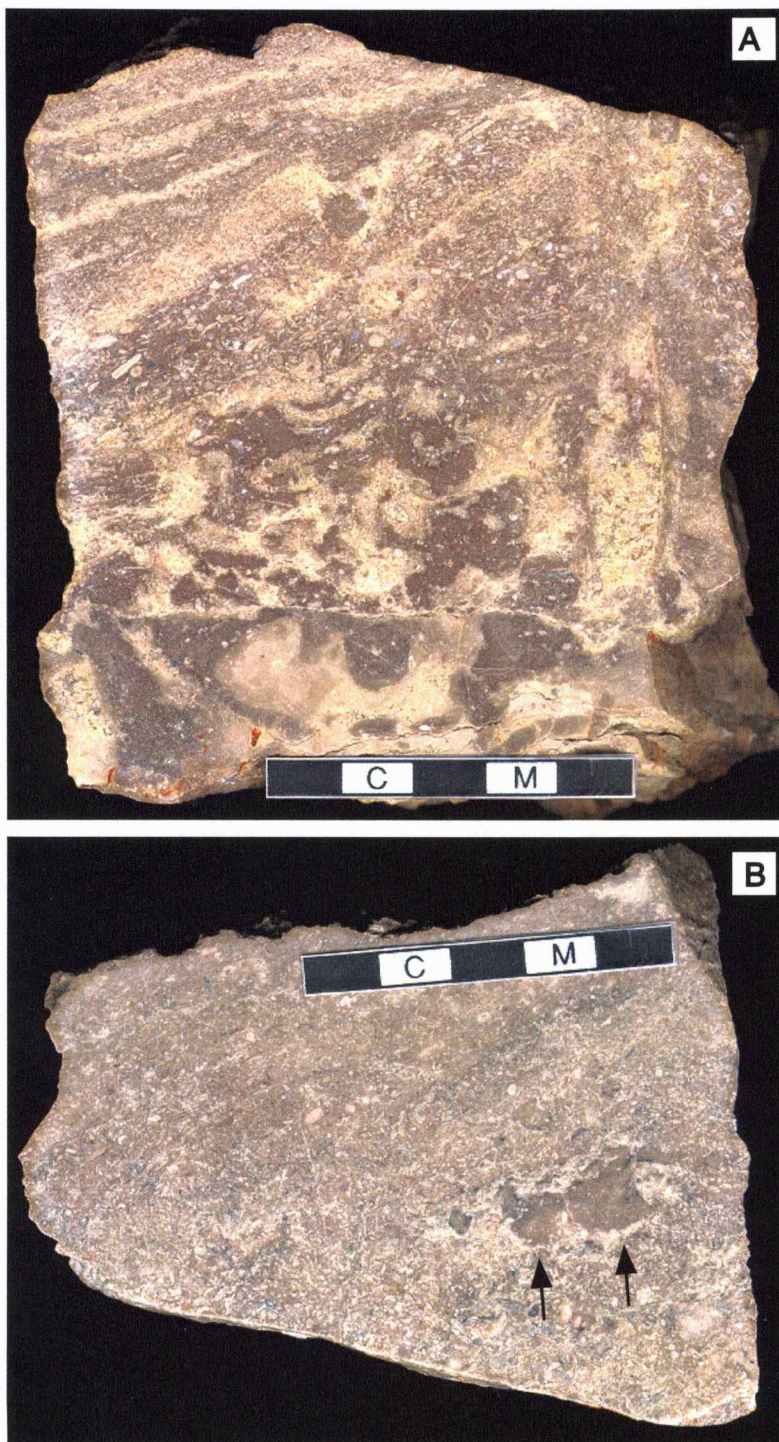


Figure 2.18.

(A) Polished slab of contact between skeletal packstone and lime mudstone. Note the cross bedding in the skeletal packstone, and the erosion at the facies contact (scale = 5 cm; sample Lake Jacomo North BF #3).

(B) Polished slab of skeletal packstone. Arrows highlight incorporated clasts of underlying lime mudstone facies incorporated within (scale = 5 cm; sample Lake Jacomo South BF #3).

vast majority of the rock. Skeletal grains are disarticulated, abraded and commonly oriented with the long axis parallel to the dip of the cross-beds. Biota represented include brachiopods, bryozoans, crinoids, serpulid worm tubes, bivalves, and gastropods. Peloids were also observed.

Clasts of the underlying lime mudstone are incorporated into the matrix of the skeletal grainstone in places (Figure 2.18b). In the field, erosional truncation of the lime mudstone by the skeletal grainstone is not readily observable. However, in polished hand sample, millimeter scale erosion was observed (Figure 2.18a).

Paleoenvironmental Interpretation

The difficulty in interpreting the environment for the skeletal grainstone lithofacies comes from the vertical relationships with surrounding facies. The skeletal grainstone overlies a restricted low-energy marine lime mudstone facies, and is overlain by a (pedogenically altered) restricted low-energy marine lime mudstone facies.

High-energy marine grainstones and packstones can be formed in a variety of environments. Events of catastrophic sedimentation, such as storm deposits, are relatively instantaneous events. However, examination of other outcrops in the area did not show a similar high-energy event.

The cross beds, lack of mud and incorporated clasts of underlying sediment in the Lake Jacomo North locality are all strong evidence for a high energy marine environment. At Lake Jacomo South, the fainter cross beds

and presence of mud indicates a relatively lower energy environment than at Lake Jacomo North. However, the skeletal grainstone facies of Lake Jacomo North is a relatively high-energy environment when compared to the underlying lime mudstone facies.

The most likely depositional environment for the skeletal grainstone lithofacies was in a storm dominated marine sand belt. Antecedent topography might have been higher at Lake Jacomo North and South than at the localities to the east (Figure 1.4). Shoaling indicated by transition from shallow water sediments (below) to subaerial exposure (above) could have provided a focus for tidal current. However, as sea level continued to shoal, energy levels decreased, and restricted extremely shallow low energy conditions resumed. Without detailed knowledge of the shelf topography, the specific depositional environment remains conjectural.

Fenestral Wackestone Facies

Description

The fenestral wackestone lithofacies is recognized only at the Farlinville locality, occurring immediately below the ooid grainstone facies in irregular lenses. The fenestral wackestone appears to have an erosive contact with the overlying cross-bedded ooid grainstone facies. Lenses range from 1 to 2 meters in length, and are up to 20 cm thick. The fenestral wackestone is a medium dark gray (N4) in weathered portions and a light

brownish-gray (5YR 6/1) in unweathered portions with medium gray (N5) color mottling.

Identified skeletal material includes bivalves, gastropods, bryozoans and brachiopods. Molluscan fauna dominates the observed skeletal grains, occurring in greater abundance than observed in the mottled skeletal wackestone facies. Skeletal material is disarticulated, and scattered throughout the fabric. The fabric is skeletal wackestone (Figure 2.19). The matrix is micrite, some of which has a peloidal texture. Based on fauna alone, the fenestral wackestone is a different lithofacies than the underlying mottled skeletal wackestone lithofacies.

The diagnostic feature of this facies is the abundant fenestral fabric. According to Shinn (1968), fenestrae (or bird's-eye vugs) can be divided into two discrete types. The types are 1) randomly distributed bubble-shaped voids and 2) planar shaped generally unconnected voids. Both types were observed at the Farlinville locality (Figure 2.19).

The randomly distributed fenestrae in the fenestral wackestone range in size from 5 mm to 2 cm in length, and 5 mm to 3 cm in height. The fenestrae often have a geopetal fill of silt at the base, capped with calcite spar (Figure 2.20a). A few fenestrae have a three component fill consisting of disturbed country rock, silt, and capped with coarse calcite spar (Figure 2.20b). The planar shaped vugs range in size from 3 mm to 10 cm in length, and 1 mm to 1 cm in height, and have a geopetal fill of silt at the base,

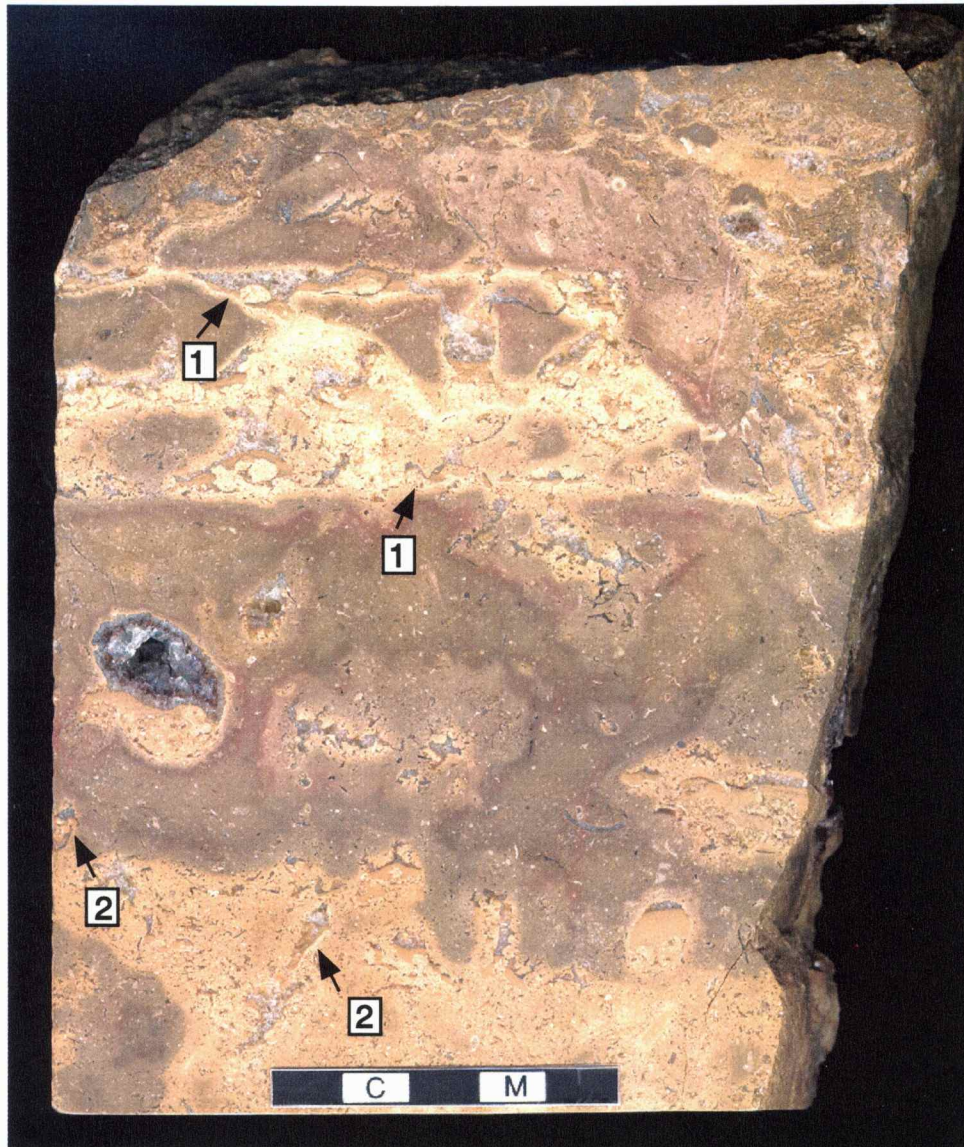


Figure 2.19. Polished slab of fenestral wackestone. Both types of bird's eye vugs 1) planar-shaped, generally unconnected voids, and 2) randomly distributed bubble-shaped voids are illustrated (scale = 5 cm; sample Farlinville RM #1). See close-up of fenestrae in Figure 2.18.

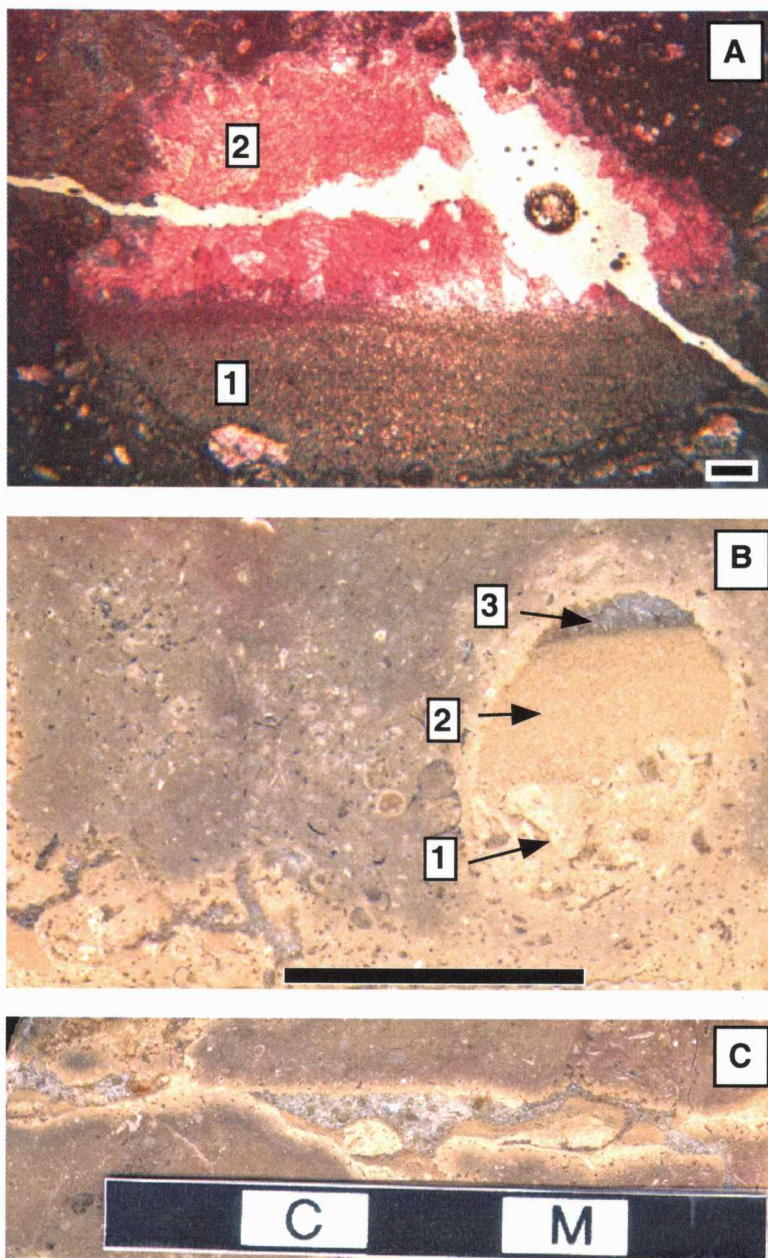


Figure 2.20.

(A) Photomicrograph of bird's eye vug within the fenestral wackestone. Silt (1) and spar (2) make a partial geopetal fill of the vug (transmitted light; scale = 1 mm; sample Farlinville 8/3 2B).

(B) Detailed photograph of polished slab in Figure 2.17. The bird's eye vug shown here has a three component geopetal fill, 1) disturbed country rock, 2) silt, 3) calcite spar (scale = 1 cm, sample Farlinville RM#1).

(C) Detailed photograph of polished slab shown in Figure 2.17. This planar shaped bird's eye vug is filled with silt and calcite spar (scale = 5 cm; sample Farlinville RM#1).

capped with coarse calcite spar (Figure 2.20c). Structures that appear to be burrows are scattered throughout the fenestral wackestone facies. The burrow-like structures range in size from 1 cm to 3 cm in width, and 2 to 7 cm in height, and are commonly floored with skeletal and peloidal material.

Paleoenvironmental Interpretation

The lateral and horizontal relationship of the fenestral wackestone lithofacies to surrounding facies is important in determining the depositional environment. The fenestral wackestone sits on top of the subtidal skeletal wackestone, and below subtidal cross-bedded oolite facies. The fenestral wackestone is not a discrete layer or bed, but only occurs in irregular lenses. Partial erosion during deposition of the high-energy ooid grainstone probably accounts for the scattered lenses of fenestral wackestone.

The fenestrae are important evidence for the depositional environment. According to Shinn (1969, 1983), fenestrae that occur in muddy rocks are a reliable indicator of upper intertidal to supratidal deposition. I interpret that the fenestral wackestone lithofacies, with its micrite matrix and fenestrae, was deposited in a upper intertidal to supratidal environment. The skeletal material, with a preponderance of molluscan fauna, indicates a restricted environment. A restricted environment is consistent with an interpretation of extremely shallow to supratidal environment, where water circulation is inhibited. I interpret the fenestral wackestone as representing a surface of subaerial exposure that is later

covered with subtidal oolitic grainstone. Ooids filling some of the fenestrae would be strong evidence for an upper intertidal to supratidal depositional environment. This was not observed however. The absence of ooids might have been the result of small fenestrae pore throats or fenestra might not have been open (i.e. cemented) to the surface.

An alternate hypothesis would be that the fenestrae observed in the wackestone are the result of organic decay and desiccation of the mud caused by the same subaerial exposure event that follows oolite deposition. In this case, the fenestral wackestone would not represent a significant surface of subaerial exposure, rather occurring as a diagenetic process on subtidal rocks. However, the lack of a continuous layer of fenestral wackestone underlying the oolite facies is evidence against this hypothesis. If the fenestrae formed as the result of organic decay and mud drying after oolite deposition, then it would be reasonable to assume that a continuous layer of mud underlying the oolite dried and fenestrae formed. Only scattered lenses of fenestral wackestone are observed at Farlinville. Deposition in an upper intertidal to supratidal environment followed by submarine erosion of the fenestral wackestone in a high energy marine sand body appears to be a better explanation for the scattered occurrence of fenestral wackestone. The abundance of molluscan fauna also is evidence against this hypothesis. The molluscan fauna observed in the lenses of fenestral wackestone differentiate the fenestral wackestone facies from the mottled skeletal wackestone facies.

If these fenestrae formed as a result of diagenetic processes acting on the subtidal mottled skeletal wackestone facies, it would be reasonable to observe similar fauna laterally in both the rock with fenestrae and the rock without fenestrae.

Paleosol Facies

Description

The paleosol lithofacies is composed of two discrete subfacies. The most common subfacies is an autoclastically brecciated lime mudstone, found from the RWD-2 #1 core north to the Raytown locality. A second subfacies is a surficial rhizolite laminated calcrete, observed only at Farlinville.

The autoclastically brecciated lime mudstone ranges in thickness from 50 to over 250 cm in thickness. It weathers a light gray (N7), with fresh surfaces being brownish gray (5YR 4/1; Figures 2.21, 2.22). Diagnostic features of the autobrecciated lime mudstone are autoclastic brecciation, color mottling, abundant millimeter scale rhizoliths, and shale infilling cracks and rhizoliths (Figures 2.21, 2.22). The original fabric and matrix of the autoclastically brecciated lime mudstone is the same as the underlying lime mudstone. Shale infilling appears to be from the overlying Galesburg Shale.



Figure 2.21. Polished slab of paleosol from Raytown locality. Note the shale filled rhizoliths and cracks (scale = 5 cm; sample Raytown BF #7).

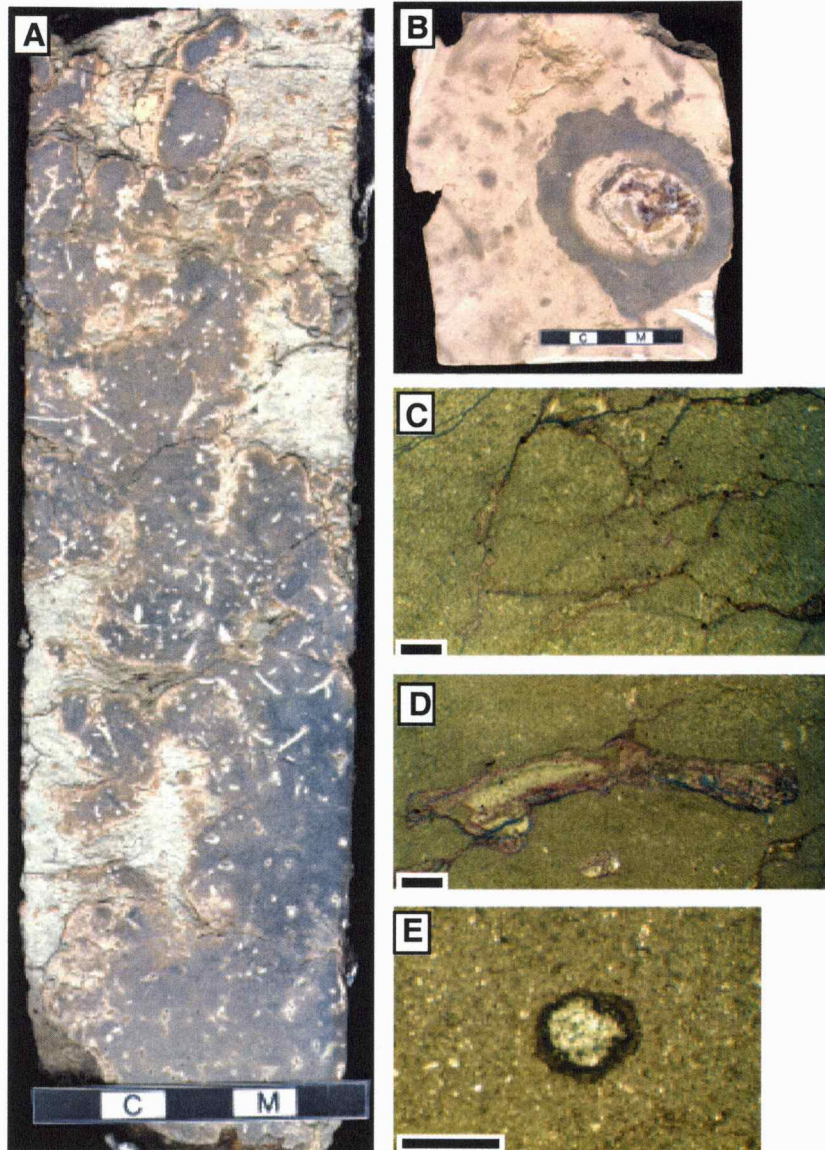


Figure 2.22. (A) Polished core section from RWD#2 #1. In outcrop, most of the shale filling the various cracks is weathered out. However, in core, this relationship is preserved (scale = 5 cm; sample RWD-2 BF#74). (B) Polished slab showing rhizocretion. The dark grey is micrite recrystallized to microspar (scale = 5 cm; sample Lake Jacomo South RM#1). (C) Photomicrograph showing autoclastic brecciation in the lime mudstone paleosol facies (transmitted light; scale = 1 mm; sample Chestnut Drive 20). (D) Photomicrograph of shale infilling a crack in lime mudstone paleosol (transmitted light; scale = 1 mm; sample Chestnut Drive 20). (E) Photomicrograph of alteration halo around rhizolith in the lime mudstone paleosol facies (transmitted light; scale = 1 mm; sample RWD-2 #2).

The contact between the autoclastically brecciated lime mudstone and the underlying lime mudstone is typically coincident with a radioactive anomaly (Figures 2.23; 2.24).

The second subfacies is a surficial rhizolite laminar calcrete, found in irregular lenses ranging from 1 to 5 cm in height, and up to 20 cm in length, The rhizolite laminar calcrete was only observed at the Farlinville locality, capping the oolite subfacies (Figure 2.25a).

The calcrete subfacies weathers a light brownish gray (5YR 6/1) color; whereas in fresh exposure, is laminated dark yellowish orange (10YR 6/6) and very pale orange (10YR 8/2). The calcrete subfacies is characterized by laminae that are sub-millimeter in scale. Typically, the dark yellowish orange laminae are separated by highly contorted lightly colored laminae (Figure 2.25b). Small tube shaped pores penetrate the calcrete subfacies (Figure 2.25b).

Paleoenvironmental Interpretation

The autobrecciated lime mudstone has abundant rhizoliths. Rhizoliths are the structures produced by the roots of terrigenous plants (Klappa, 1980). The rhizoliths and autoclastic brecciation are indicative of subaerial exposure and pedogenic processes. The autobrecciated lime mudstone subfacies formed as the result of weathering on the underlying lime mudstone lithofacies.

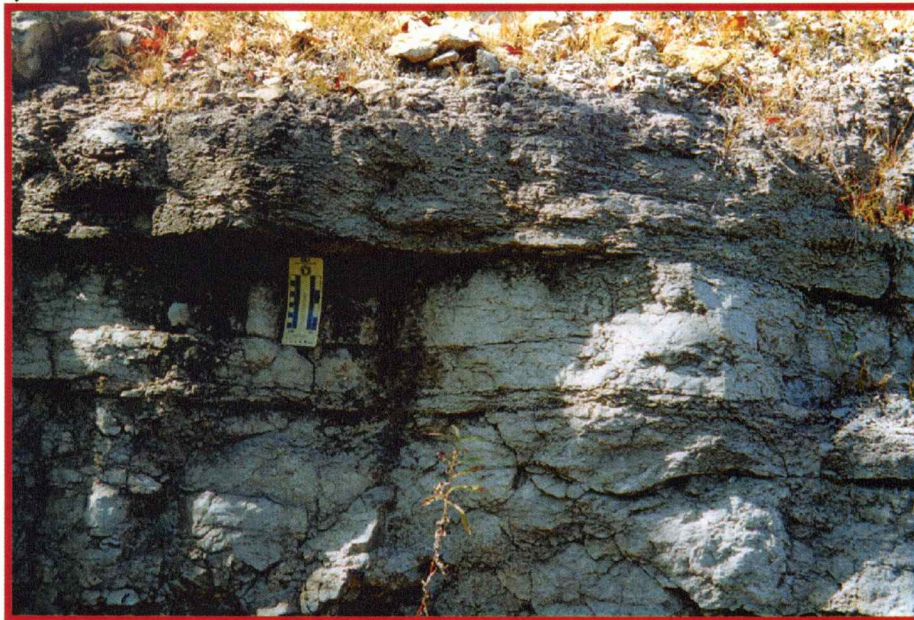
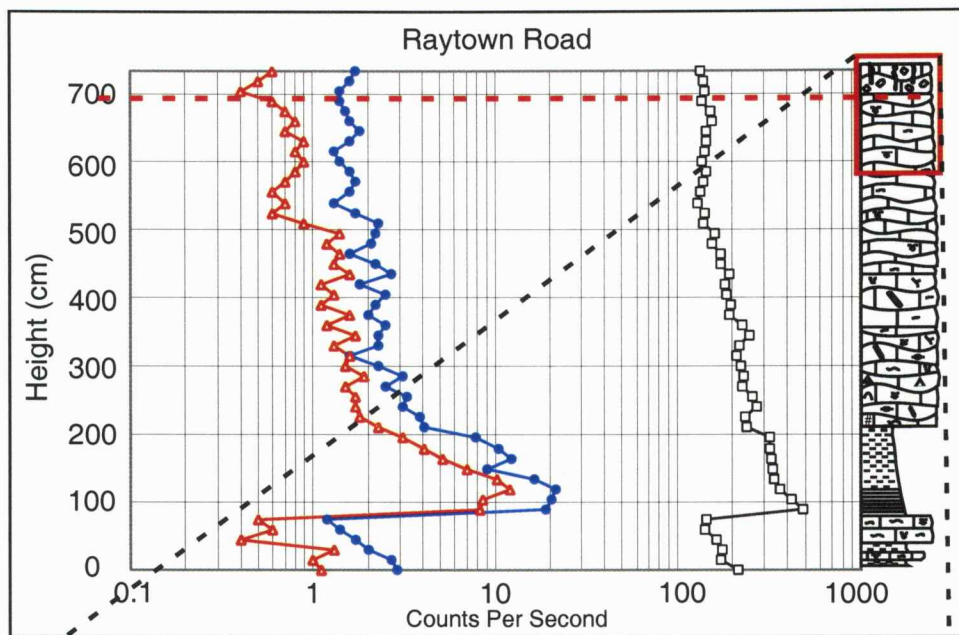


Figure 2.23. Outcrop photograph at the Raytown locality showing contact between autoclastically brecciated lime mudstone (upper) and lime mudstone (lower). This contact is coincident with a uranium and potassium rich radioactive anomaly.

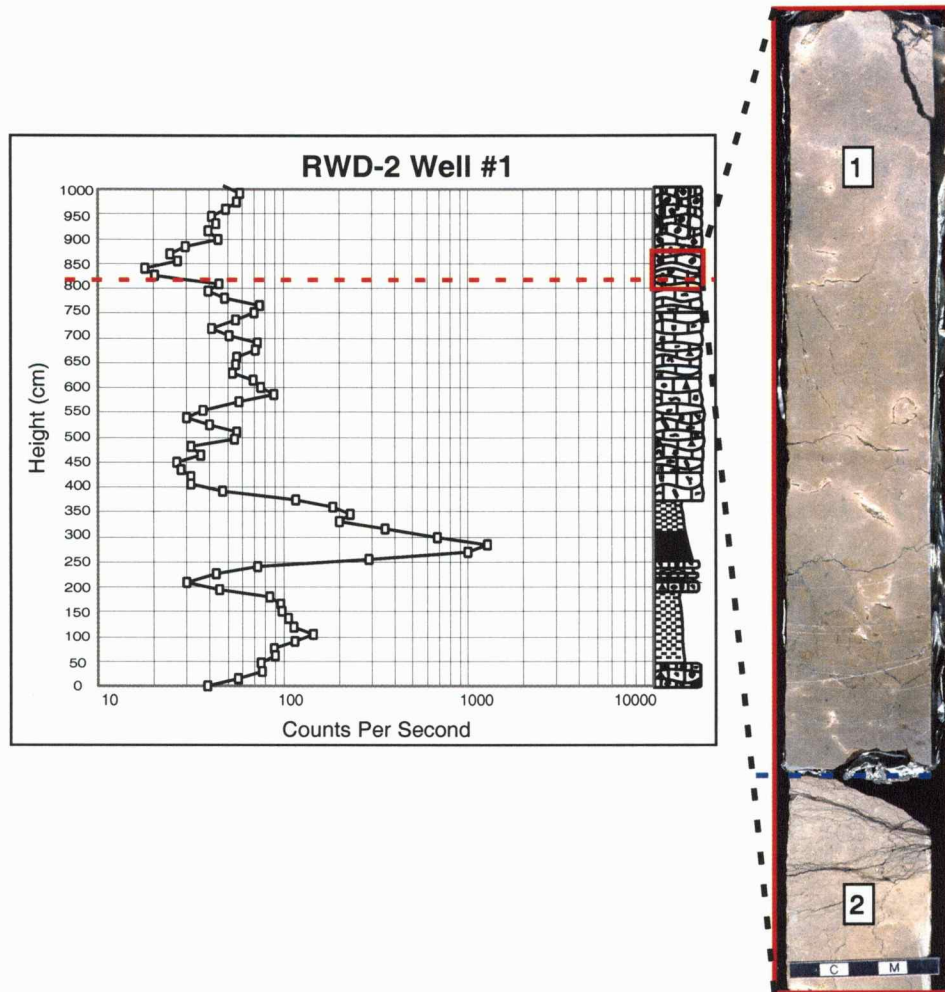


Figure 2.24. Polished core section from the RWD-2 #1 borehole showing contact between (1) autoclastically brecciated lime mudstone and (2) lime mudstone. This contact is coincident with a radioactive anomaly.

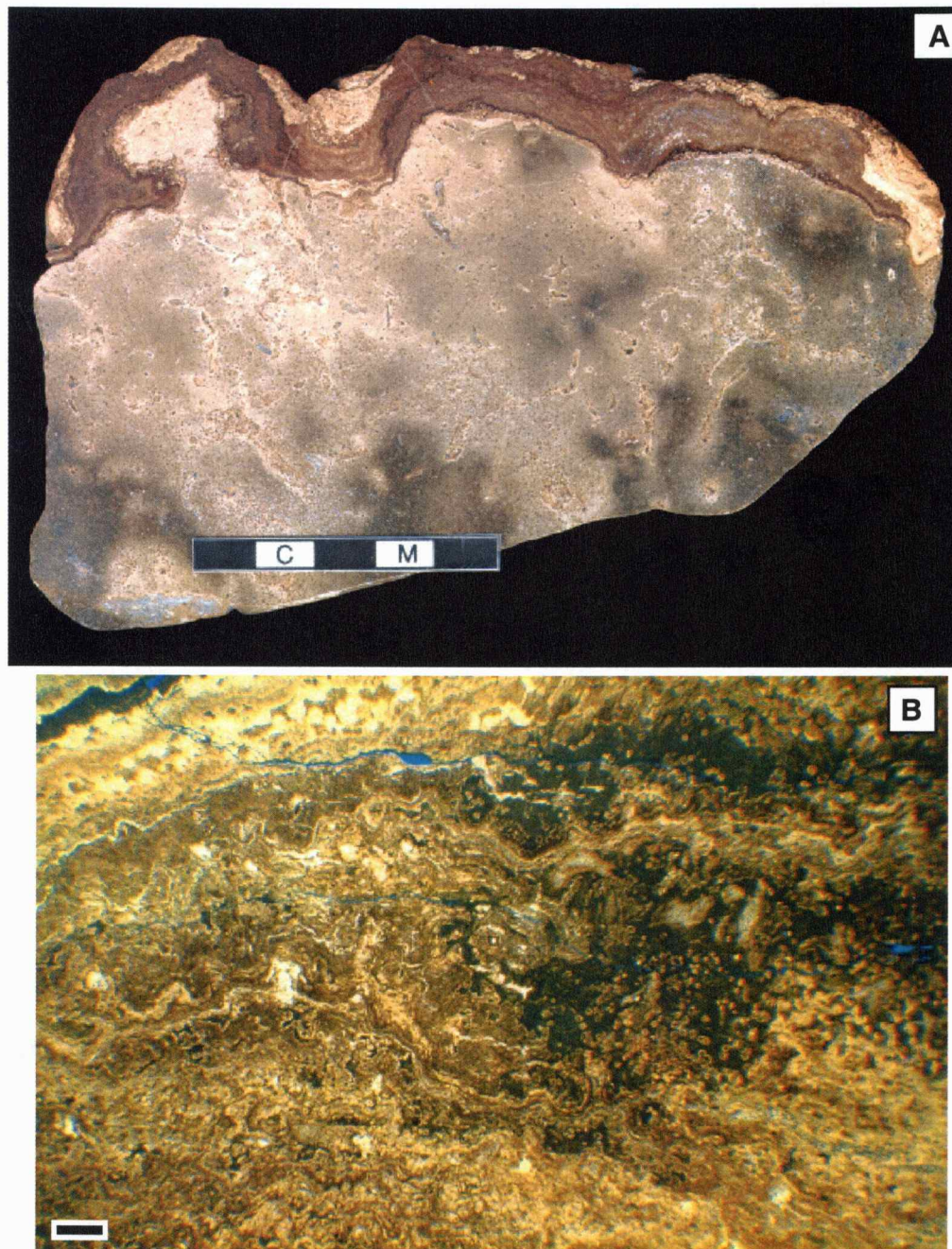


Figure 2.25. (A) Polished slab showing surficial laminar calcrete subfacies on ooid packstone subfacies (scale = 5 cm; sample Farlinville RM#2). (B) Photomicrograph of laminar calcrete. Note the laminated micrite and the rhizoliths (transmitted light; scale = 1 mm; sample Farlinville 12.5B).

Studies of Pleistocene calcretes by Perkins (1977) and the studies of surficial laminar calcretes by Wright et al. (1988) show similarities between Pleistocene calcretes and the laminated calcrete observed at Farlinville. The presence of the rhizoliths in the laminated calcrete subfacies suggests that the formation of this facies was in part rootlet aided. Root activity has been interpreted as playing an important role in the formation of surficial laminated calcretes (Wright et al., 1988). Simple dissolution and precipitation of calcium carbonate probably occurred in this facies, but root activity played an important role in the formation of the laminated calcrete at the Farlinville locality. The laminated calcrete subfacies is not a weathered zone like the autobrecciated lime mudstone, but is instead a carbonate formed under subaerial conditions.

Both the autobrecciated lime mudstone and laminated calcrete subfacies formed as the result of pedogenic processes occurring in a subaerial environment, and they are a pedogenic overprint of pre-existing depositional lithofacies.

Lithofacies and Depositional Environments of the Elm Branch Shale, the Hushpuckney Shale, and the Middle Creek Limestone.

Though not the main focus of this study, the depositional environments represented in the Elm Branch Shale, the Middle Creek Limestone, and the

Hushpuckney Shale play an important role in the development of any paleo-environmental model of this interval. Within these three units, there are six discrete lithofacies.

Elm Branch Shale

Blocky Mudstone Facies

Description

The blocky mudstone facies is found in the lower portion of the Elm Branch Shale. Diagnostic features are the slickensides and the blocky and weathered appearance, which occur even in fresh core (Figure 2.26). The blocky mudstone facies is medium gray (N5) to light brownish gray (5YR 6/1) in color. Calcareous nodules are present in the lower portion, but decrease upwards, leaving a homogenous mudstone (Figure 2.26). These calcareous nodules are very light gray (N8), irregular in shape, but are typically oval shaped, 1 to 3 cm in length, and 1 to 2 cm in height.

Interpretation

The blocky appearance, soil slickensides, and caliche nodules are evidence that the blocky mudstone lithofacies represents a paleosol. Marine fossils were not observed. The blocky mudstone facies was probably formed in some sort of overbank area within an interfluvial setting, with the sediment being derived from pedogenic processes acting on the underlying limestone, wind transported sediment, and occasional fluvial processes.

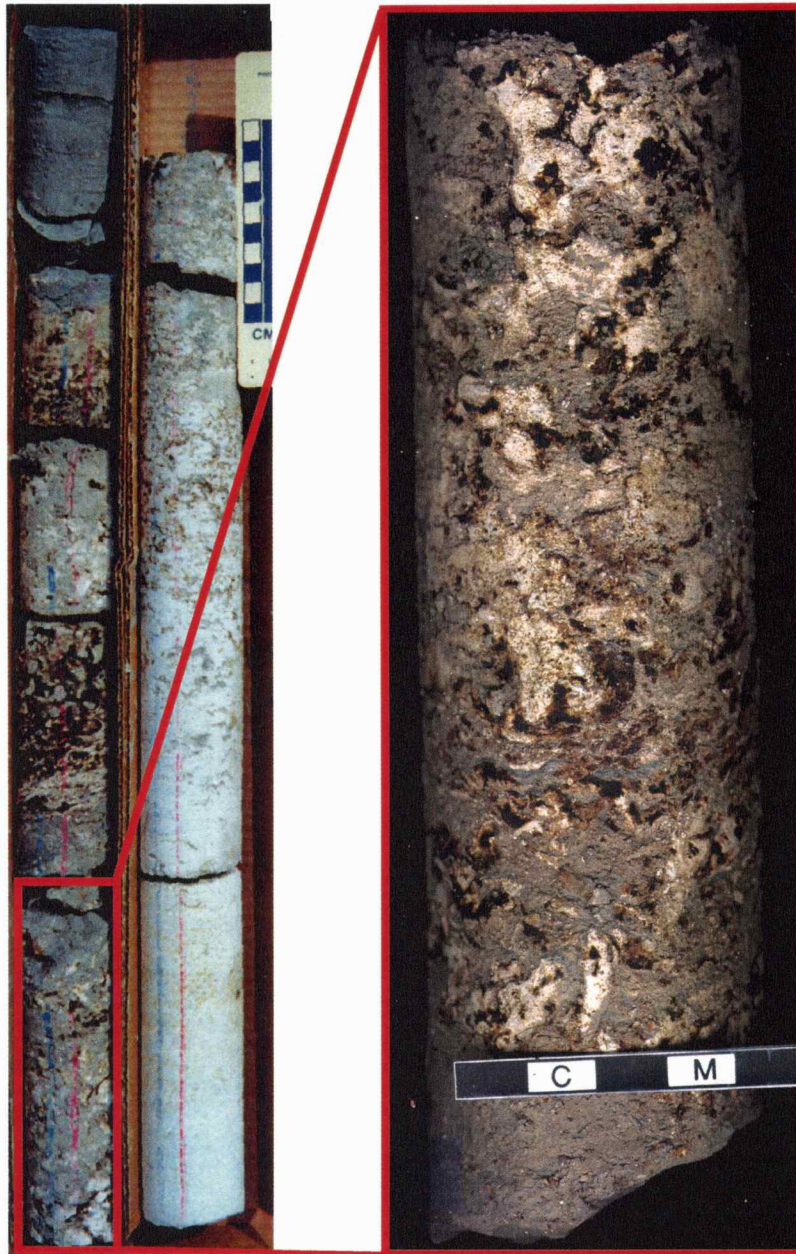


Figure 2.26. Photographs of the Elm Branch Shale from the RWD-2 core hole. Note the blocky nature of the mudstone, and the weathered appearance. Inset picture shows calcareous lumps within mudstone. Lumps are both caliche nodules and reworked clasts of the underlying Sniabar Limestone. Soil slickensides are also seen within within the blocky mudstone (scale = 5 cm).

Skeletal Wackestone Facies

Description

Observed sporadically in the upper portion of the Elm Branch Shale, the skeletal wackestone lithofacies is typically 5 to 10 cm thick. Medium light gray (N6) in appearance, the skeletal wackestone facies has abundant marine fossils. Identified fossils include brachiopods, crinoids, bryozoans, molluscs, gastropods and foraminifera. Skeletal grains are typically disarticulated, but relatively well-preserved (Figure 2.27). Wackestones are the dominant fabric. Matrix appears to be completely depositional micrite. No sedimentary structures were recognized.

Interpretation

Disarticulation of skeletal material is interpreted as being the result of bioturbation. The abundant marine skeletal material and the presence of depositional micrite are evidence that the skeletal wackestone lithofacies was deposited in a relatively normal-marine low-energy environment, below wave base.

Middle Creek Limestone

Phylloid Algal Wackestone/Packstone Facies

Description

The phylloid algal wackestone/packstone facies is composed of two beds of limestone 10 to 15 cm thick, sporadically separated by calcareous

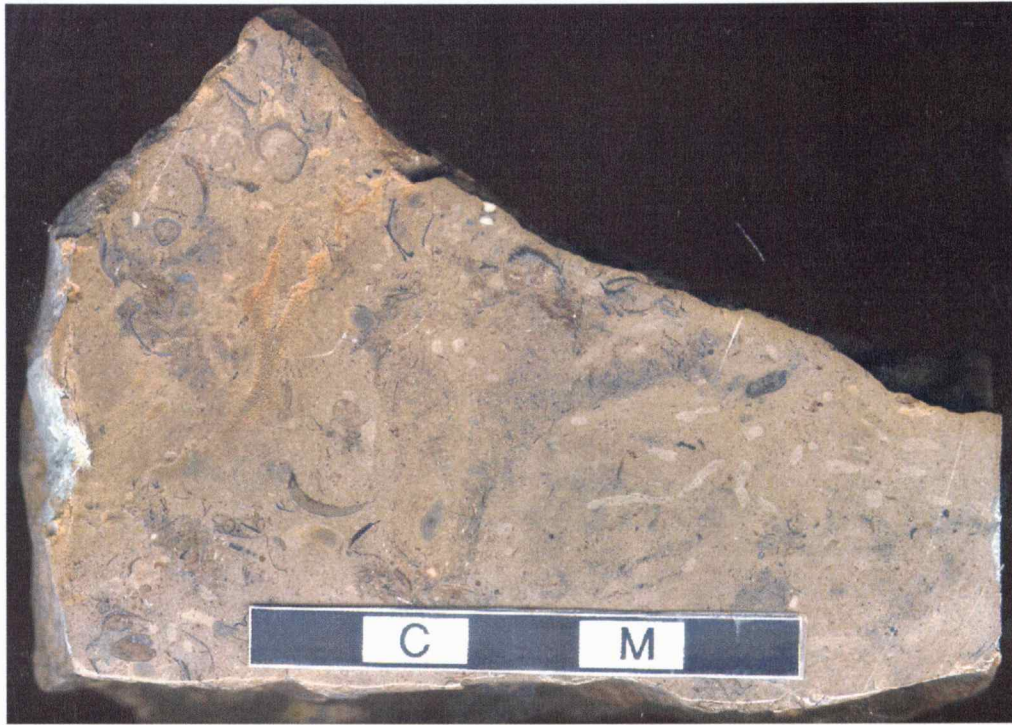


Figure 2.27. Polished slab of limestone from within the upper Elm Branch Shale. Note the marine fossils (scale = 5 cm; sample Raytown EB#1).

shale. Medium dark gray (N4) on fresh surfaces, the phylloid algal facies weathers a brownish gray (5YR 4/1) in outcrop. Skeletal material is abundant. Identified skeletal material consists of phylloid algal blades, brachiopods, crinoids, molluscs, gastropods, bryozoans, and foraminifera. Most bioclasts are disarticulated, but relatively well-preserved (Figure 2.28).

Fabric ranges from wackestones to packstones (Figure 2.28). In both fabrics, matrix appears to be depositional micrite.

Interpretation

The abundance of phylloid algal blades and the occurrence of diverse marine biota in a depositional micrite matrix are strong evidence for a low-energy, photic zone normal marine environment.

Calcareous Shale

Description

The calcareous shale facies is found interbedded with the phylloid algal wackestone/packstone lithofacies described above. The bed size is typically about 10 cm thick. Color is medium light gray (N6), but a little lighter than the surrounding limestones (Figure 2.28b). Marine fossils, including foraminifera, molluscs, and brachiopods are found within. This shale is calcareous.

Interpretation

Since the calcareous shale lithofacies is bounded by marine limestones, and contains marine fossils, it is interpreted as a marine

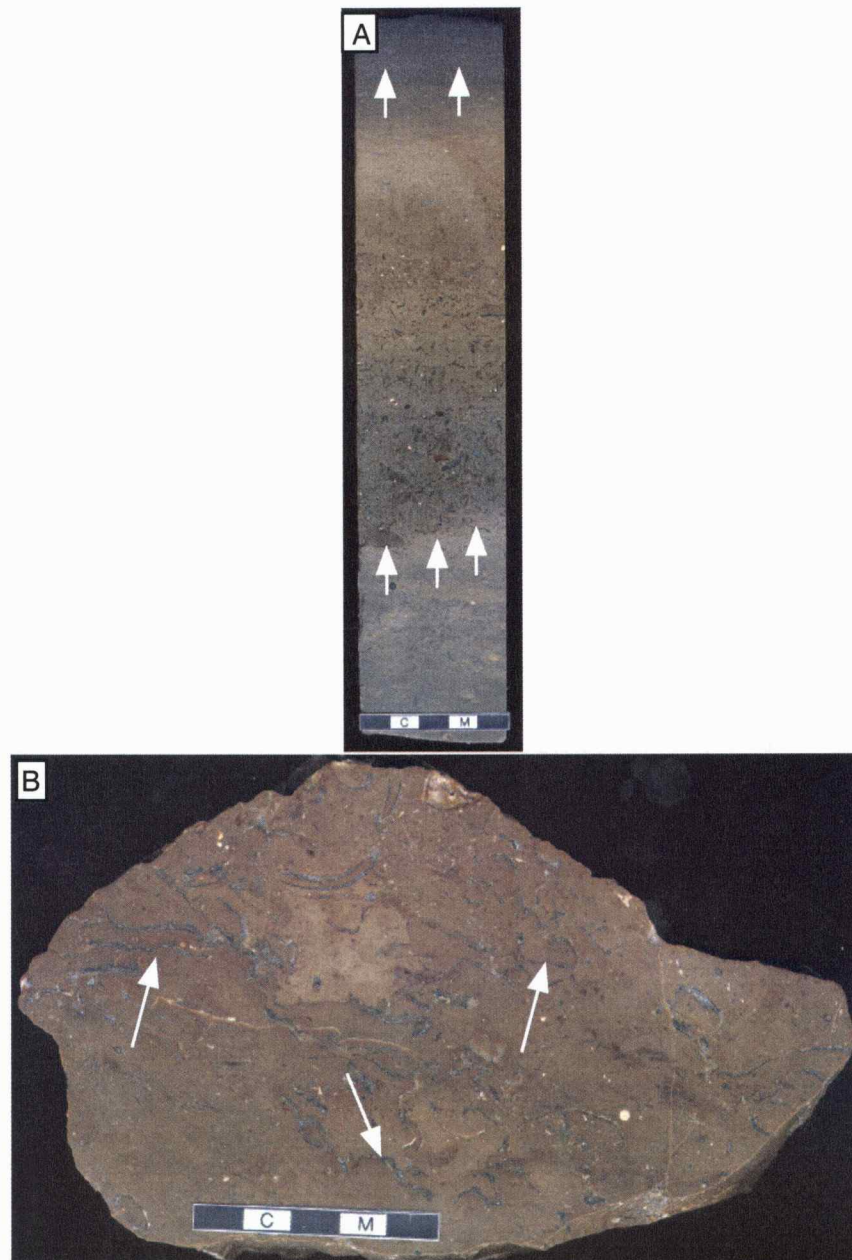


Figure 2.28. (A) Polished core section of the Middle Creek Limestone. Note the abundant marine fossils, and the arrows highlighting the sharp contact with the overlying Hushpuckney Shale and the underlying gray calcareous shale (scale = 5 cm; sample RWD-2 MC#23). (B) Polished slab of the Middle Creek Limestone. Arrows highlight the abundant and well-preserved phylloid algal blades (scale = 5 cm; sample Raytown MC#2).

environment deposit. Decreased oxygen levels might explain the fluctuation from limestone to calcareous shale. Other possibilities might include a combination of abnormal nutrient level, fluctuating salinity, and turbidity.

Hushpuckney Shale

Fissile Black Shale Facies

Description

A dark black color (N1), fissility and millimeter-scale laminae are diagnostic for the fissile black shale facies (Figure 2.29). Fossils were not observed, however, abundant planktonic fauna, such as conodonts and fish, have been described within the Hushpuckney Shale (Watney et al., 1989). Enrichment in metals such as molybdenum and uranium has been noted within this facies (Coveney et al., 1989). Phosphate nodules were observed.

Interpretation

Fissile black shales such as the Hushpuckney may be deposited in either shallow or deep-water environments. Examination of the fissile black shale facies in any one particular outcrop is probably not indicative of all of its depositional environments. However, the widespread occurrence of the fissile black shale facies, correlatable from eastern Kansas into eastern Colorado, and north into Iowa, suggests deposition in similar deep-water environments (Watney et al., 1989).

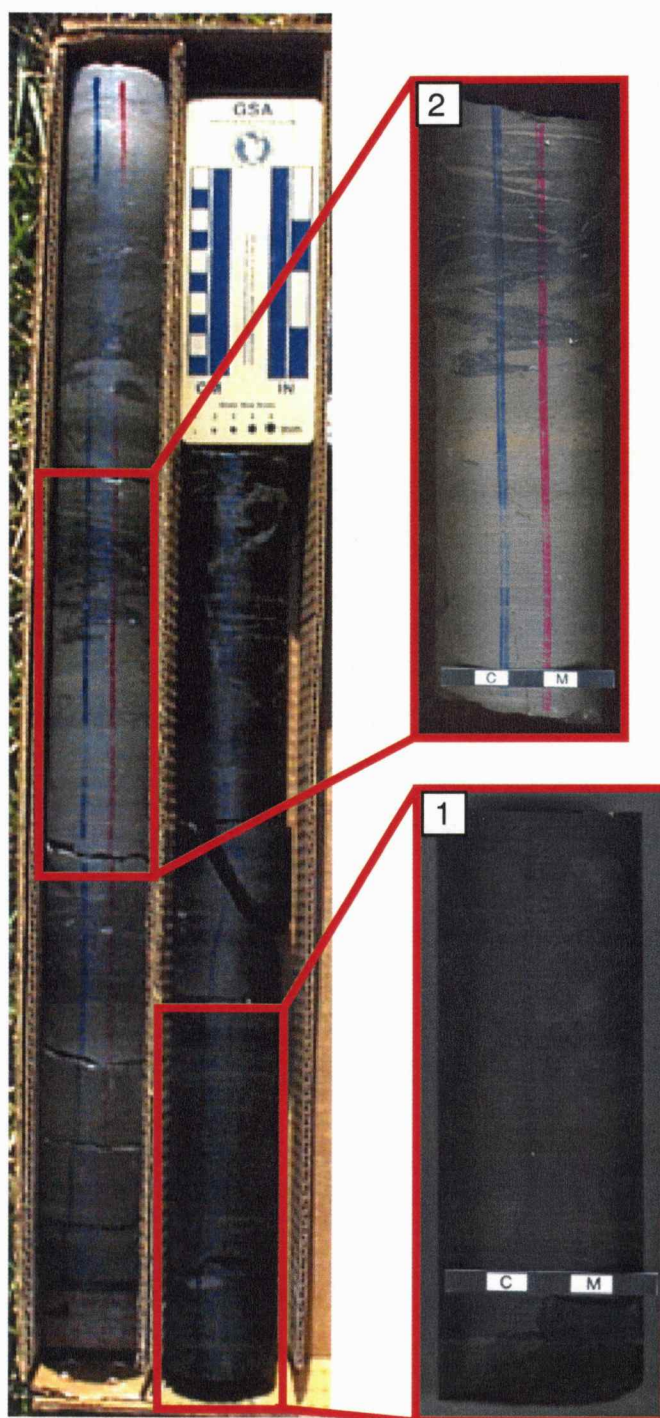


Figure 2.29. Core section of the Hushpuckney Shale from the RWD-2 well. Note the transition from 1) fissile black shale to 2) gray shale (scale = 5 cm;).

Total Organic Content (TOC) of the Hushpuckney Shale in Kansas has been measured as high as 20 percent (Jewett, 1994). High TOC is the cause of the black appearance of the fissile shale facies. High TOC, and the occurrence of phosphate, are all indicative of anoxic conditions. Without oxygen, the organic matter cannot be broken down. Various models for this anoxia have been proposed, including upwelling and pseudo estuarine circulation (Heckel, 1977), upwelling through Ekman's transport (Parrish, 1982), and thermocline (Rossignol-Strick, 1982; Heckel, 1985). The specific cause of the anoxia in the lower Hushpuckney Shale is not within the scope of this thesis.

Gray Shale Facies

Description

Diagnostic features of the gray shale lithofacies are marine fossils, medium gray color (N5), lack of laminations, and relation to the fissile black shale. Unlike the fissile black shale, the gray shale is not laminated, and has a more blocky appearance in outcrop. Rare marine fossils, such as brachiopods, occur within this facies. Near the upper portion, some burrowing is evident (Figure 2.29).

Interpretation

The gray shale facies is likely from an environment relatively low in oxygen, probably dysaerobic (0.3-1.0 O₂ ml/l), due to the paucity of body fossils and burrowing, except in the uppermost parts (Rhoads and Morse,

1971). The sharp contact with the Bethany Falls Limestone is probably related to seawater reaching sufficient oxygen levels to support abundant shelled bottom fauna.

**Chapter 3: Sequence Stratigraphy of the Elm Branch Shale, Middle
Creek Limestone, Hushpuckney Shale, and the Bethany Falls Limestone**

Chapter Three

Sequence Stratigraphic Nomenclature

Sequence stratigraphic nomenclature will be used to discuss the vertical, lateral and temporal relationships of the lithofacies in the Bethany Falls Limestone and related lithostratigraphic units. A complete review of sequence stratigraphy terminology is beyond the scope of this study. However, a brief summary of basic concepts and nomenclature will be provided.

The depositional sequence is considered to be the essential unit of sequence stratigraphy (Vail et al., 1991). Mitchum et al. (1977) defined the depositional sequence as a genetically related succession of strata bounded by unconformity surfaces and their correlative conformities. Galloway (1989), however, defined a genetic stratigraphic sequence as being bounded by surfaces that reflect the depositional hiatus that occurs during maximum marine flooding.

In the Lansing and Kansas City groups, reservoir facies are intimately associated with subaerial exposure (e.g. Heckel, 1983; Watney, 1984; Watney and French, 1988; Hoth et al., 1998). Within the Bethany Falls Limestone, subaerial exposure surfaces are well developed, and are distinctive. For these reasons, this study used evidence for a significant fall in relative sea-level to define sequence boundaries. Evidence included

pedogenic features on subtidal rock (e.g. paleo-karst, rhizoliths, calcrete, autoclastic brecciation) and lateral relationships of these surfaces of subaerial exposure.

Cyclothems have the same scale of formation, but have different bounding surfaces than depositional sequences (Figure 1.1). Duration of Upper Pennsylvanian cyclothems, and consequently depositional sequences, have typically been considered to be between 300 and 500 ka (Watney et al., 1989). However, Rasbury et al. (1998) used U-Pb ages of paleosols to constrain the duration of Upper Pennsylvanian cyclothems to 143 ± 64 ka.

The parasequence is defined as a relatively conformable succession of genetically related beds bounded by marine flooding surfaces, or their correlative conformities (Van Wagoner et al., 1988). Marine flooding surfaces are surfaces that separate younger from older strata, across which there is evidence for a significant increase in water depth (Van Wagoner et al., 1988). Parasequence sets are successions of genetically related parasequences that form a distinctive stacking pattern; they are typically bounded by major marine flooding surfaces (Van Wagoner et al., 1988). While marine flooding surfaces are recognized within the study area, section and core control was not sufficient to correlate individual beds, and consequently, parasequences and parasequence sets were not defined.

Identification of Sequences

Sequences are genetically related, relatively conformable successions of strata bounded by unconformities. Unconformities are surfaces along which there is evidence of significant subaerial exposure (Van Wagoner et al., 1988). Within the study area, there is evidence for three surfaces of significant subaerial exposure defining two sequences (Figure 3.1 *in packet*). Within the Bethany Falls Limestone there is evidence of subaerial exposure at the top of the formation and in the southern part of the study area an additional significant exposure surface is observed beneath the ooid grainstone subfacies. A surface of subaerial exposure between the Elm Branch Shale and the Sniabar Limestone has been previously noted (Watney et al., 1989; French and Watney, 1993; Watney and Heckel, 1994). These widespread surfaces of subaerial exposure at the top of the Sniabar Limestone and at the top and within the Bethany Falls Limestone are interpreted as sequence boundaries. Two sequences are recognized within the Bethany Falls Limestone and associated units (Figures 3.1, 3.2 *in packet*).

Sequence A

Sequence A is distributed over the entire field area and contains the Elm Branch Shale, the Middle Creek Limestone, the Hushpuckney Shale, and portions of the Bethany Falls Limestone (Figures 3.1, 3.2). A surface of subaerial exposure on the top of the Sniabar Limestone is the basal

boundary for Sequence A. The Sniabar Limestone shows extensive paleokarst features and pedogenic alteration superimposed on subtidal carbonates (Watney et al., 1989). From Raytown to RWD-2 #1, and from Raines #1 south to Farlinville, the upper boundary of Sequence A lies at the top of the Bethany Falls Limestone, at the contact between the oolite facies and the skeletal wackestone facies.

The surface of subaerial exposure at the top of the Bethany Falls Limestone is well defined by rhizoliths, karst tubes, distinctive color mottling and in situ brecciation occurring on subtidal rocks, features that occur throughout the field area. This evidence suggests that this upper surface of subaerial exposure is a widespread and significant episode of subaerial exposure. At Farlinville, a fenestral wackestone was found in lenses underlying the subtidal oolite facies, and overlying the subtidal skeletal wackestone facies. As discussed in Chapter Two, the fenestral wackestone is interpreted as being deposited in an upper intertidal to supratidal environment. Subsequent erosion in the oolite lithofacies environment resulted in patchy distribution of the fenestral wackestone at Farlinville (Stover 1992; this study). Fenestral wackestone is not found at any other section containing the oolite facies. However, it is likely that this fenestral wackestone was present at the contact between the skeletal wackestone and oolite, but subsequent submarine erosion destroyed the fenestral wackestone. Examination of Figures 3.1 and 3.2 illustrates the vertical and

lateral relationship of the fenestral wackestone observed at Farlinville to adjacent sections. The fenestral wackestone is laterally equivalent to subtidal rocks in all sections studied. The interrelationship suggests that relative sea-level fell significantly across the field area, subaerially exposing subtidal rocks located to the north of Farlinville (Figures 3.1, 3.2). I interpret the fenestral wackestone at Farlinville to represent a significant surface of subaerial exposure.

Sequence B

Sequence B, composed of portions of the upper Bethany Falls Limestone, is only found in the southern portion of the field area, from Raines #1 to Farlinville (Figures 3.1, 3.2).

An interpreted subaerial exposure surface characterized by fenestral wackestone at the top of sequence A is the basal boundary of sequence B. The upper boundary of sequence B is a surface of subaerial exposure found on top of the subtidal oolite lithofacies. This surface of subaerial exposure is defined by karst tubes, rhizoliths, and laminar calcretes observed occurring on subtidal rocks. A drop in relative sea-level occurred, exposing subtidal rock to subaerial processes, resulting in the formations of karst, rhizoliths, and laminar calcretes. These features, and the drop in relative sea-level they reflect, are evidence for a significant surface of subaerial exposure.

Stratigraphic Datum

A stratigraphic datum is used in cross sections to give an idea of depositional topography. Ideally, a stratigraphic datum should be a bed contemporaneously deposited in a similar environment and occurring on a relatively flat depositional surface. The use of an appropriate marker as a datum is extremely important to determine the original stratigraphic configuration (Tearpock and Boschke, 1991).

The biologically influenced nature of carbonates is unique among sediment sources due to the biota's ability to grow both vertically and laterally. Reefs and various bioherms are examples of the ability of carbonate producing organisms, and consequently carbonate deposits, to grow (e.g., Harbaugh, 1964; Heckel and Cocke, 1969; James, 1983). If bioherms are present within the Bethany Falls, the use of a datum above the Bethany Falls would tend to draw the edges of the mound up, distorting its true shape (i.e. any positive feature would appear as a channel-like feature). For this reason, the use of a datum underlying possible positive features is desirable.

The widespread nature of the Hushpuckney Shale, which can be correlated across the midcontinent, has been interpreted as occurring in a synchronous, relatively flat, deep-water environmental setting (Watney et al., 1989). Vail (1987) points out that relatively deep-water, such as the environment in which the Hushpuckney Shale was deposited, leads to

preservation of depositional topography. The Hushpuckney Shale represents one of the most significant glacial-eustatic inundations in the midcontinent (Heckel, 1986). The transition for the top of the Hushpuckney Shale to the base of the Bethany Falls Limestone likely represents changing oxygen levels, from dysaerobic to aerobic. Aerobic oxygen levels (≥ 1.0 ml O₂ per liter) allow deposition of calcareous, shelled fauna, as observed in the Bethany Falls Limestone (Rhoads and Morse, 1971). Since the Hushpuckney Shale was probably deposited isochronously across a relatively flat, deep-water environment, the top of the Hushpuckney Shale is used as stratigraphic datum for Figure 3.1. Using the top of the Hushpuckney Shale provides a consistent datum for mapping overlying depositional topography. Various authors however, suggest that the area had a slight south-southwest depositional dip (e.g., Hamblin, 1969, Watney et al., 1989). Subsidence of sediments was also occurring. For these reasons, it should be emphasized that the depositional topography shown in Figure 3.1 is interpreted depositional topography relative to the datum and is not exact depositional topography.

An alternative marker near the base of the Bethany Falls Limestone might provide a useful stratigraphic datum. Examination of measured sections and core reveals the phylloid algal packstone is found through the entire field area, near the base of the Bethany Falls Limestone. In the southern portion of the field area, a skeletal packstone underlies the phylloid

algal packstone. I have interpreted the skeletal packstone as representing deposition below the photic limits for significant growth of phylloid algae, while the phylloid algal packstone was deposited in the photic zone, within the limits of the photic zone ideal for phylloid algae production.

The assumption that the photic limit was in the same location throughout the field area is essential for using the base of the phylloid algal packstone as a datum. If water conditions were similar in terms of sunlight penetration, then the base of the photic zone would be of equal depth throughout the field area and provide another very useful stratigraphic datum for understanding depositional patterns (Figure 3.2).

Of the two datums used, I prefer the use of the base of the phylloid algal facies to the use of the top of the Hushpuckney Shale. The use of the top of the Hushpuckney Shale is a lithostratigraphic datum, and does not reflect a consistent shift in environmental conditions. The transition for dysaerobic (gray shale deposition) to aerobic (limestone deposition) is not well defined by the lithostratigraphy. This is evidenced by the observation of extraneous shale units within the skeletal packstone in the southern portion of the field area (Figure 3.1). The use of the base of the phylloid algal packstone appears to reflect a more consistent change in environmental conditions, from light penetration being inadequate for phylloid algal growth (skeletal packstone) to light penetration supporting significant phylloid algal growth (phylloid algal packstone).

Sequence A

Elm Branch Shale Interval

Description

Within the study area, a sequence boundary separates the subaerially exposed Sniabar Limestone and the blocky mudstone of the Elm Branch Shale (Figures 3.1, 3.2: Surface A). Surface A is the basal boundary of the Elm Branch Shale interval. Moving up section, the non-marine blocky mudstone of the Elm Branch Shale is separated from a marine limestone in the upper Elm Branch Shale or from marine limestones in the Middle Creek Limestone by an interpreted marine flooding surface (Figures 3.1, 3.2: Surface B; Features 1, 2). The transition from non-marine mudstones of the Elm Branch Shale to marine skeletal wackestones and phylloid algal packstones represents an abrupt increase in relative sea-level. This marine flooding surface is interpreted as a transgressive surface and the upper boundary on the Elm Branch Shale interval (Figures 3.1, 3.2: Surface B).

Lithologies remain relatively consistent across the field area. The Elm Branch Shale is primarily a blocky mudstone. In some locations, however, a thin skeletal wackestone is present at the upper portion of the Elm Branch Shale, which is often capped by calcareous shale (Figures 3.1, 3.2: Feature 1).

Interpretation

The Elm Branch Shale interval was deposited following a fall in relative sea-level. The mudstone in the Elm Branch Shale is a paleosol. As sea level fell, conditions changed from the open-marine environment of the subtidal Sniabar Limestone to the non-marine environment of the lower Elm Branch Shale (Figure 3.3). Fluvial and eolian processes provided sediments that were modified by soil processes in this paleosol. An abrupt rise in relative sea-level formed the transgressive marine flooding surface (Figures 3.1, 3.2: Surface B).

Lower Hushpuckney Shale Interval

Description

Portions of the Elm Branch Shale, the entire Middle Creek Limestone and portions of the Hushpuckney Shale are interpreted as parts of the lower Hushpuckney Shale interval. The transgressive marine flooding surface is the basal boundary of the lower Hushpuckney Shale interval, and is delineated based on using lithologies that reflect an abrupt increase in relative sea-level (Figures 3.1, 3.2: Surface B). Lithologies reflecting an abrupt increase in relative sea-level are marine limestones of the upper Elm Branch Shale and Middle Creek Limestone that overlie the paleosols of the Elm Branch Shale. The maximum flooding surface, the upper boundary of the lower Hushpuckney Shale interval, was picked on the highest gamma ray values in the Hushpuckney Shale (Figures 3.1, 3.2: Surface C). High gamma ray

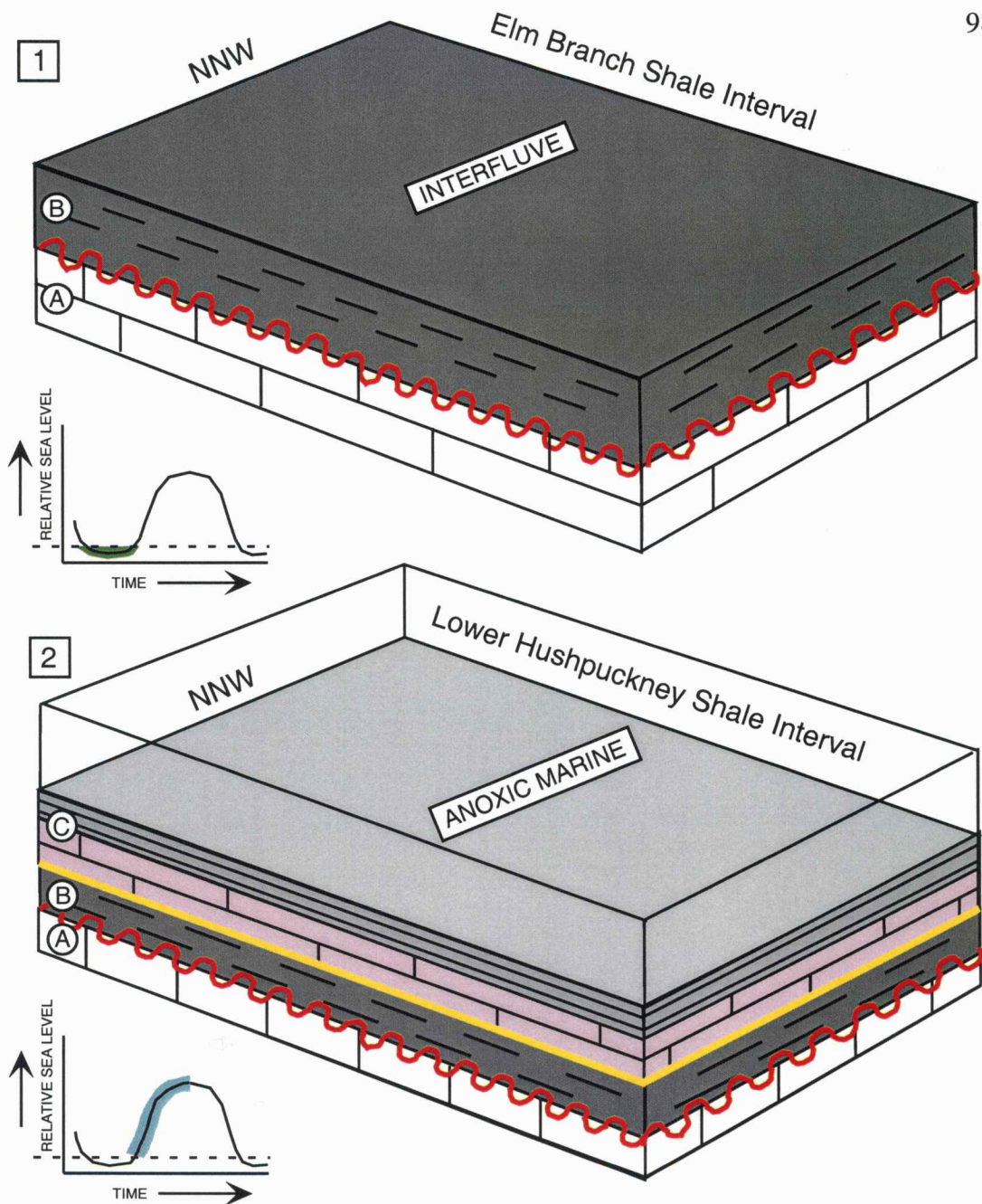


Figure 3.3. Generalized depositional model for Sequence A. For legend, refer to Figure 3.1. Circled letters are A) Sniabar Limestone, B) Elm Branch Shale, C) limestones and shales in the Elm Branch Shale, Middle Creek Limestone and the Hushpuckney Shale. Unfilled box on top indicates relative water depth

values provided a consistent marker, and appear related to depositional condensation during maximum flooding.

The Middle Creek Limestone has a consistent character of a phylloid algal packstone throughout the lower Hushpuckney Shale interval. In some locations, thin calcareous shale separates beds of the packstone (Figures 3.1, 3.2: Feature 3). The lower portion of the Hushpuckney Shale is consistently black, fissile shale with phosphate nodules throughout the lower Hushpuckney Shale interval.

Interpretation

The abrupt change from non-marine paleosols to phylloid algal packstone and marine conditions reflects a period of rapid relative sea-level rise. Moving up section from the open marine packstone, the razor sharp contact with a highly radioactive black fissile shale reflects rapidly deepening of water conditions, and a change in oxygen levels from normal marine to anoxic (Figures 2.25; 3.1, 3.2: Feature 4; 3.3; Rhoads and Morse, 1971).

High radioactivity within the lower Hushpuckney Shale is the result of condensation of radioactive wind-blown dust from the granitic craton, and concentration of radioactive elements in phosphate nodules and organic material (high Total Organic Carbon - TOC). Anoxic bottom water conditions precluded the oxidation of organic matter, preserving the condensed accumulations of organic remains, keeping the uranium in a reduced, immobile state in organic remains. The surface of highest radioactivity is

interpreted as the surface of maximum inundation, and maximum condensation of radioactive cratonic dust, organic material, and preservation of phosphate (Figures 3.1, 3.2: Surface C).

Bethany Falls Limestone Interval

Description

Portions of the Hushpuckney Shale and the Bethany Falls Limestone are included in the Bethany Falls Limestone interval. In the northern portion of the field area, the Bethany Falls Limestone interval includes the entire Bethany Falls Limestone to the contact with the Galesburg Shale (Figures 3.1, 3.2). In the southern portion, however, the Bethany Falls Limestone interval of sequence A is interpreted to extend about two thirds of the way through the Bethany Falls Limestone (Figures 3.1, 3.2).

The base of the Bethany Falls Limestone interval is bounded by the maximum flooding surface, and the top is defined by a sequence boundary (Figures 3.1, 3.2: Surfaces C; D, E). The lower boundary was picked on the highest gamma ray count within the Hushpuckney Shale (i.e. maximum flooding surface). In the north, the upper sequence boundary is placed at a surface of subaerial exposure, based on abundant evidence (e.g. rhizoliths, color mottling, and autobrecciation). In the southern part of the study area, the fenestral wackestone lithofacies is interpreted as being indicative of subaerial exposure, followed by submarine erosion. The contact between the

oolite and skeletal wackestone lithofacies is considered one of significant subaerial exposure (Figures 3.1, 3.2: Surfaces D, E).

The Hushpuckney Shale within the Bethany Falls Limestone interval is black fissile shale that grades up section into gray calcareous shale. The lithologies present in the Bethany Falls Limestone include skeletal packstone, phylloid algal packstone, skeletal wackestone, skeletal grainstone, and in the upper parts a lime mudstone (Figures 3.1, 3.2). Thicknesses of the lithofacies vary within the Bethany Falls Limestone. Examination of Figure 3.1 shows a thickening of the phylloid algal packstone to the south, until the interpreted contact with the pinchout of the underlying skeletal packstone is reached (Figure 3.1: Feature 8). The skeletal packstone was observed in the southern portion of the field area and is interbedded with calcareous shale that is similar to the calcareous shale observed in the uppermost Hushpuckney Shale.

In Figure 3.2, the phylloid algal packstone thickens into a mound or bank like geometry towards the Raines #1 core. Overlying sediments thin over this mound-like shape, preserving the topography up section. Moving south from the Raines #1 borehole, the skeletal packstone underlying the phylloid algal packstone interfingers with calcareous shale similar to shale observed in the upper Hushpuckney Shale, and appears to flank and support phylloid algal packstone (Figure 3.2: Features 6, 7, and 8).

The skeletal wackestone has a relatively consistent thickness in the northern portion. Moving to the south, however, the skeletal wackestone thicken where the phylloid algal and skeletal packstones are thinner, and thin where these packstones are thicker (Figures 3.1, 3.2: Features 9, 10). The lime mudstone is restricted to the northern half of the field area. (Figure 3.1). Inclusion of the pedogenically altered lime mudstone into the lime mudstone facies results in a relatively constant thickness across the northern part of the study area (Figures 3.1, 3.2: Features 11, 13). However, in the extreme northern portion of the field area, the lime mudstone tends to thicken where the underlying skeletal wackestone is thinner (Figures 3.1, 3.2: Feature 11). The skeletal grainstone is only found in two sections in the northern area (Figures 3.1, 3.2: Feature 12). Overlying the lime mudstone is pedogenically altered lime mudstone. The autobrecciated lime mudstone facies was only observed in the northern half of the field area and thins towards the north (Figures 3.1, 3.2: Feature 13).

Interpretation

During deposition of the Bethany Falls Limestone interval sediments, relative sea level was falling. The highest gamma ray values within the black fissile shale of the lower Hushpuckney Shale are interpreted as representing maximum flooding. As relative sea level fell, oxygen levels within the basin changed from anoxic to dysoxic allowing deposition of a calcareous shale with lower gamma ray values (Figures 3.1, 3.2: Feature 5). Whatever the

cause of the anoxia, relative sea level was falling at this point, illustrated by the widespread correlatable nature of these facies (Watney et al, 1989). The contact between the calcareous shale of the Hushpuckney, and the overlying carbonates of the Bethany Falls Limestone reflects a further increase in oxygen levels to oxic conditions that would support a shelly bottom fauna and initiation of limestone accumulation (Figure 3.1; Feature 6). The Hushpuckney Shale has been interpreted to represent up to 100 to 200 m of water depth (e.g. Heckel, 1977, Heckel 1980).

In the southern half of the field area, the first limestone produced was a skeletal packstone. This skeletal packstone is characterized by absence of phylloid algae. Phylloid algae are dependent on sunlight for photosynthesis, and have to be within their photic limits. Modern photosynthetic algae, which serve as an analog to the phylloid algae found within the Bethany Falls Limestone, thrive in 20 to 30 m of water, but can grow as deep as 70 to 100 m (Phipps and Roberts, 1988). However, at these deep depths, phylloid algal production is greatly decreased. It should be emphasized that water depth under 30 m is the ideal depth for phylloid algal production.

Local conditions, such as sediment input, have an effect on the depth of effective sunlight illumination. Moving vertically within the section, the skeletal packstone overlies interpreted deep-water dysoxic marine shale (Figures 3.1, 3.2: Feature 6). Moving laterally, the skeletal packstone pinches out into a phylloid algal packstone (Figure 3.1: Feature 8). Lateral

and vertical relationships of this skeletal packstone are evidence that water depth played a significant role in photic zone location (Figure 3.4). The skeletal packstone lithofacies has interbedded calcareous shale beds that reflect either changing oxygen levels within the environment, or pulses of increased terrigenous sedimentation. Causes for changing oxygen levels and increased sediment influx could be due to changes in eustatic sea level, climate, or local tectonic activity affecting terrigenous sources to the south. The transition from the Hushpuckney Shale, which might reflect deposition in water depths around 100 m, to a phylloid algal packstone, which reflects deposition in under 30 m depth, represents a significant fall in relative sea-level.

With the deposition of photic zone phylloid algal packstones to the north, and relatively deeper water skeletal packstone to the south, carbonate production was established (Figure 3.3). Without internal time lines, it is impossible to say if these two lithofacies are time equivalent. However, it is reasonable that as relative sea-level fell, deposition of the lower phylloid algal packstone and skeletal packstone facies was synchronous. Changes in relative sea level brought the southern area into the photic zone, and phylloid algal production was initiated over the entire field area (Figures 3.1, 3.2: Feature 8). These phylloid algal packstones contain depositional micrite, which indicates a low energy environment, probably below wave base. Wave base for epeiric seas has been estimated at between 10 to 20 meters

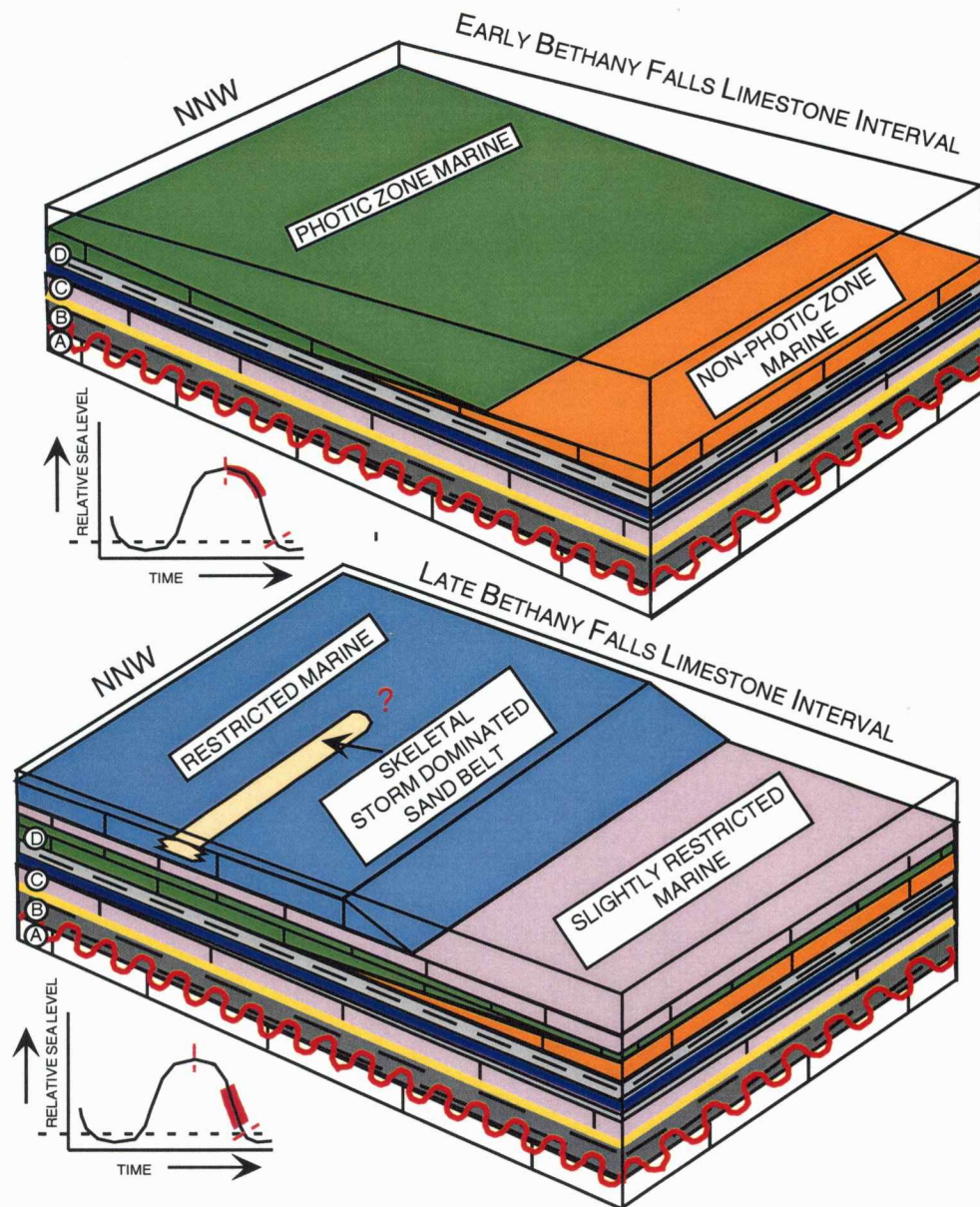


Figure 3.4. Generalized depositional model illustrating development with falling relative sea level, for Sequence A. For legend, refer to Figure 3.1. Circled letters are A) Sniabar Limestone, B) Elm Branch Shale, C) limestones and shales in the Elm Branch Shale, Middle Creek Limestone and the Hushpuckney Shale and D) shales and limestones within the Hushpuckney Shale and Bethany Falls Limestone. Unfilled box on top indicates relative water depth.

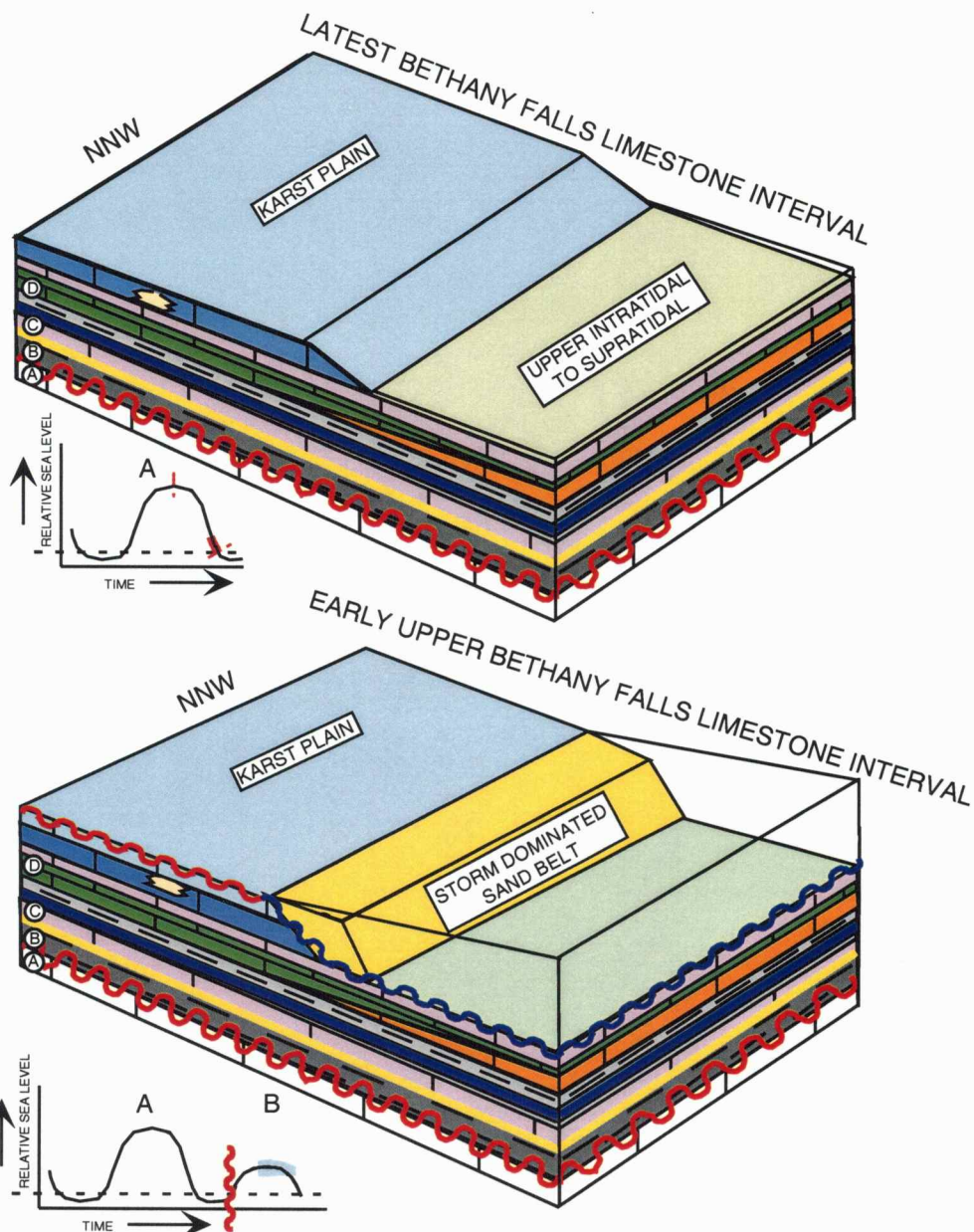


Figure 3.5. This figure illustrates the latest Bethany Falls Limestone interval of sequence A and the early upper Bethany Falls Limestone interval of Sequence B. For legend, refer to Figure 3.1. Circled letters are A) Sniabar Limestone, B) Elm Branch Shale, C) limestones and shales in the Elm Branch Shale and Middle Creek Limestone and D) fissile black shales within the Hushpuckney Shale and E) shales and limestones within the Hushpuckney Shale and Bethany Falls Limestone and F) limestones within the Bethany Falls Limestone. Unfilled box on top indicates relative water depth.

(Brenner, 1980). The phylloid algal packstone was probably deposited between 20 and 30 meters, below wave base, and within the photic zone.

Figure 3.2, using the base of the phylloid algal packstone as a datum, presents a slightly different depositional topography. In Figure 3.2, as opposed to Figure 3.1, the skeletal packstone appears to act as a base for interpreted phylloid algal mound or bank development (Figure 3.2: Features 6 and 8). Based on the topography presented in Figure 3.2, I interpret the skeletal packstones as representing bases to the mound form seen in Raines #1. Skeletal packstones act as foundations to phylloid algal deposits, reflecting deposition in non-photoc zone conditions until relative sea level changed enough to bring the sea floor into the photic zone. The interpreted phylloid algal mound in the Raines #1 also appears to occupy a minor local high or local break in the depositional shelf.

Carbonate production was now well established across the field area. The transition from the phylloid algal packstone to the skeletal wackestone probably indicates very slight restriction. Both environments were probably relatively normal marine, but the decrease in abundance of biota suggests a slight restriction (Figures 3.1, 3.2: Feature 9). As relative sea level dropped, circulation of marine waters probably decreased. Physiographic barriers are not necessary for restriction in epeiric seas. As relative sea level dropped, the broad expanse of water damped out tidal and wave energy (Enos, 1983).

Restriction, caused by dropping relative sea level, could result in abnormal salinities, depleted nutrients, and possibly temperature extremes (Enos, 1983). As restriction increased, deposition of the lime mudstone lithofacies of the Bethany Falls Limestone increased (Figures 3.1, 3.2: Feature 11; 3.4). The lime mudstone lithofacies, with its sparse biota, extensive burrowing, and abundance of depositional mud, probably reflects these restricted conditions.

The skeletal packstone found at Lake Jacomo North and South is interpreted as an isolated storm dominated carbonate belt (Figures 3.1, 3.2: Feature 12; 3.4). Cross beds, orientation of skeletal material, and the lack of mud indicate a high-energy environment. This high-energy marine sand belt might have occurred as a result of localized focusing of tidal flows. Tidal flows would provide increased energy levels to winnow mud. Contributing factors for this focus might be due to an interaction of antecedent topography and relative sea level change. Both Lake Jacomo North and South have thicker sections of the Bethany Falls Limestone than adjacent sections (Figures 3.1 and 3.2). This could reflect subtle paleo-topography, which, in combination with dropping relative sea level, focused tidal flows, and resulted in deposition of a high-energy storm dominated marine sand belt (Figures 3.1; 3.2; 3.4). However, outcrop data is limited, and without detailed knowledge of the shelf configuration, which due to erosion is not possible, the specific depositional environment remains conjectural.

As relative sea level continued dropping, deposition of restricted lime mudstones resumed, as energy levels dissipated (Figures 3.1, 3.2: Feature 13). Falling eustatic sea level resulted in subaerial exposure throughout the field area. This subaerial exposure surface is characterized by in situ brecciation, rhizoliths, color mottling and karst tubes in the north. In the southern field area, the upper intertidal to supratidal fenestral wackestones were being deposited (Figures 3.1, 3.2: Surface D).

Sequence B

Upper Bethany Falls Limestone Interval

Description

A marine flooding surface is coincident with the basal boundary of Sequence B (Figures 3.1, 3.2: Surface E). The upper Bethany Falls Limestone interval is composed entirely of units assigned to the Bethany Falls Limestone. The oolite lithofacies has varying thickness throughout the field area, and a lime mudstone facies is restricted to the area from Raines #1 south to 383rd Street (Figures 3.1, 3.2: Feature 15).

The upper surface of the Bethany Falls Limestone assigned to sequence B has evidence for significant subaerial exposure (e.g. karst tubes, rhizoliths, color mottling and laminated calcretes). The upper surface of the upper Bethany Falls Limestone interval of the Bethany Falls Limestone is interpreted as a sequence boundary.

Interpretation

Following the relative sea level fall that resulted in the sequence boundary capping Sequence A, relative sea level rose. This rise is represented by marine carbonates lying on top of subaerially exposed carbonates (Figures 3.1, 3.2: Surface E).

The oolite lithofacies represents high-energy storm dominated marine sand belts that appear related to highs or breaks in the shelf (Figures 3.1, 3.2: Feature 14). These paleo-topographic highs might have provided a focus for tidal currents, resulting in high-energy environments. The northern oolitic storm dominated sand belt probably reflects the oldest oolite deposited and preserved during sequence B (Figures 3.1, 3.2: Feature 14, 3.5). This sand belt reflects deposition during a highstand in the formation of sequence B. As relative sea-level fell, a younger storm dominated sand belt formed (Figures 3.1, 3.2: Feature 16). This sand belt appears on a subtle topographic high. This topographic high could have provided a focus for current and tidal energy. Separating these marine sand belts is a restricted lime mudstone. This lime mudstone is interpreted to represent a restricted, lagoon type environment behind the storm dominated sand belt illustrated by Feature 16 (Figures 3.1, 3.2: Feature 15, 3.6).

Following deposition of the high-energy upper Bethany Falls Limestone interval sediments, relative sea level dropped. This apparently rapid drop in combination with the extreme updip shelf position did not allow

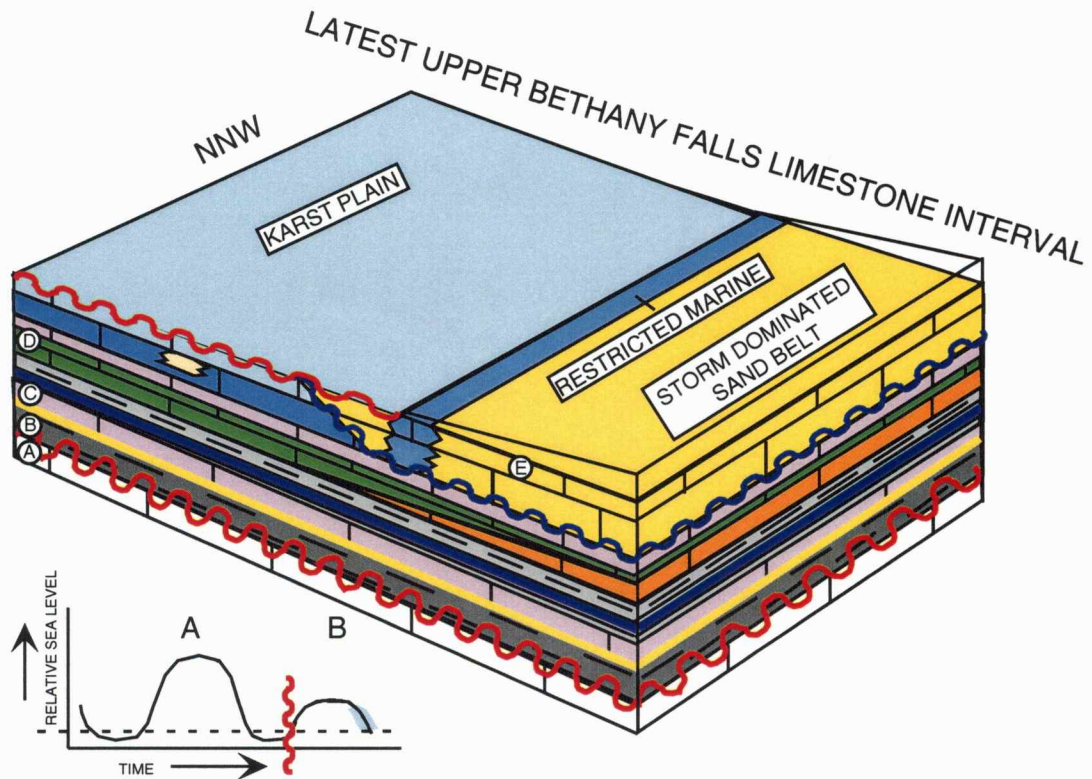


Figure 3.6. This figure illustrates the latest upper Bethany Falls Limestone interval of Sequence B. For legend, refer to Figure 3.1. Circled letters are A) Sniabar Limestone, B) Elm Branch Shale, C) limestones and shales in the Elm Branch Shale and Middle Creek Limestone and D) fissile black shales within the Hushpuckney Shale and E) shales and limestones within the Hushpuckney Shale and Bethany Falls Limestone and F) limestones within the Bethany Falls Limestone. Unfilled box on top indicates relative water depth.

for accumulation of upper intertidal to supratidal restricted lime mudstone.

The sediments of sequence B were exposed to subaerial processes.

Rhizoliths, karst tubes, laminar calcretes and color mottling are evidence of this eustatic sea level drop.

To the south of this field area Watney et al. (1989) has recognized an extra shale and limestone couplet overlying the Bethany Falls Limestone, and underlying the Galesburg Shale. This extra shale and limestone have been classified as the Ladore Shale and the Mound Valley Limestone (Watney et al., 1989, and Watney and Heckel, 1994). The Ladore Shale has been described as a fine-grained marine clastic shale, and interpreted as representing a lowstand clastic wedge, derived from the Ouachita Mountains to the south (Watney et al., 1989). The clastic Ladore Shale directly overlies the Bethany Falls Limestone.

The Mound Valley Limestone has been described as consisting of a skeletal wackestone and oolitic grainstone, and interpreted as representing marine flooding of the underlying Ladore Shale. Figure 3.7 illustrates the vertical and lateral relationships of the Ladore Shale and Mound Valley Limestone to the Bethany Falls Limestone. It is likely that the upper Bethany Falls Interval of sequence B and the Ladore Shale and Mound Valley Limestone are in the same sequence, based upon these lateral and vertical relationships (Figure 3.7).

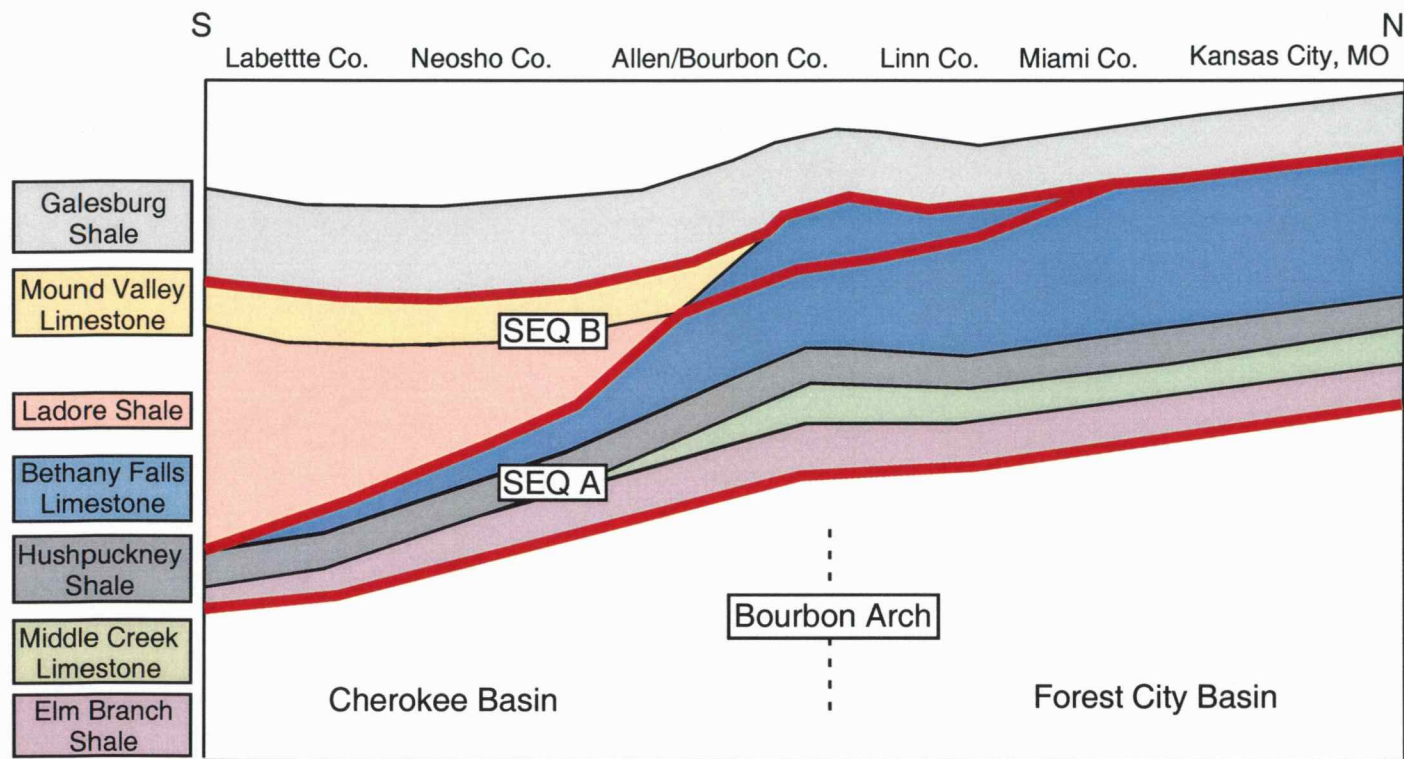


Figure 3.7. Diagrammatic south to north stratigraphic cross section of Missourian strata, illustrating relationships of the Ladore Shale, the Mound Valley Limestone, and the Bethany Falls Limestone. The Ladore Shale and Mound Valley Limestone have been recognized to the south of Linn County, and have tentatively been included as systems tracts within sequence B (defined in this study). Red lines are sequence boundaries. Cross section not to scale (Modified from Watney et al., 1989).

Casual Mechanisms for Sequence Development

Various allogenic and autogenic causes have been proposed for Upper Pennsylvanian cyclothemic strata. Numerous studies have documented extensive upper Paleozoic glacial deposits on Gondwana (e.g., Wanless and Sheperd, 1936; Heckel, 1977; Crowell, 1978; Heckel, 1986). These studies established that the upper Paleozoic was a time of large-scale continental glaciation on Gondwana and associated glacial-eustasy. Pleistocene glaciation and associated eustatic sea-level changes have served as an analogue to the upper Paleozoic.

Using the pinning-point method of Goldstein and Franseen (1995), Soreghan and Siles (1999) have demonstrated amplitudes of at least 80 m and probably in excess of 100 m for Late Pennsylvanian glacioeustasy. The widespread and correlatable nature of Late Pennsylvanian cyclothemic deposits over the midcontinent are cited as evidence of allogenic controls (Watney et al., 1989). The widespread nature, late Paleozoic glaciation, and amplitudes of over 80 m are evidence for glacial-eustasy being an important control on sequence development. Also, localized events and features such as tectonic disturbances and subtle topographic differences probably contribute to the nature of Upper Pennsylvanian sequences.

Chapter 4: Conclusions

Chapter Four

Conclusions

Lansing and Kansas City Group limestones are important petroleum reservoirs over a large area in central and western Kansas (Carr, 1995). Many of the reservoirs in the Kansas City Group are located in isolated grainstones with oomoldic porosity. In the Lansing and Kansas City groups, formation of oomoldic porosity is related to adjacent subaerial exposure surfaces (French and Watney, 1993). In the midcontinent, recognition and mapping of subaerial exposure surfaces can be improved by replacing the traditional cyclothem stratigraphy with a sequence stratigraphic approach. A high-resolution sequence stratigraphic model of the Bethany Falls Limestone was developed to recognize and map subaerial exposures and to improve understanding of the interaction of factors that affect deposition of Kansas City Group carbonates in the midcontinent. Detailed study of Upper Pennsylvanian outcrops, cores, thin sections, polished slabs, and spectral gamma-ray profiles of the Bethany Falls Limestone were used to establish lithofacies, and to infer depositional environments and the genesis of sequences present.

The Bethany Falls Limestone consists of eight lithofacies. The skeletal packstone, phylloid algal packstone and mottled skeletal wackestone lithofacies were deposited in open marine environments, probably below

wave base. The skeletal grainstone and oolite lithofacies were deposited in a high-energy relatively shallow environment. The lime mudstone lithofacies was deposited in a restricted, shallow marine environment. The fenestral wackestone was deposited in an intertidal to supratidal environment. The paleosol lithofacies is a pedogenic overprint on the lime mudstone and oolite lithofacies. The pedogenic features in the paleosol lithofacies are crucial for recognition of surfaces of subaerial exposure, which might be sequence boundaries. However, distinct lithologic and petrographic evidence of subaerial exposure is often absent.

Within the study area, from the top of the Sniabar Limestone, to the base of the Galesburg Shale, two sequences were observed. Three sequence boundaries, two marine flooding surfaces, and one maximum flooding surface were observed. The sequence boundaries and flooding surfaces resulted from changes in relative sea level.

Paleosols observed within the Elm Branch Shale indicate a subaerial depositional environment. The normal marine phylloid algal packstones of the Middle Creek Limestone overly the Elm Branch Shale, providing evidence for a relatively rapid rise in relative sea-level. Anoxic and dysoxic deep-water shales of the Hushpuckney Shale overlie the Middle Creek Limestone, providing evidence for a further increase in relative sea-level, perhaps up to 100 to 200 m of total depth. Normal marine, relatively shallow water phylloid algal packstones of the Bethany Falls Limestone lie on top of dysoxic shales

of the Hushpuckney Shale, indicating a significant fall in relative sea-level, perhaps up to 80 m. Shoaling trends were observed continuing up through the Bethany Falls Limestone, until a significant surface of subaerial exposure was observed, terminating sequence A. An additional sequence was observed within the southern portion of the field area. Subtidal rocks of sequence B lie on top of the surface of subaerial exposure bounding sequence A, providing evidence for a rise in relative sea-level. The lower boundary of sequence B is a coincident marine flooding surface and sequence boundary. An extensive surface of subaerial exposure covers subtidal rocks of sequence B, providing an upper sequence boundary.

Both the lateral and vertical variability observed in the Elm Branch Shale, Middle Creek Limestone, Hushpuckney Shale, and Bethany Falls Limestone results from the interaction of changing eustatic sea level, relative sea level, and antecedent topography. Understanding of the lateral and vertical changes in depositional facies can be improved through careful selection of a stratigraphic datum related to presumed regional events. Eustatic sea level changes acted on a regional basis to drive large-scale changes in deposition. Events such as relatively deep marine anoxic shales and subaerial exposure appear to be synchronous over large regions and support eustatic influence. Relatively deep-water skeletal packstones overlain by relatively shallow water phylloid algal packstones illustrates the vertical variations caused by changes in relative sea level. Antecedent

topography provided foci for tidal energy, facilitating deposition of high-energy grainstones. Lateral variations, illustrated by pinchout of relatively deep-water skeletal packstones into relatively shallow water phylloid algal packstones, are likely caused by variation in antecedent topography.

Long noted anomalies such as “fortuitous” limestones within formations, subaerial exposure within a sequence, and shoaling trends should not be ignored. Shoaling and subaerial exposure in the upper Bethany Falls Limestone is interpreted as the positionally updip extent of an additional sequence (sequence B). Sequence B appears related to the enigmatic “Mound Valley Limestone” and exposure event described in the counties immediately to the south of the study area. Sequence B of the Bethany Falls Limestone may be the extreme updip shelf equivalent to the Ladore Shale and Mound Valley Limestone.

References

- Arakel, A.V., and McConchie, D., 1982, Classification and genesis of calcrete and gypsite lithofacies in paleodrainage systems of inland Australia and their relationship to carnotite mineralization; *Journal of Sedimentary Petrology*, v. 52, p. 1149-1170.
- Ball, M.M., 1967, Carbonate sand bodies of Florida and the Bahamas; *Journal of Sedimentary Petrology*, v. 37, p. 556-591.
- Brenner, R.L., 1980, Construction of process-response models for ancient epicontinental seaway depositional systems using partial analogs; *American Association of Petroleum Geologists Bulletin*, v. 64, p. 1223-1244.
- Broadhead, G.C., 1868, Coal measures from northwestern corner of Missouri to Glasgow, Howard County, Missouri, in *St. Louis Academy of Science, Transactions*, v. 2, p. 320.
- Brown, L.F., and Fisher, W.L., 1977, Seismic-stratigraphic interpretation of depositional systems: examples from Brazilian rift and pull-apart basin, in C.E. Payton, ed., *Seismic stratigraphy – applications to hydrocarbon exploration*, *American Association of Petroleum Geologists Memoir 26*, p. 213-248.
- Budd, D.A., Saller, A.H., and Harris, P.M., 1995, Unconformities and porosity in carbonate strata; *American Association of Petroleum Geologists Memoir 63*, p. vii-xii.
- Carlisle, D., 1983, Concentration of uranium and vanadium in calcretes and gypcretes, in R.C.L. Wilson, ed., *Residual Deposits; Geological Society of London Special Publication 11*, p. 185-195.
- Carr, T.R., Jaech, J., Guy, W.J., Hopkins, J.F., and Hoth, P., 1995, Use of gamma-ray spectral log to recognize exposure surfaces and associated water tables in a midcontinent carbonate sequence, Kansas, in *Annual Meeting Abstracts: American Association of Petroleum Geologists 1995 annual convention*, p. 14.
- Chung, G.C., and Swart, P.K., 1990, The concentration of uranium in freshwater vadose and phreatic cements in a Holocene ooid cay: A method of identifying ancient water tables; *Journal of Sedimentary Petrology*, v. 60, p. 735-746.
- Crowell, J.C., 1978, Gondwanan glaciation, cyclothem, continental positioning, and climate change; *American Journal of Science*, v. 278, p. 1345-1372.
- Enos, Paul, 1983, Shelf environment, in P.A. Scholle, D.G. Bebout, and C.H. Moore, eds., *Carbonate Depositional Environments: American Association of Petroleum Geologists Memoir 33*, p. 268-295.

- Enos, Paul, and Sawatsky, L.H., 1981, Pore space in Holocene carbonate sediments: *Journal of Sedimentary Petrology*, v. 51, no.3, p. 961-985.
- Esteban, M., and Klappa, C.R., 1983, Subaerial Exposure in P.A. Scholle, D.G. Bebout, and C.H. Moore, eds., *Carbonate Depositional Environments: American Association of Petroleum Geologists Memoir 33*, p. 1-54.
- Evans, C.C., 1984, Development of an ooid shoal complex: the importance of antecedent and syndepositional topography, in P.M. Harris, ed *Carbonate sands – a core workshop: SEPM Core Workshop No. 5*, p. 392-428.
- French, J.A., Watney, W.L., and Franseen, E.K., 1989, Stop 8 - Farlinville North Quarry, in W. L. Watney, J.A. French, and E.K. Franseen, eds., *Guidebook for a Field Conference on sequence stratigraphic interpretation and modelling of cyclothems in the Upper Pennsylvanian (Missourian) Lansing and Kansas City groups in eastern Kansas: Kansas Geological Survey 41st annual field trip*, p. 147-153.
- French, J.A., and Watney, W.L., 1993, Stratigraphy and depositional setting of the lower Missourian (Pennsylvanian) Bethany Falls and Mound Valley limestones, analogues for age-equivalent ooid-grainstone reservoirs, Kansas, in *Current Research on Kansas Geology: Kansas Geological Survey Bulletin 235*, p. 27-39.
- Galloway, W.E., 1989, Genetic stratigraphic sequences in basin analysis I: architecture and genesis of flooding-surface bounded depositional units: *American Association of Petroleum Geologists Bulletin*, v. 73, no. 2, p. 125-142.
- Goldhammer, R.K., Lehman, P.J., and Dunn, P.A., 1993, The origin of high-frequency platform carbonate cycles and third-order sequences (Lower Ordovician El Paso Group, west Texas): constraints from outcrop data and stratigraphic modelling: *Journal of Sedimentary Petrology*, v. 63, p. 318-359.
- Goldstein, R.H., and Franseen, E.K., 1995, Pinning points: A method of providing quantitative constraints on relative sea-level history: *Sedimentary Geology*, v. 95, p. 1-10.
- Halley, R.B., Harris, P.M., and Hine, A.C., 1983, Bank margin environment, in P.A. Scholle, D.G. Bebout, and C.H. Moore, eds., *Carbonate Depositional Environments: American Association of Petroleum Geologists Memoir 33*, p. 464-506.
- Hamblin, W.K., 1969, Marine paleocurrent directions in limestones of the Kansas City Group (Upper Pennsylvanian) in eastern Kansas: *Kansas Geological Survey Bulletin 194*, part 2, 25 p.
- Harbaugh, J.W., 1964, Significance of marine banks in southeastern

- Kansas in interpreting cyclic Pennsylvanian sediments: Kansas Geological Survey Bulletin 169, p. 199-203.
- Harris, P.M., 1984, Cores from a modern carbonate sand body; the Joulter's ooid shoal, Great Bahama Bank, in P.M. Harris, ed Carbonate sands – a core workshop: SEPM Core Workshop No. 5, p. 429-464.
- Heckel, P.H., 1972, Recognition of ancient shallow marine environments in J.K. Rigby, and W.K. Hamblin, eds., Recognition of Ancient Sedimentary Environments: Society of Economic Palaeontologists and Mineralogists, Special Publication, No. 16, p.226-286.
- Heckel, P.H., 1977, Origin of phosphatic black shale facies in Pennsylvanian cyclothems of midcontinent North America: American Association of Petroleum Geologists Bulletin, v. 61, p. 1045-1068.
- Heckel, P.H., 1980, Palaeogeography of eustatic model for deposition of midcontinent Upper Pennsylvanian cyclothems, in Fouch, T.D., and Magathan, E.R. eds., Paleozoic Palaeogeography of West-Central United States: Society of Economic Paleontologists and Mineralogists, West-Central United States Paleogeography Symposium 1, Rocky Mountain Section, p. 197-214.
- Heckel, P.H., 1985, Current views of midcontinent Pennsylvanian cyclothems; in W.L. Watney, R.L. Kaesler, K.D., Newell, Recent Interpretations of Late Paleozoic Cyclothems: Proceedings of the Third Annual Meeting, midcontinent Section, Society of Economic Paleontologists and Mineralogists, p. 1-21.
- Heckel, P.H., 1986, Sea-level curve for Pennsylvanian eustatic marine transgressive-regressive depositional cycles along mid-continent outcrop belt, North America: *Geology*, V. 14, p. 330-334.
- Heckel, P.H., and Cocke, J.M., 1969, Phylloid algal-mound complexes in outcropping Upper Pennsylvanian rocks of Mid-continent: American Association of Petroleum Geologists Bulletin 53, p. 1058-1074.
- Hine, A.C., 1977, Lily Bank, Bahamas; history of an active oolite sand shoal: *Journal of Sedimentary Petrology*, v. 47, p. 1554-1581.
- Hoth, P., Carr, T.R., Bau, M., and Dulski, P., 1998, Trace and rare-earth elemental variation in a midcontinent carbonate sequence - a key to understanding reservoir development: in Proceedings Pennsylvanian and Permian Geology and Petroleum in the Southern midcontinent, Oklahoma Geological Survey Workshop, April 7-8, 1998, p 20.
- Hyne, N.J, 1995, Sequence stratigraphy - A new look at old rocks, in N.J. Hyne, ed., Sequence Stratigraphy of the Mid-Continent: Tulsa Geological Society Special Publication No. 4, p. 5-17.

- James, N.P., 1983, Reef, in P.A. Scholle, D.G. Bebout, and C.H. Moore, eds., Carbonate Depositional Environments: American Association of Petroleum Geologists Memoir 33, p. 345-440.
- Jewett, C.H., 1994, Microfabric and petrology of the Hushpuckney Shale (Pennsylvanian), midcontinent, U.S.A., in Geological Society of America, Northeastern Section, 29th Annual Meeting Abstracts with Programs, v. 26, no. 3, p. 26.
- Klappa, C.F., 1980, Rhizoliths in terrigenous carbonates: classification, recognition, genesis and significance, in V. P. Wright, and M.E. Tucker, eds., Calcretes: Blackwell Scientific Publications, London, p. 149-165.
- Mann, A.W., and Horowitz, R., 1979, Groundwater calcrete deposits in Australia: some observations from western Australia; Geological Society of Australia Journal, v. 26, p. 293-303.
- Merriam, D.F., 1963, The geologic history of Kansas: Kansas Geological Survey Bulletin 162, p. 128.
- Miller, D.E., 1966, geology and ground-water resources of Miami County, Kansas; Kansas Geological Survey Bulletin 181, 66 p.
- Mitchum, R.M. Jr., Vail, P.R., and Thompson, S. III, 1977, Seismic stratigraphy and global changes of sea level, part 2: The depositional sequence as a basic unit for stratigraphic analysis, in C.E. Payton ed., Seismic Stratigraphy - applications to hydrocarbon exploration: American Association of Petroleum Geologists Memoir 25, p. 53-62.
- Mitchum, R.M., and Van Wagoner, J.C., 1991, High-frequency sequences and their stacking patterns: sequence stratigraphic evidence of high-frequency eustatic cycles: American Association of Petroleum Geologists memoir 26, p. 117-133.
- Moore, R.C., 1932, Kansas Geological Society, 6th annual field conference, Guidebook, p. 85.
- Mossler, J.H., 1971, Facies and diagenesis of Swope Limestone (Upper Pennsylvanian) southeast Kansas: Unpublished thesis, University of Iowa, 228 p.
- Mossler, J.H., 1973, Carbonate Facies of the Swope Limestone Formation (Upper Pennsylvanian) Southeast Kansas: Kansas Geological Survey Bulletin 206, Part 1, 17 p.
- Newell, K.D., Watney, W.L., Stephens, B.P., and Hatch, J.R., 1987, Hydrocarbon potential in Forest City Basin: Oil and Gas Journal, v. 85, no. 42, p. 58-62.
- Nollisch, D.A., 1983, Diagenesis of Middle Creek and Bethany Falls Limestones, Swope Formation, Upper Pennsylvanian (Missourian), midcontinent North America: Unpublished M.S. thesis, Department of Geology, University of Iowa, Iowa City, IA,

- 168 p. (available as Kansas Geological Survey, Open-file Report. no. 83-29)
- Parrish, J.T., 1982, Upwelling and petroleum source beds, with reference to Paleozoic: American Association of Petroleum Geologists Bulletin, v. 66, no. 6, p. 750-774.
- Payton, C.E., 1966, Petrology of the carbonate members of the Swope and Dennis Formation (Pennsylvanian), Missouri and Iowa: Journal of Sedimentary Petrology, v. 36, no. 2, p. 576-601.
- Perkins, R.D., 1977, Depositional framework of Pleistocene rocks in south Florida: Geological Society America Memoir 147, p. 131-198.
- Phipps, C.V., and Roberts, H.H., 1988, Seismic characteristics and accretion history of Halimeda bioherms on Kalukalukuang Bank, eastern Java Sea (Indonesia): Coral Reefs, v. 6, p. 149-159.
- Posamentier, H.W., Allen, G.P., James, D.P., and Teeson, M., 1992, Forced regressions in a sequence stratigraphic framework: concepts, examples, and exploration significance: American Association of Petroleum Geologists Bulletin, v. 76, no. 11, p. 1687-1709.
- Rasbury, E.T., Hanson, G.N., Meyers, W.J., Holt, W.E., Goldstein, R.H., and Saler, A.H., 1998, U-Pb dates of paleosols: constraints on late Paleozoic cycle durations and boundary ages: Geology, v. 26, no. 5, p. 403-406.
- Rhoads, D.C., and J.W. Morse, 1971, Evolutionary and ecologic significance of oxygen-deficient marine basins: Lethaia, v. 4, p. 413-428
- Rossignol-Strick, M., 1982, Petroleum origin – heavy rain, river plume, ocean stratification: American Association of Petroleum Geologists Bulletin, v. 66, p. 625-626.
- Sarg, J.F., 1988, Carbonate sequence stratigraphy: in Sea-level Changes: An Integrated Approach, Society of Economic Paleontologists and Mineralogists Special Publication No. 42, p. 155-181.
- Schutter, S.R., 1983, Petrology, clay mineralogy, paleontology, and depositional environments of four Missourian (Upper Pennsylvanian) shales of the midcontinent and Illinois Basin: Ph.D. dissertation, University of Iowa, 1,208 p.
- Shinn, E.A., 1968, Practical significance of birdseye structures in carbonate rocks: Journal of Sedimentary Petrology, v. 38, no. 1, p. 215-223.
- Shinn, E.A., 1983, Tidal Flat Environment, in P.A. Scholle, D.G. Bebout, and C.H. Moore, eds., Carbonate Depositional Environments: American Association of Petroleum Geologists Memoir 33, p. 172-210.

- Soreghan, G.S., and Giles, K.A., 1999, Amplitudes of Late Pennsylvanian glacioeustasy: *Geology*, v. 27, no. 3, p. 255-258.
- Stover, S.G., 1992, Stratigraphy and depositional environment of the upper Bethany Falls limestone member, Farlinville North quarry, Linn County, Kansas: Unpublished thesis, University of Kansas, 47 p.
- Tearpock, D.J., and Bischke, R.E., 1991, Applied subsurface geological mapping: Prentice Hall, p. 142.
- Tedesco, L.P., and Wanless, H.R., 1989, Role of burrow excavation and infilling in creating the preserved depositional fabric of Pennsylvanian phylloid mounds of southeastern Kansas in W. L. Watney, J.A. French, and E.K. Franseen, eds., Guidebook for a Field Conference on sequence stratigraphic interpretation and modelling of cyclothems in the Upper Pennsylvanian (Missourian) Lansing and Kansas City groups in eastern Kansas: Kansas Geological Survey 41st annual field trip, p. 179-191.
- Vail, P.R., 1987, Part 1 – Seismic stratigraphy interpretation procedure – Key definitions of sequence stratigraphy; in A.W. Bally, ed., *Atlas of Seismic Stratigraphy: American Association of Petroleum Geologists, Studies in Geology* 27, v. 1, p. 1-10.
- Vail, P.R., Audemard, F., Bowman, S.A., Eisner, P.N., and Perez-Cruz, C., 1991, The stratigraphic signatures of tectonics, eustasy and sedimentology – an overview, in C. Einsele, W. Ricken, and A. Seilacher, eds., *Cycles and events in stratigraphy*: New York, Springer-Verlag, p. 617-659.
- Van Wagoner, J.C., Posamentier, H.W., Mitchum, R.M., Vail, P.R., Sarg, J.F., Loutit, T.S., and Hardenbol, J., 1988, An overview of the fundamentals of sequence stratigraphy and key definitions: in *Sea-level Changes: An Integrated Approach*, Society of Economic Paleontologists and Mineralogists Special Publication No. 42, p. 39 – 45
- Wanless, H.R., and Shepard, F.P., 1936, Sea level and climatic changes related to Late Paleozoic cycles: *Geological Society of America Bulletin*, v. 47, p. 1177-1206.
- Watney, W.L., 1980, Cyclic sedimentation of the Lansing-Kansas City Groups in northwestern Kansas and southwestern Nebraska: *Kansas Geological Survey Bulletin* 220, 72 p.
- Watney, W.L., 1984, Recognition of favorable reservoir trends in Upper Pennsylvanian cyclic carbonates in western Kansas and southwestern Nebraska – a guide for petroleum exploration: *Kansas Geological Survey, Bulletin* 220, 72 p.
- Watney, W.L., 1985, Evaluation of the significance of tectonic, sedimentary control versus eustatic control of Upper Pennsylvanian

- cyclothems in the western midcontinent; in W.L. Watney, R.L. Kaesler, K.D., Newell, Recent Interpretations of Late Paleozoic Cyclothems: Proceedings of the Third Annual Meeting, midcontinent Section, Society of Economic Paleontologists and Mineralogists, p. 105-140.
- Watney, W.L., and French, J., 1988, Characterization of carbonate reservoirs in the Lansing-Kansas City groups (Upper Pennsylvanian) in Victory Field, Haskell County, Kansas; in S.M. Goolsby, M.W. Longman, eds., Occurrence and Petrophysical Properties of Carbonate Reservoirs in the Rocky Mountain Region: 1988 Carbonate Symposium, Rocky Mountain Association of Geologists, p. 27-46.
- Watney, W.L., French, J.A., and Franseen, E.K., 1989, Guidebook for a field conference on sequence stratigraphic interpretation and modelling of cyclothems in the Upper Pennsylvanian (Missourian) Lansing and Kansas City groups in eastern Kansas: Kansas Geological Survey 41st annual field trip, p. 1-70.
- Watney, W.L., French, J.A., and Franseen, E.K., 1989, Stop 7 - Raytown section along I-435 just south of 350 Highway; Hertha, Swope and Dennis cycles, *in* W. L. Watney, J.A. French, and E.K. Franseen, eds., Guidebook for a field conference on sequence stratigraphic interpretation and modelling of cyclothems in the Upper Pennsylvanian (Missourian) Lansing and Kansas City groups in eastern Kansas: Kansas Geological Survey 41st annual field trip, p. 141-145.
- Watney, W.L., and Heckel, P.H., 1994, Kansas Geological Survey Open File Report 94-34, p. 8.
- Watney, W.L., French, J.A., Doveton, J.H., Youle, J.C., and Guy, W.J., 1995, Cycle hierarchy and genetic stratigraphy of middle and upper Pennsylvanian strata in the upper mid-continent, in N.J. Hyne ed., Sequence stratigraphy of the Mid-Continent: Tulsa Geological Society Special Publication No. 4, p. 141-192.
- Wright, V.P., Platt, N.H., and Wimbledon, W.A., 1988, Biogenic laminar calcretes: evidence of calcified root-mat horizons in paleosols; *Sedimentology*, v. 35, p. 603-620.
- Zeller, D.E. (ed.), 1968, The Stratigraphic Succession in Kansas: Kansas Geological Survey Bulletin 189, p. 28-29.

Appendix 1: Measured Stratigraphic Sections

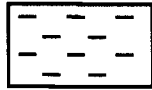
Outcrop and Core Locations

- 1) Farlinville Quarry
Linn County KS
N1/2 Section 34, T.20 S., R.23 E
- 2) LaCygne West
Linn County KS
NE 1/4 Section 2, T.20 S., R.23 E
- 3) LaCygne East
Linn County KS
NE 1/4 Section 1, T.20 S., R.24 E
- 4) LaCygne North
Linn County KS
NE 1/4 Section 31, T.19 S., R.25 E
- 5) Fontana
Miami County KS
NW 1/4 Section 30, T.18 S., R.24 E
- 6) 383rd Street
Miami County KS
SW 1/4 Section 31, T.18 S., R.25 E
- 7) Ridgeview Road
Miami County KS
SW 1/4 Section 18, T.18 S., R.24 E
- 8) Raines #1 Core
Miami County KS
NE 1/4 Section 30, T.17 S., R. 25 E
- 9) RWD#2 Well #1 Core
Miami County KS
NW 1/4 Section 29, T.16 S., R. 25 E
- 10) Chestnut Drive
Jackson County MO
NE 1/4 Section 5, T.47 N., R.33 W

- 11) Dodson
Jackson County MO
NE1/4 Section 22, T.48 N., R.33 W
- 12) Lake Jacomo South
Jackson County MO
NW 1/4 Section 27, T.48 N., R.31 W
- 13) Lake Jacomo North
Jackson County MO
SW 1/4 Section 16, T.48 N., R.31 W
- 14) Raytown Road
Jackson County MO
NW 1/4 Section 6, T.48 N., R.32 W

SYMBOLS FOR SECTIONS

LITHOLOGIC



shale



black fissile shale



limestone

FEATURES



rhizolith



caliche



autobrecciation



fenestra



stylolite



geopetal

PARTICLES



ooid



peloid



coated grain

SCALE

5 mm equals 15 cm.
All measurements in cm.

SYMBOLS FOR SECTIONS**FOSSILS**

brachiopod



gastropod

general shell
fragment

bryozoan



crinoid



coral



foraminifera



algae



bivalve



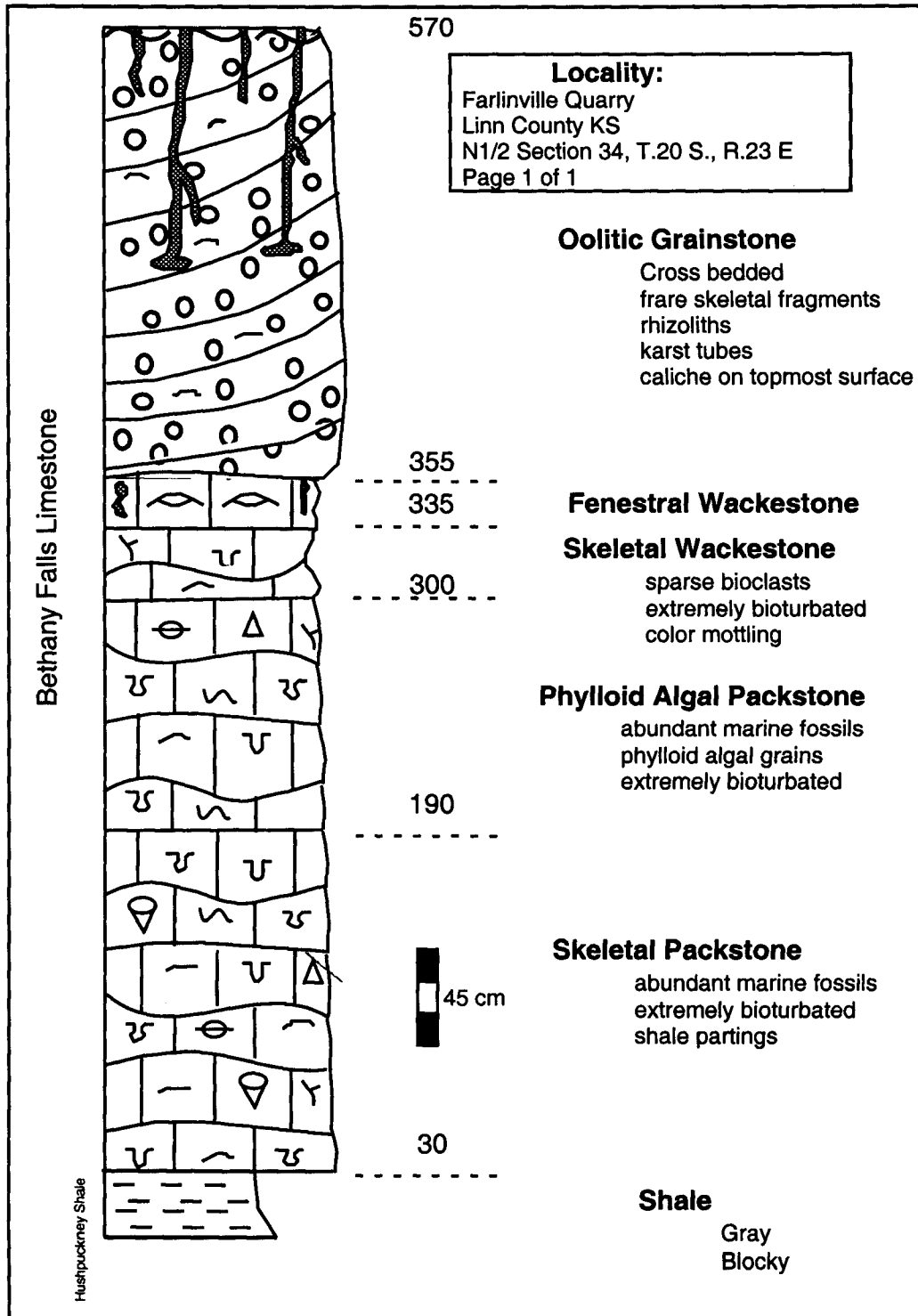
ostracod

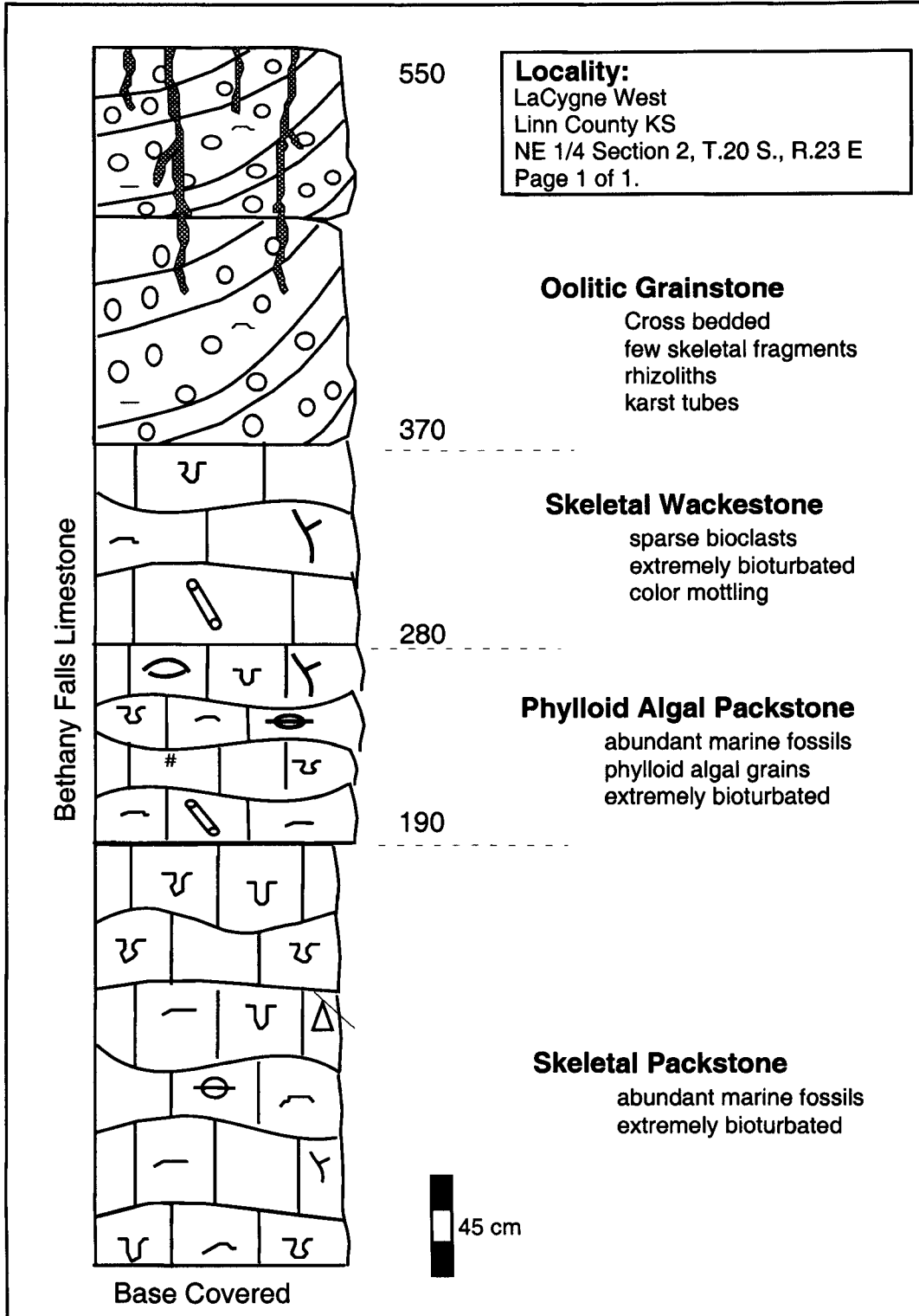


trilobite

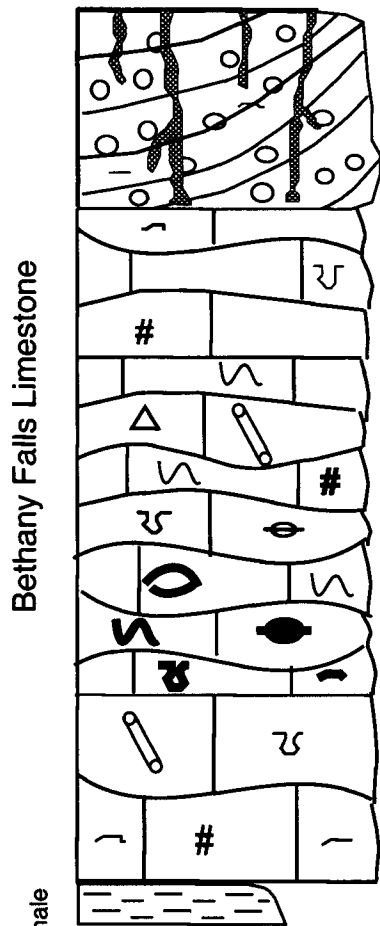


worm tube





Locality:
 LaCygne East
 Linn County KS
 NE 1/4 Section 1, T.20 S., R.24 E
 Page 1 of 1.



Bethany Falls Limestone

Hushpuckney Shale

360

280

220

90

15

Oolitic Grainstone

Cross bedded
 sparse skeletal frag
 ments
 rhizoliths
 karst tubes

Skeletal Wackestone

sparse bioclasts
 extremely bioturbated
 color mottling

Phylloid Algal Packstone

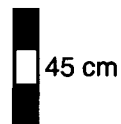
abundant marine fossils
 phylloid algal grains
 extremely bioturbated

Skeletal Packstone

abundant marine fossils
 extremely bioturbated

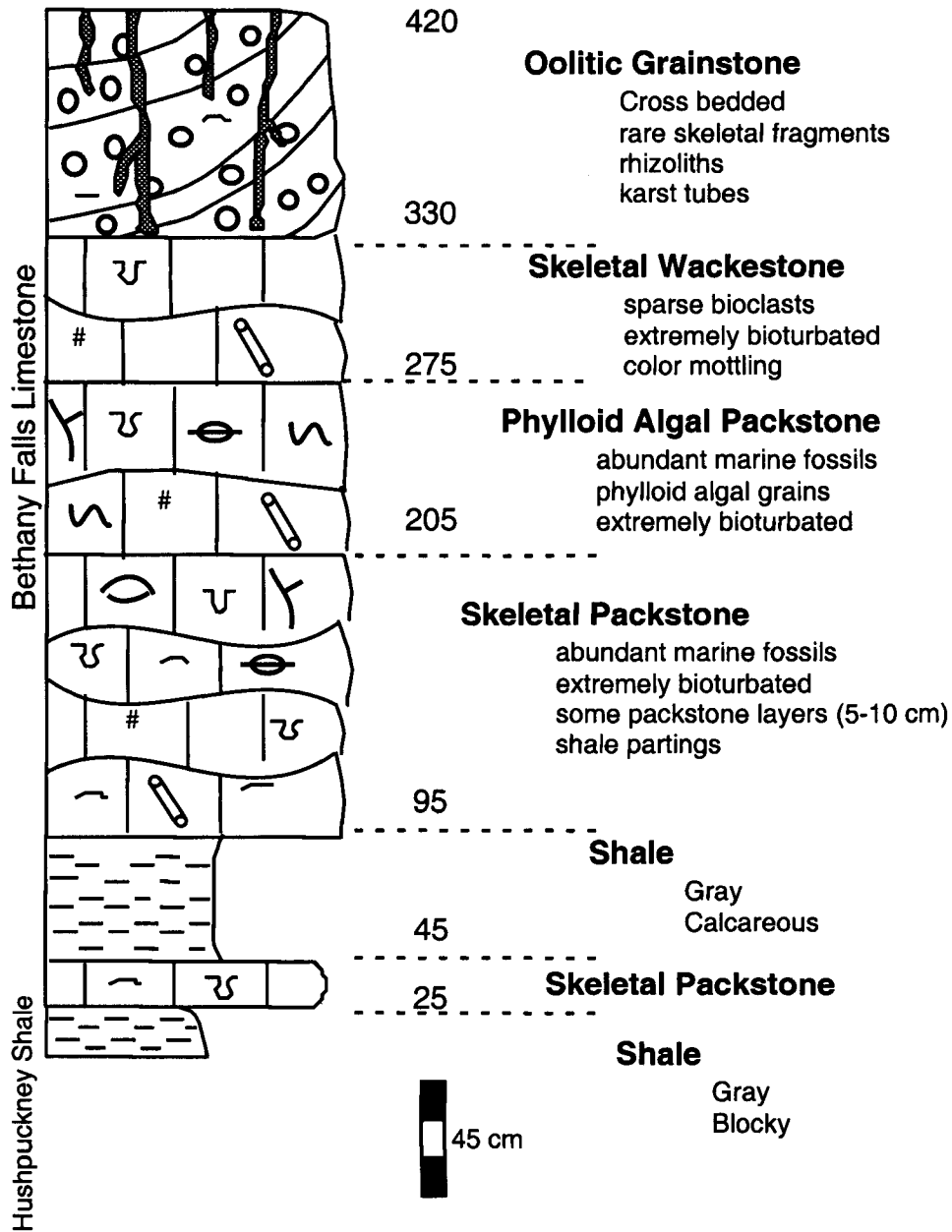
Shale

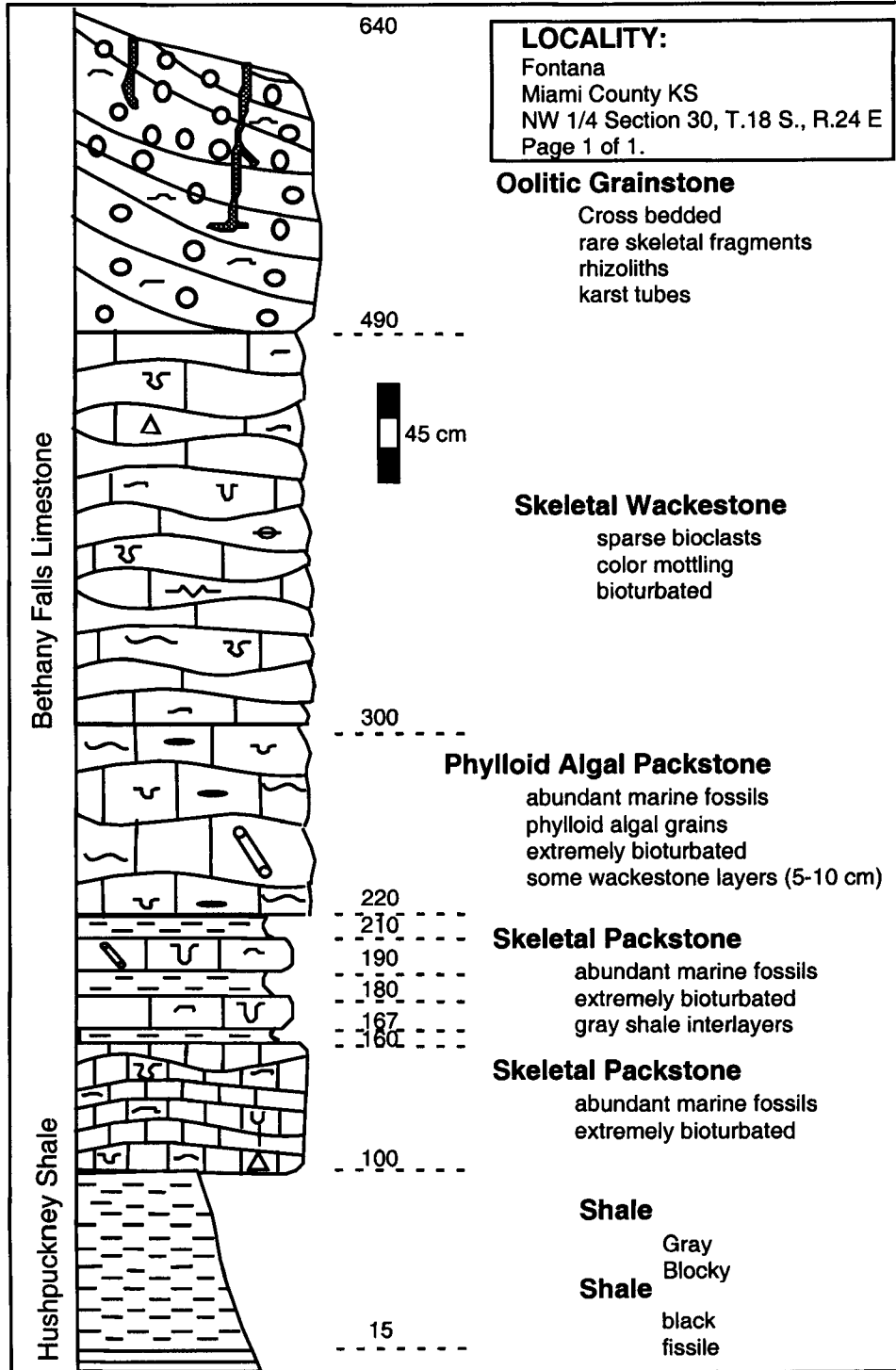
Gray
 Blocky

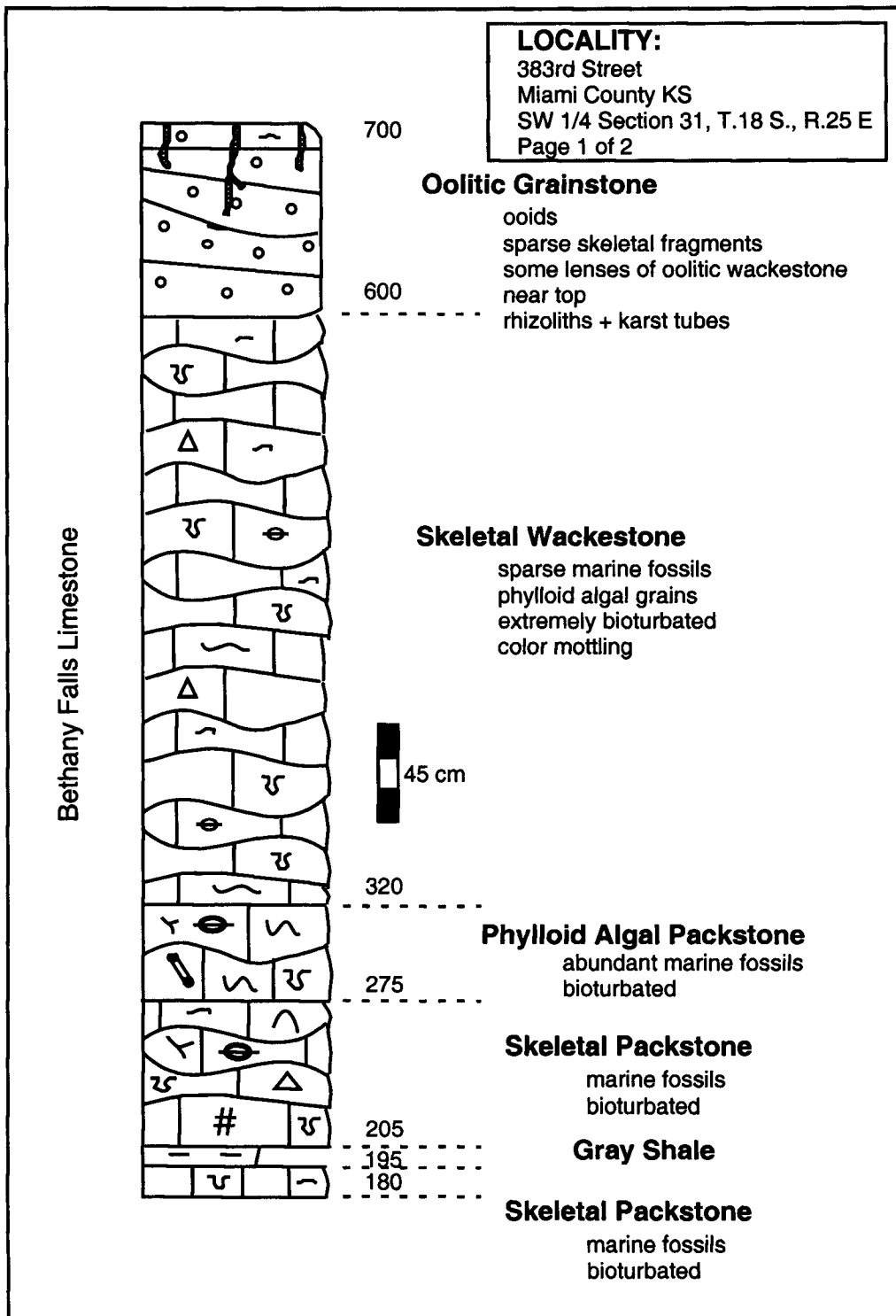


Locality:

LaCygne North
 Linn County KS
 NE 1/4 Section 31, T.19 S., R.25 E
 Page 1 of 1.



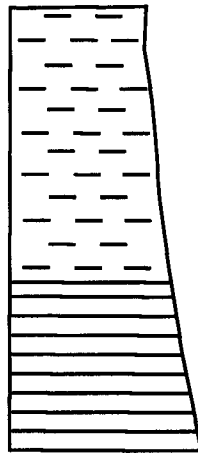




LOCALITY:

383rd Street
Miami County KS
SW 1/4 Section 31, T.18 S., R.25 E
Page 2 of 2

Hushpuckney Shale



180

70



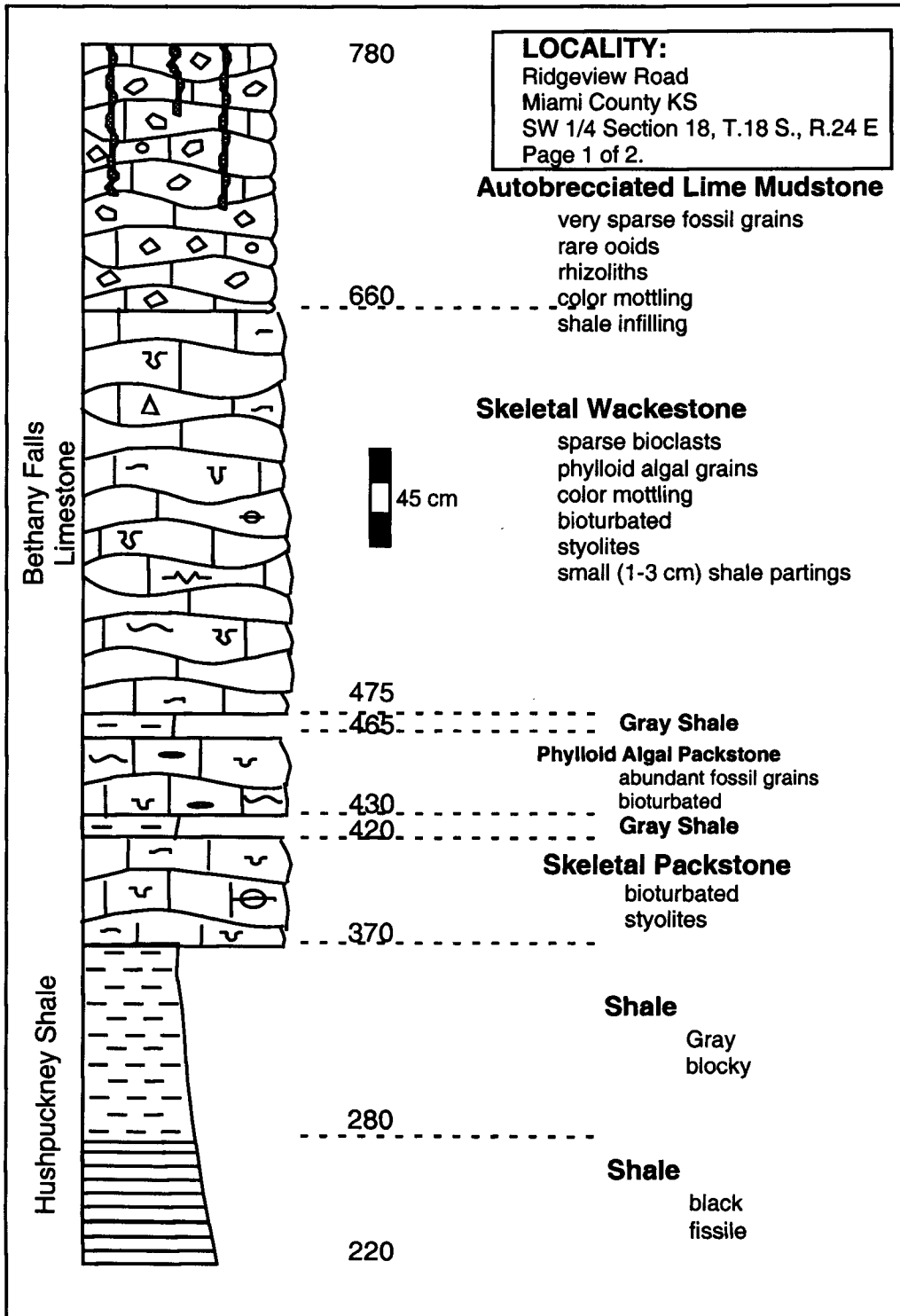
45 cm

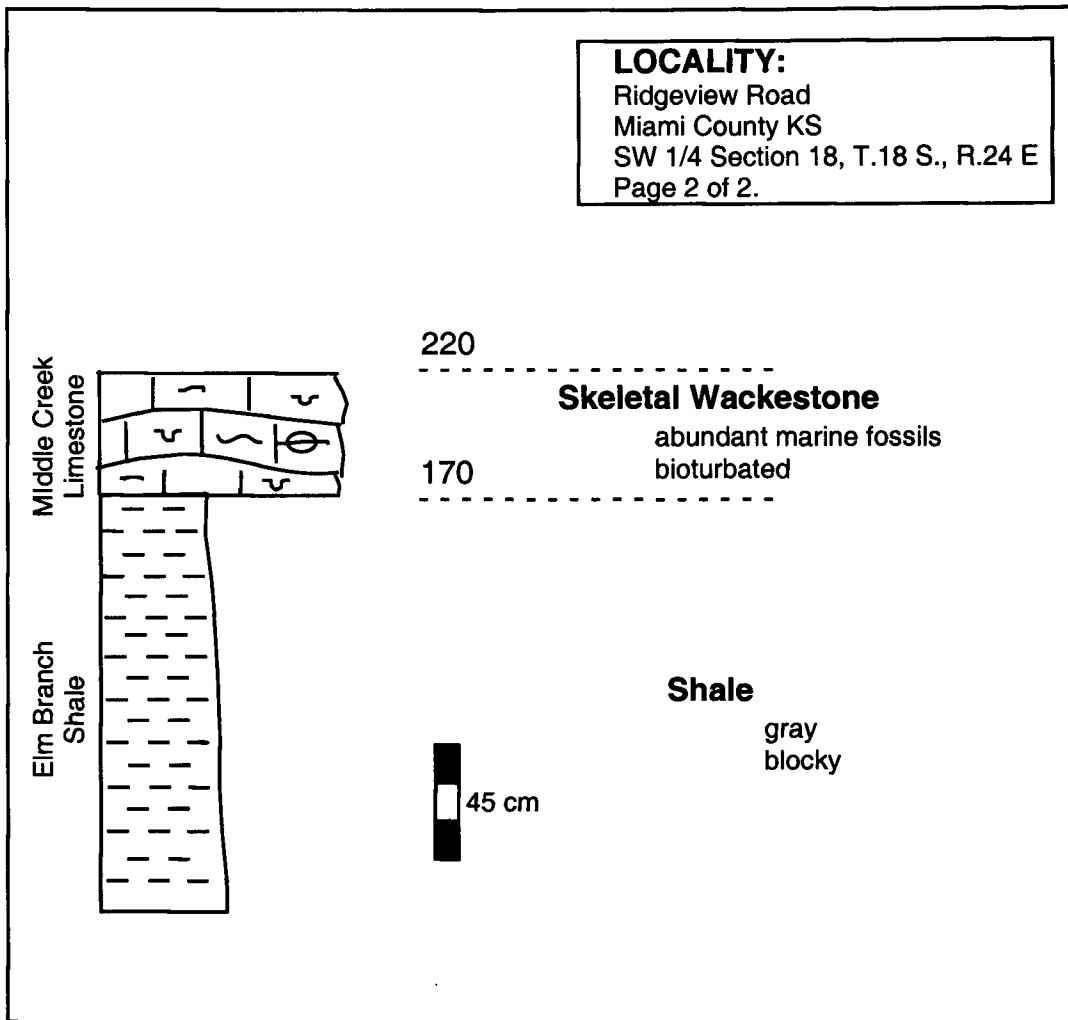
Shale

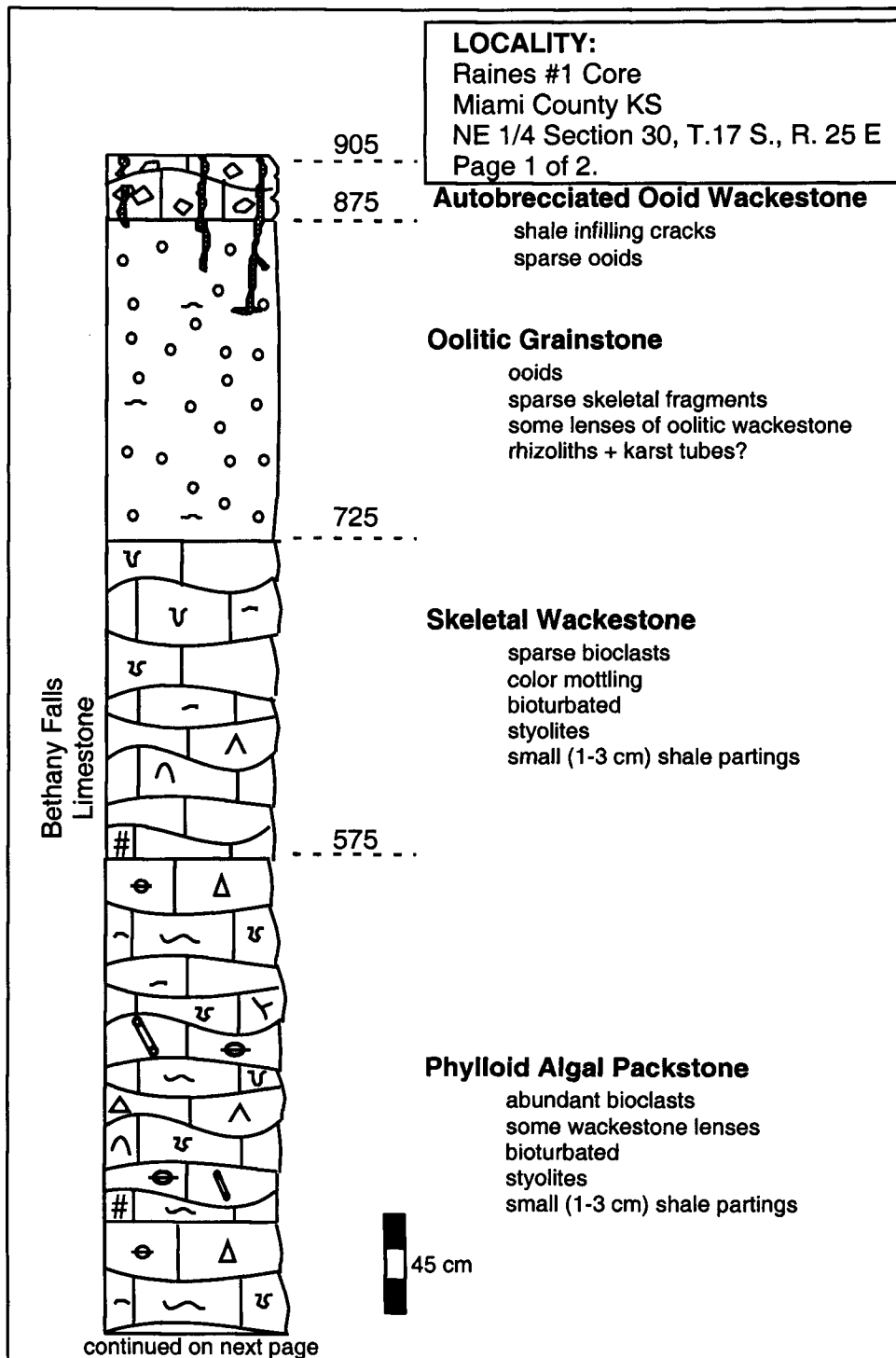
Gray
Blocky

Shale

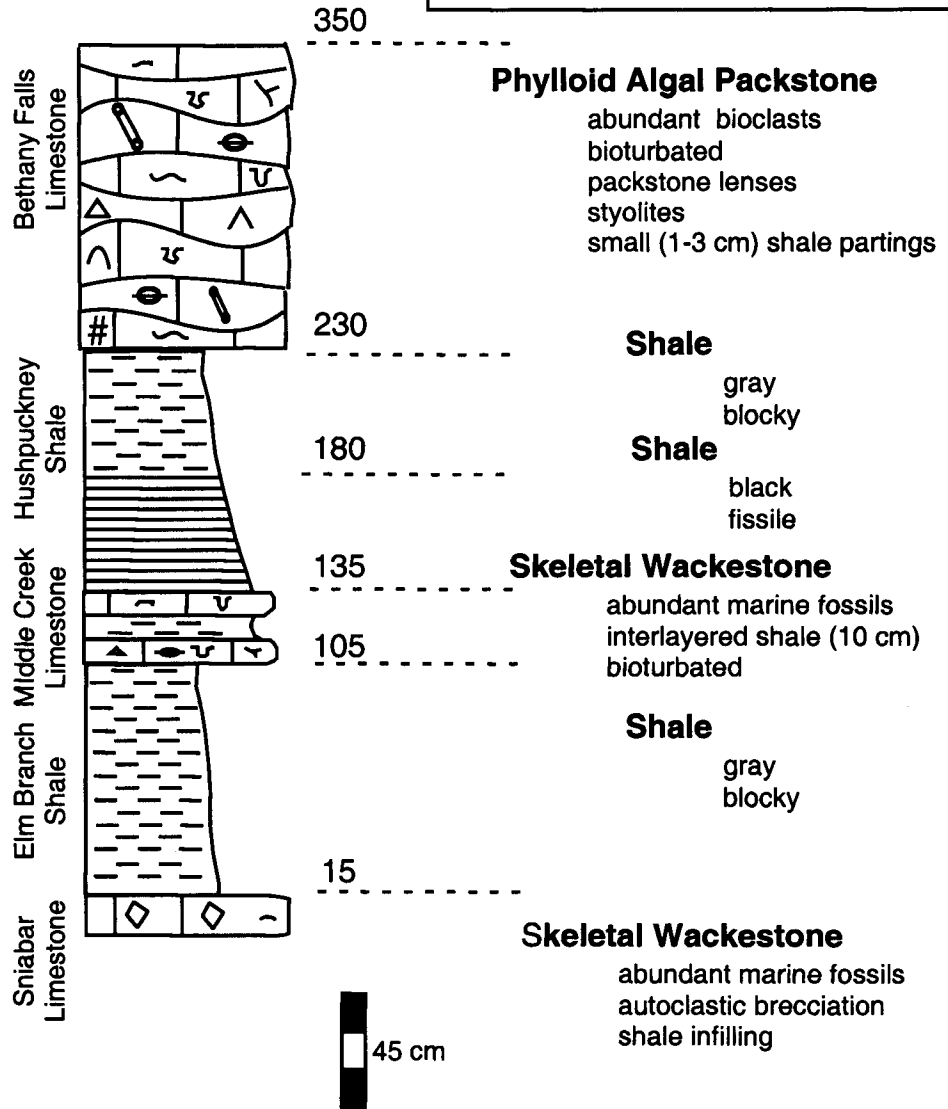
black
fissile







LOCALITY:
 Raines #1 Core
 Miami County KS
 NE 1/4 Section 30, T.17 S., R. 25 E
 Page 2 of 2.



LOCALITY:

RWD#2 Well #1 Core
Miami County KS
NW 1/4 Section 29, T.16 S., R. 25 E
Page 1 of 2.

Autobrecciated Lime Mudstone

very sparse fossil grains
rhizoliths
color mottling
shale infilling

1018

853

Mottled Lime Mudstone

very sparse fossil grains
color mottling
extremely bioturbated
peloids

768

Skeletal Wackestone

sparse fossil grains
phyloid algal grains
color mottling
bioturbated
stylolites
small (1-3 cm) shale partings

628

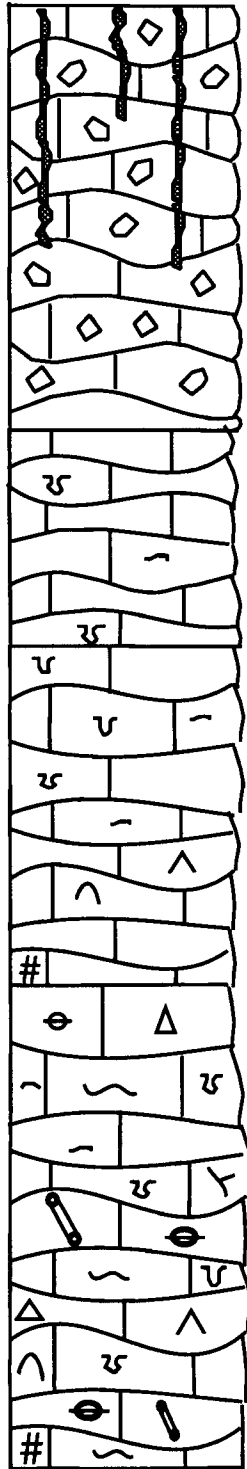
Phylloid Algal Packstone

abundant bioclasts
some wackestone layers
bioturbated
stylolites
small (1-3 cm) shale partings

45 cm



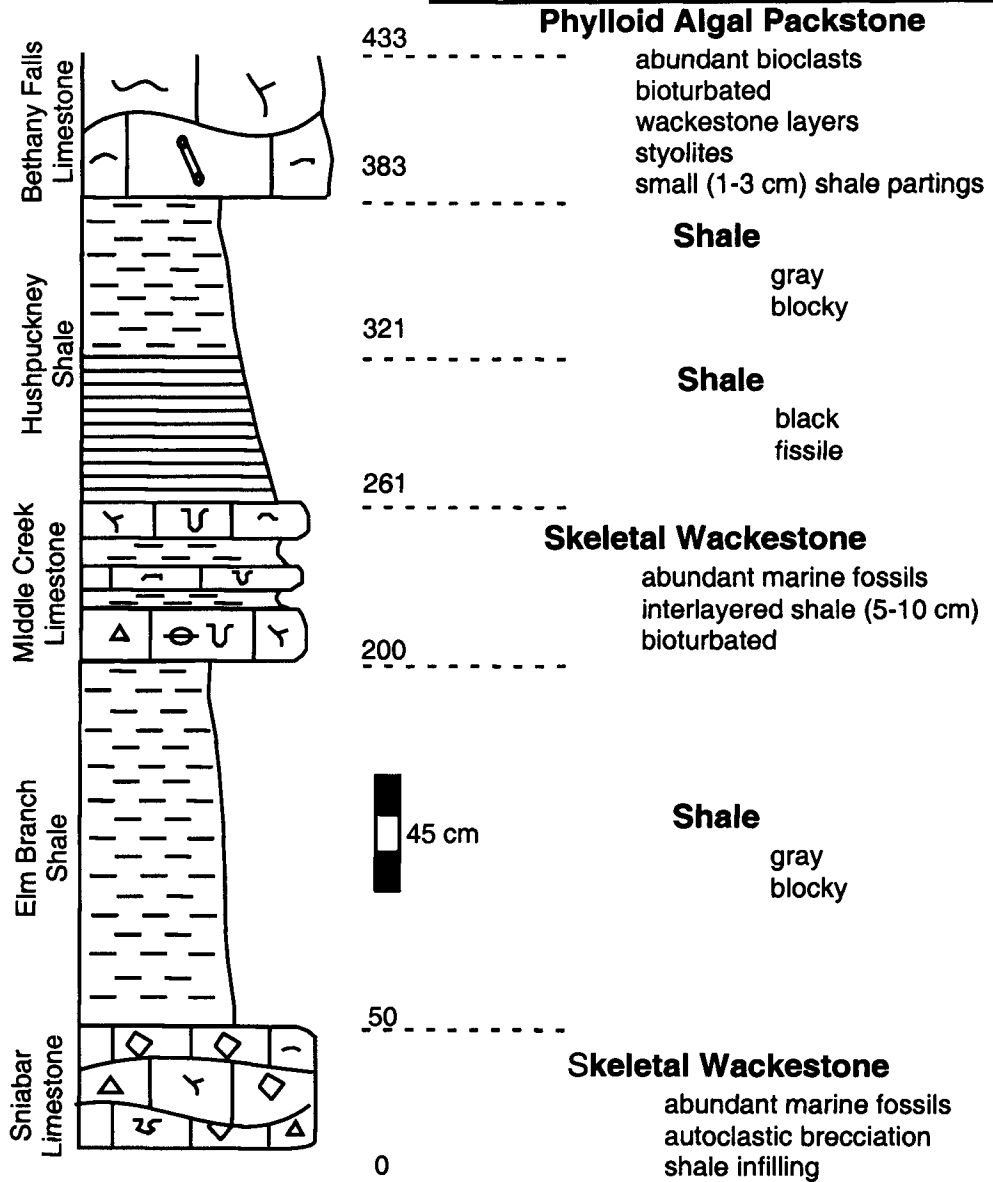
Bethany Falls
Limestone

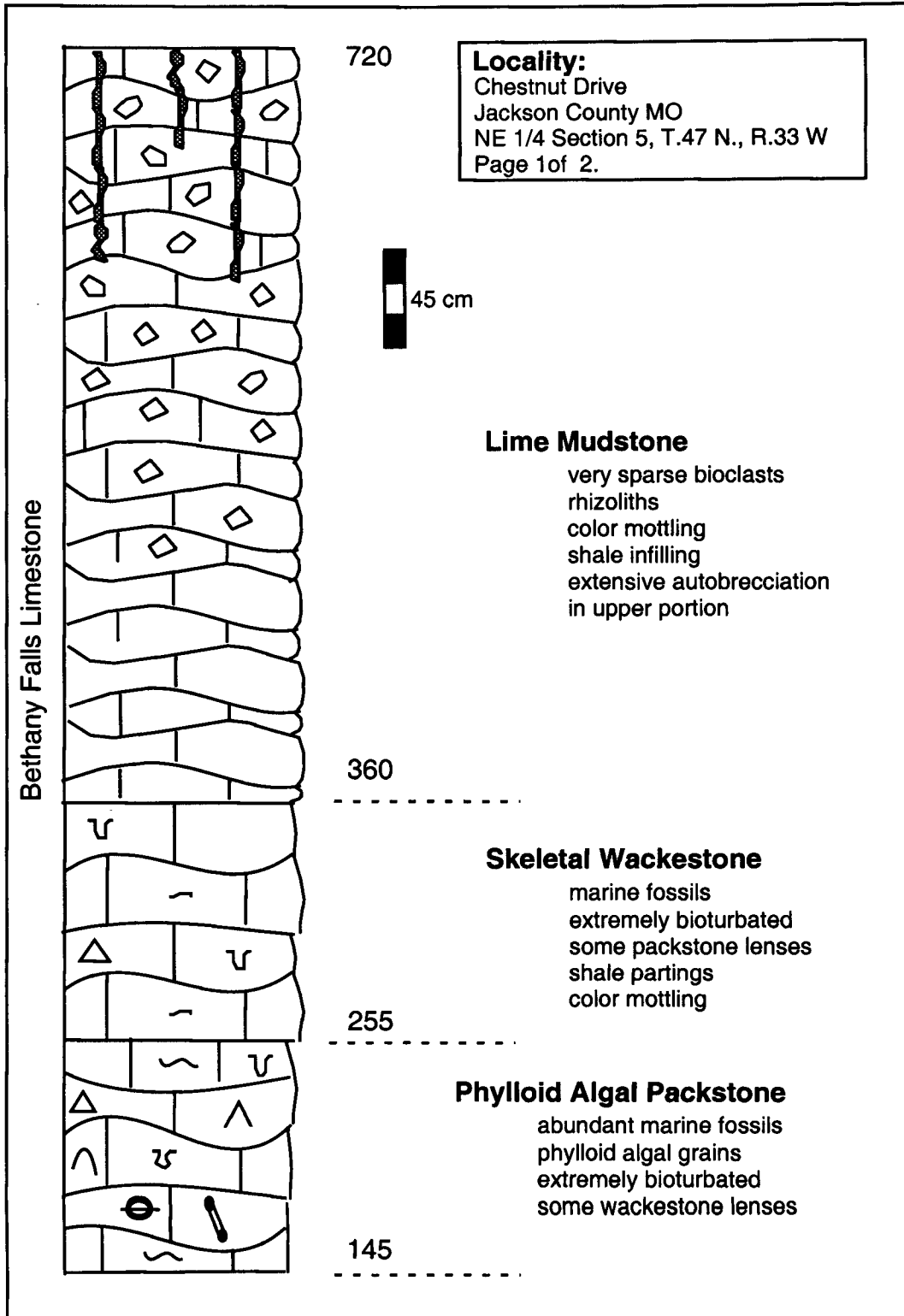


433

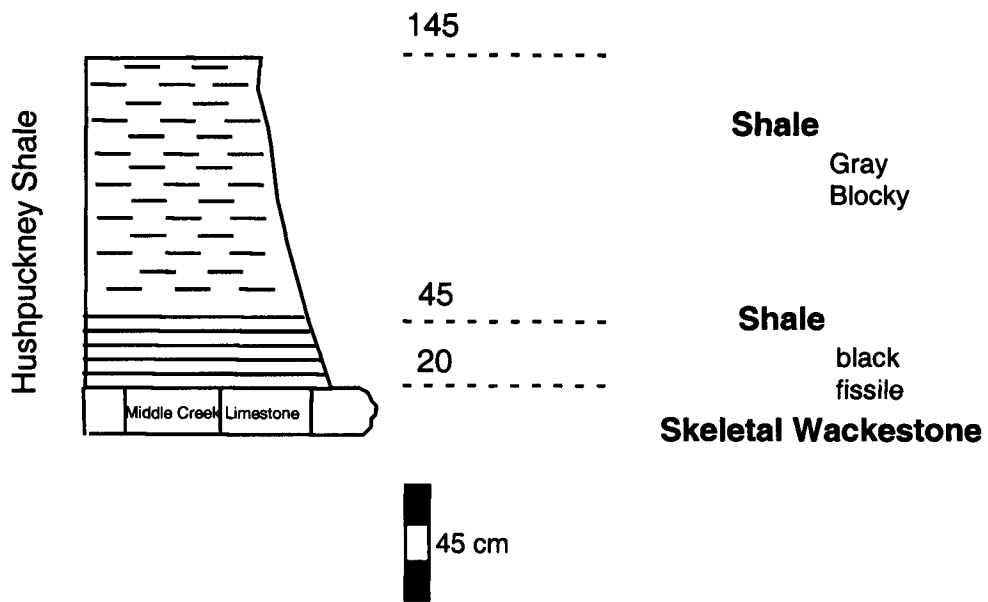
continued on next page

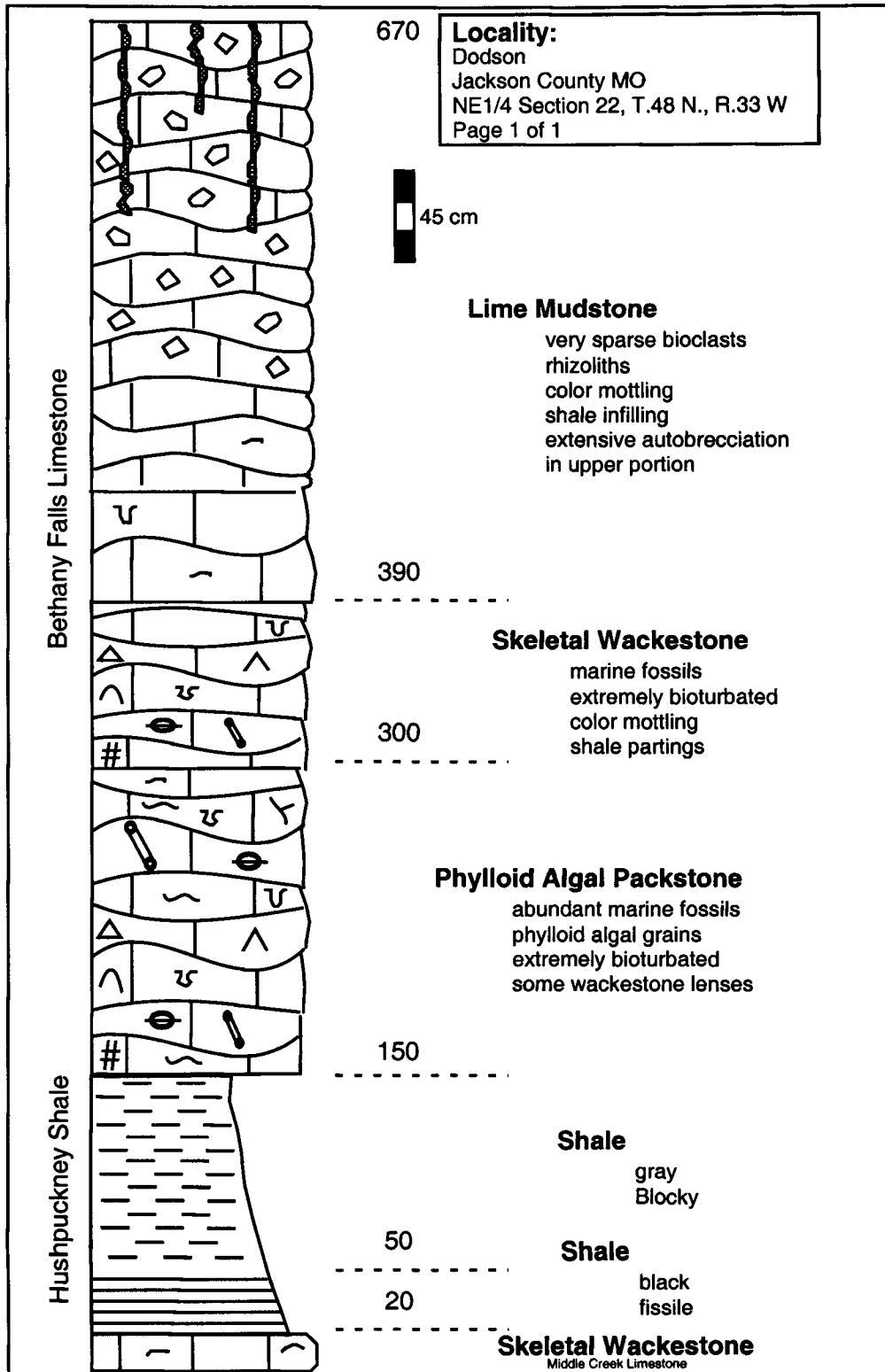
LOCALITY:
 RWD#2 Well #1 Core
 Miami County KS
 NW 1/4 Section 29, T.16 S., R. 25 E
 Page 2 of 2.





Locality:
Chestnut Drive
Jackson County MO
NE 1/4 Section 5, T.47 N., R.33 W
Page 2 of 2.

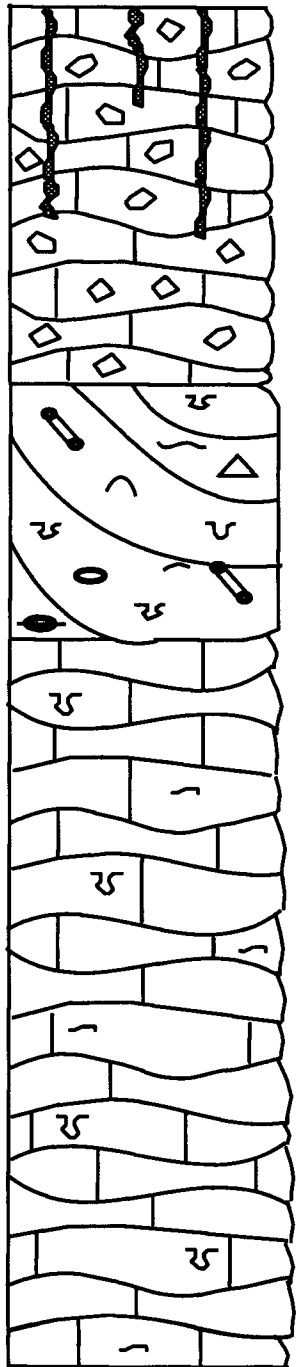




LOCALITY:

Lake Jacomo South
Jackson County MO
NW 1/4 Section 27, T.48 N., R.31 W.
Page 1 of 2.

Bethany Falls Limestone



755

Autobrecciated Lime Mudstone

very sparse bioclasts
rhizoliths
color mottling
shale infilling

605

Skeletal Packstone/Grainstone

abundant marine fossils
faintly cross bedded
some lime mudstone clasts
grains abraded and rounded

505

Lime Mudstone

very sparse bioclasts
color mottling

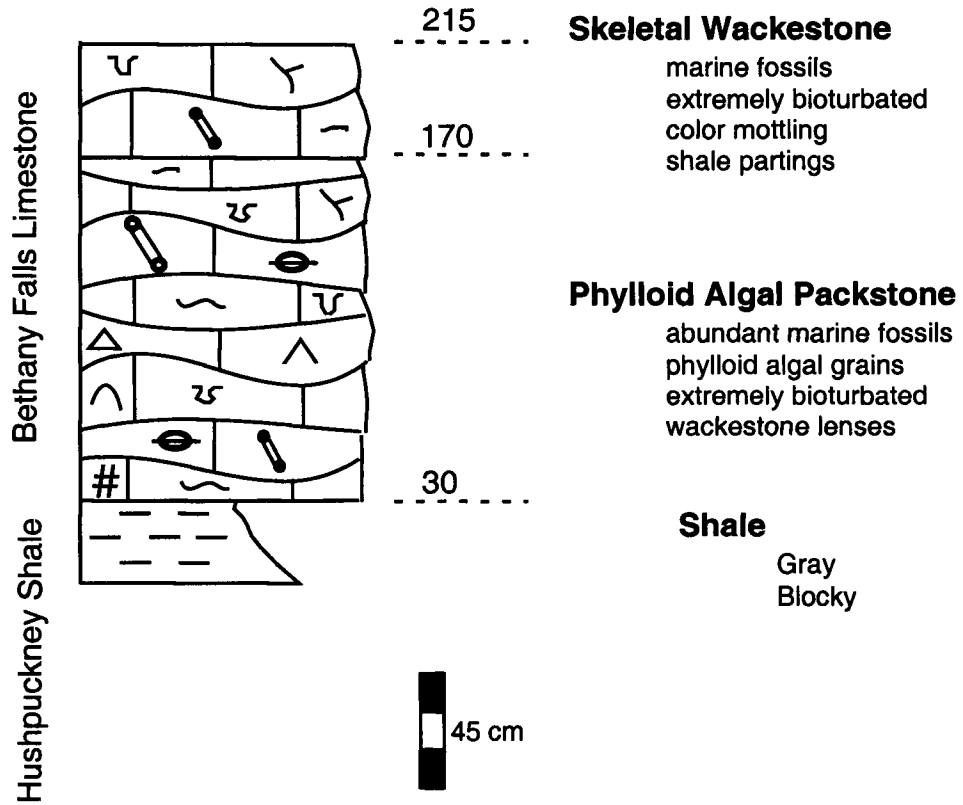
215



45 cm

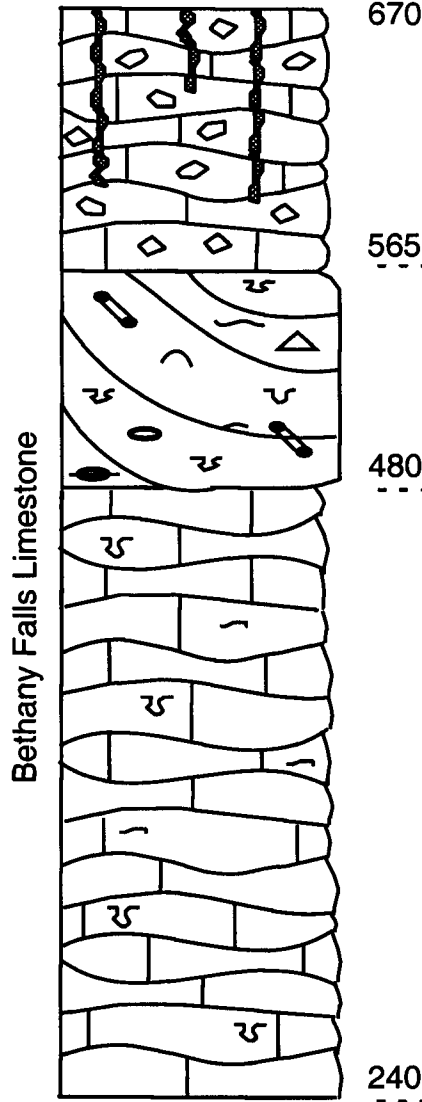
LOCALITY:

Lake Jacomo South
 Jackson County MO
 NW 1/4 Section 27, T.48 N., R.31 W.
 Page 2 of 2.



LOCALITY:

Lake Jacomo North
Jackson County MO
SW 1/4 Section 16, T.48 N., R.31 W
Page 1 of 2.



Autobrecciated Lime Mudstone

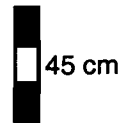
very sparse bioclasts
rhizoliths
color mottling
shale infilling

Skeletal Packstone/Grainstone

abundant marine fossils
cross bedded
some lime mudstone clasts
grains abraded and rounded

Lime Mudstone

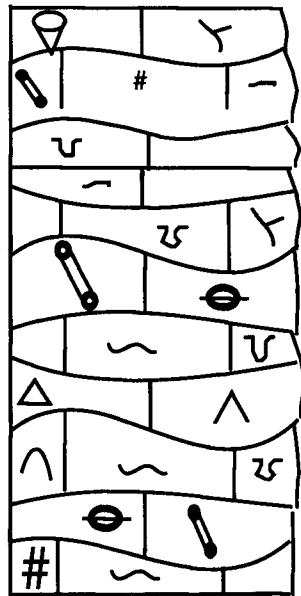
very sparse bioclasts
color mottling



LOCALITY:

Lake Jacomo North
Jackson County MO
SW 1/4 Section 16, T.48 N., R.31 W
Page 2 of 2.

Bethany Falls Limestone



240

Skeletal Wackestone

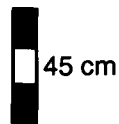
marine fossils
extremely bioturbated
color mottling
shale partings

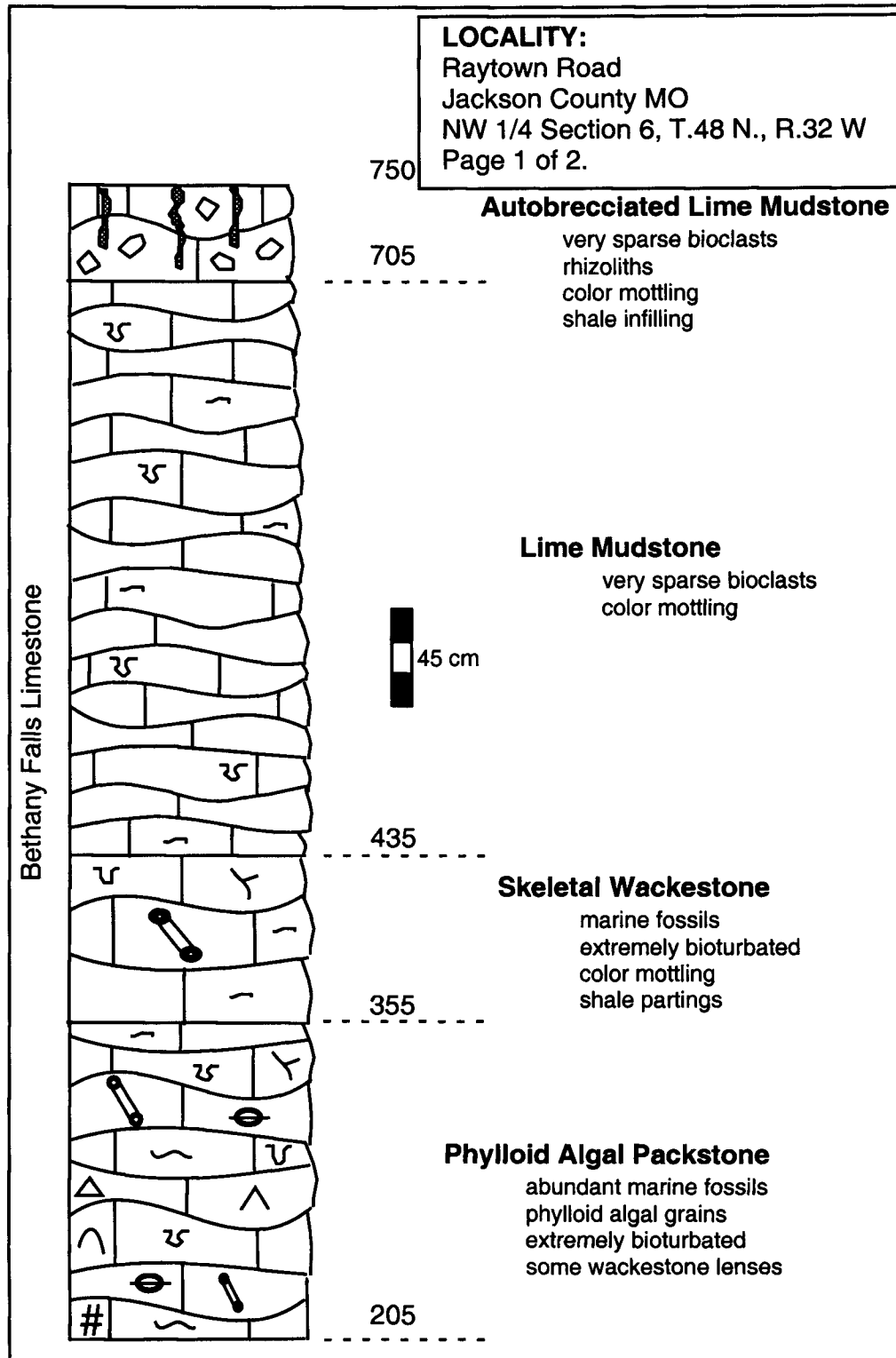
170

Phylloid Algal Packstone

abundant marine fossils
phylloid algal grains
extremely bioturbated
wackestone lenses

Base Covered

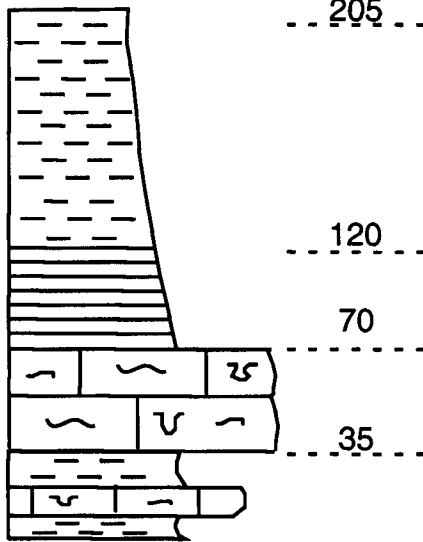




LOCALITY:
Raytown Road
Jackson County MO
NW 1/4 Section 6, T.48 N., R.32 W
Page 2 of 2.

Hushpuckney Shale

Elm Branch Sh.: Middle Creek LS.

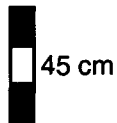


Shale
gray
blocky

Shale
black
fissile

Skeletal Wackestone
abundant marine fossils
bioturbated

Shale
gray
blocky
10 cm wackestone layer



Appendix 2: Spectral Gamma Ray Logs
Discussion and Interpretation.

Logfacies of the Bethany Falls Limestone and Hushpuckney Shale

Measured sections of the Bethany Falls Limestone and Hushpuckney Shale were logged at 15 cm intervals with a handheld differential spectrometer, the Scintrex GRS 500. The spectrometer measures natural gamma radiation, and can differentiate between potassium, thorium, and uranium. In this study, the total count, potassium and uranium were measured. Boreholes were logged with a slimline natural gamma and induction tool, which only records the total gamma ray count (Century 9511). Based upon gamma ray profiles, the Bethany Falls and Hushpuckney Shale could be subdivided into five discrete logfacies. These logfacies are based upon the character of the log profile and radioactive anomalies that act as bounding surfaces.

Logfacies A

Logfacies A is only recognized in the southern portion of the field area, from Farlinville to Raines #1 (Figure 1.4). Logfacies A is characterized by having a relatively low gamma ray profile. The lower boundary is a radioactive anomaly. This anomaly, while recognizable on all gamma ray profiles, is especially evident on the uranium profile (Figure App 2.1).

The radioactive anomaly marking the base of logfacies A does not appear to correspond to changes in depositional facies. However, some physical features of the rocks are related to this anomaly. At the Farlinville locality, vertical rhizoliths terminate in a horizontal manner coincident with the

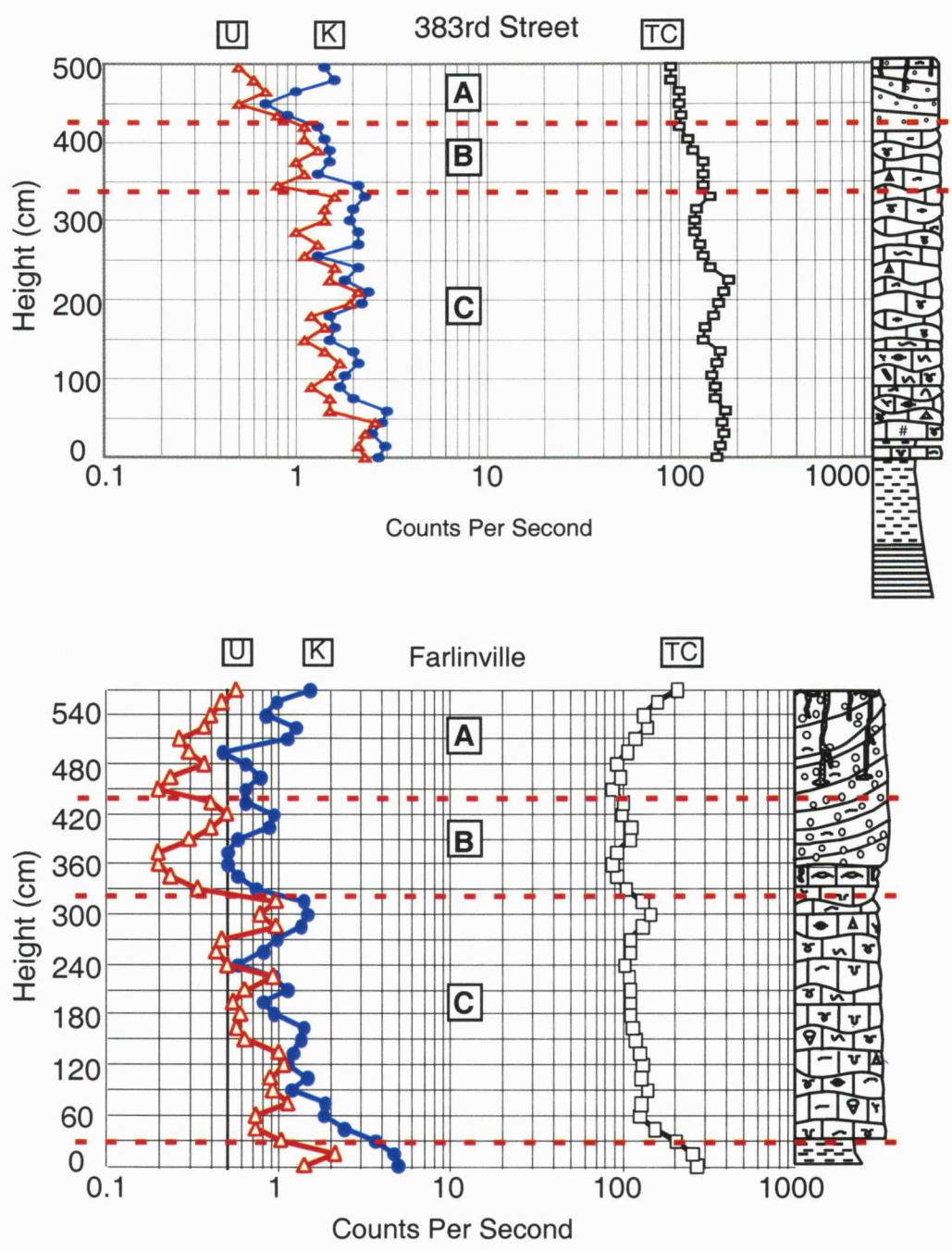


Figure App 2.1. Spectral gamma ray profiles of 383rd Street and Farlinville localities. Dashed red lines are radioactive anomalies separating logfacies. Logfacies are marked A, B, and C. The red profile is uranium, the blue profile is potassium, and the black profile is total count.

radioactive anomaly (Figure App 2.2). At other localities rhizoliths are restricted to logfacies A and do not extend into the lower logfacies (Figure App 2.1). In all sections and core containing ooid grainstones, the basal anomaly of logfacies A separates oomoldic porosity below the anomaly, and low porosity grainstone above (Figures App 2.3, App 2.4a).

Figure App 2.4 illustrates the differences in cement below, just above, and above the uranium rich radioactive anomaly. The oomoldic porosity seen in Figure App 2.4b results from the unstable aragonitic ooid grains being leached, either by corrosive mixing zone waters, or freshwater. Oomolds are observed filled by coarse calcite spar above the interpreted paleo-water table (Figure App 2.4c, d). Some grains were not dissolved, probably due to micritization occurring early in the grain's history (Figure App 2.4d). The curved cement features shown in Figure App 2.4c might be a very mature gravitational cement feature. These gravitational cement features have occasionally been termed microstalactitic or pendulous. The curved face on the cement feature would suggest it grew along a meniscus front and the lack of cement at the bottom of the pore would argue against a water-saturated pore. Both points suggest vadose zone. The large size of the mold-filling crystals might argue against vadose zone cementation, however, the large size could be related to a lack of competition between crystals and slow growth; features that could be accommodated if waters percolated slowly into

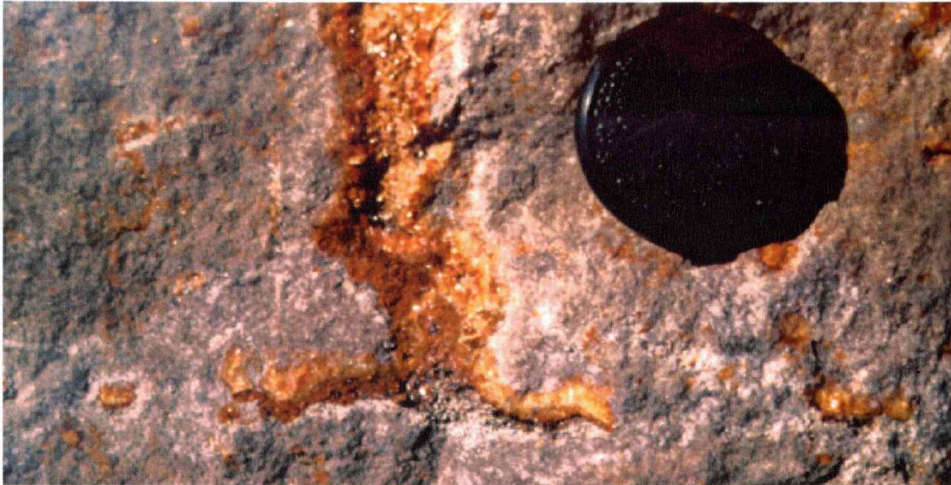


Figure App 2.2. Rhizolith terminating at a horizontal root mat coincident with radioactive anomaly separating logfacies A from logfacies B (locality Farlinville Quarry).

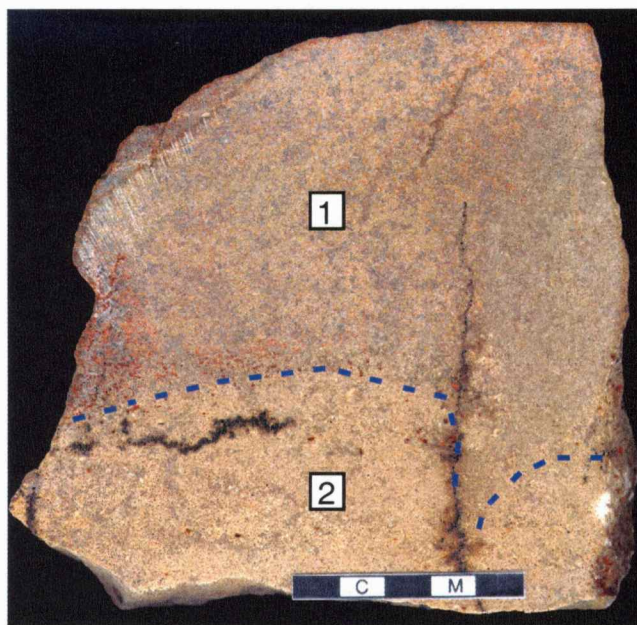
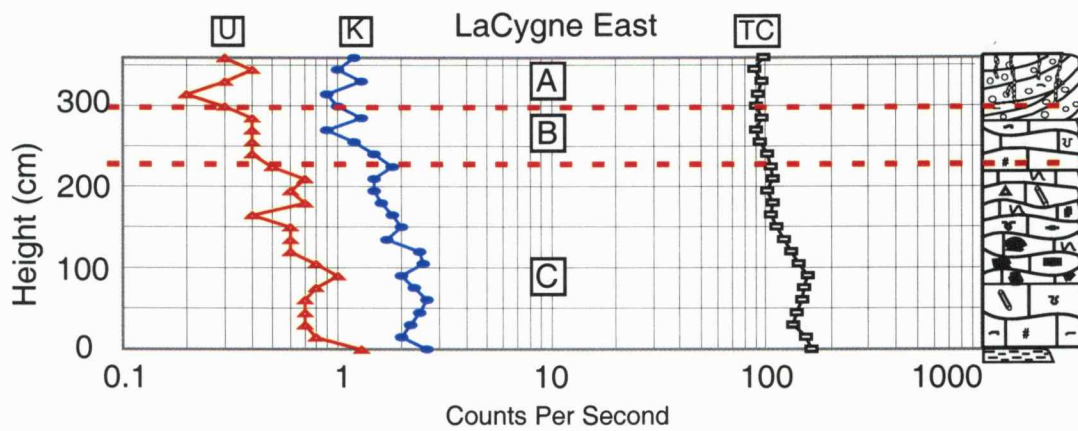


Figure App 2.3. Polished slab of ooid grainstone from 300 cm height at LaCygne East. The dashed blue is the contact between the portion of the rock with 1) oomoldic porosity and 2) the portion without. This contact coincides with the radioactive anomaly separating logfacies A from logfacies B. The red profile is uranium, the blue profile is potassium, and the black profile is total count (scale = 5 cm).

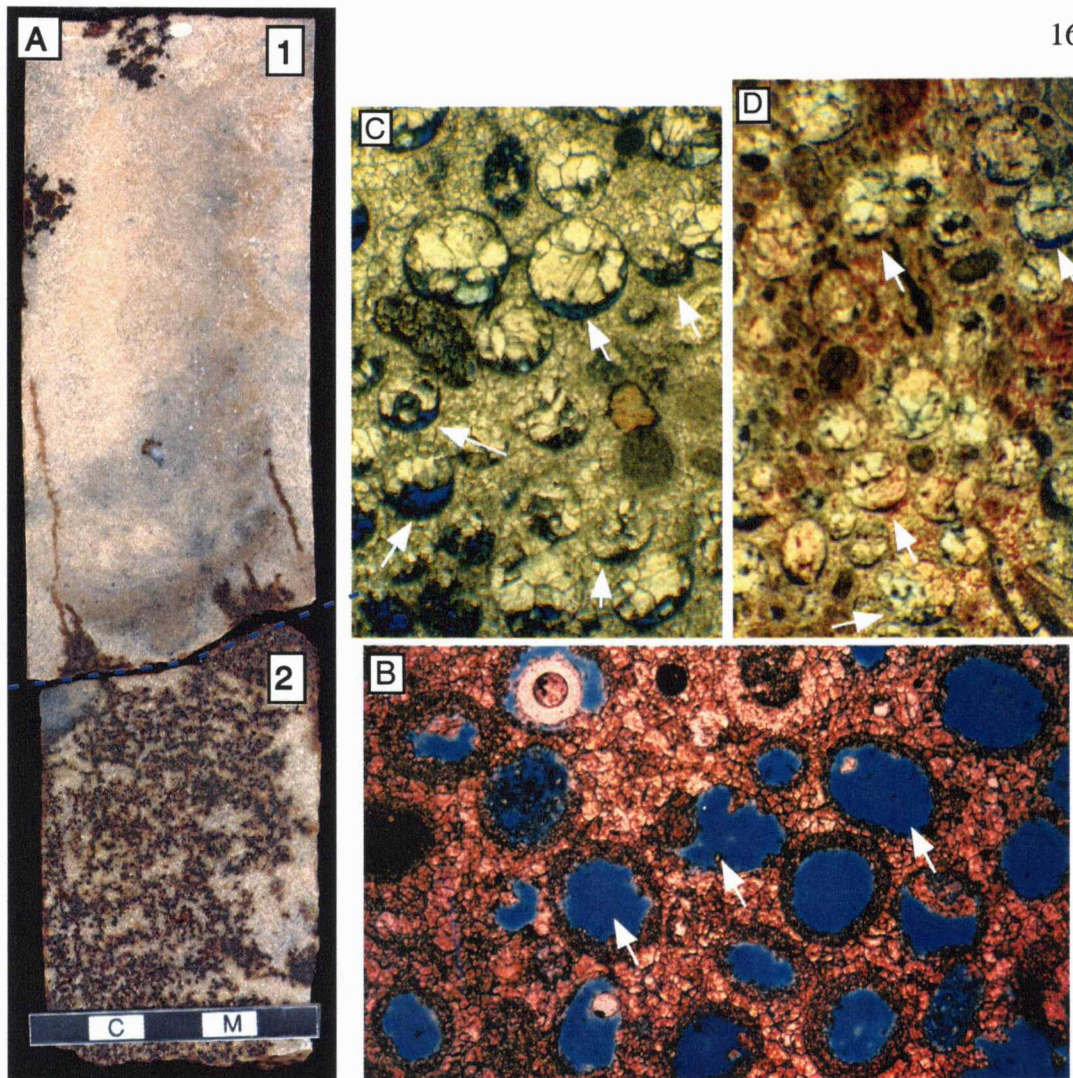


Figure App 2.4 (A) Polished core section of ooid grainstone from the Raines #1 well. The contact between the 1) low porosity section and 2) oomoldic section is coincident with a radioactive anomaly (blue dashed line). Oil staining highlights oomoldic porosity. The dashed blue line is the contact between logfacies A (1) and logfacies B (2).

(B) Photomicrograph of oomoldic porosity below upper radioactive anomaly at Farlinville (arrows; transmitted light; scale = 1mm; sample Farlinville 7).

(C) Photomicrograph of possible microstalactitic (gravitational) cement largely filling oomolds with blocky calcite spar. Arrows highlight porosity at base of oomolds. Sample is slightly above upper radioactive anomaly at Farlinville (transmitted light; scale = 1mm; sample Farlinville 9).

(D) Photomicrograph of completely filled oomolds with calcite spar (arrows). Some original structure is preserved in micritized ooids. Sample is 30 cm above C (transmitted light; scale = 1mm; sample Farlinville 10).

the pores and then sat there for some time. The drive for precipitation would presumably have been degassing of the infiltrating water into the oomoldic pore once the water settled into the meniscus. Moving up section from the interpreted paleo-water table to the surface of subaerial exposure, coarse calcite spar completely fills oomolds, with the curved cement features decreasing in abundance, and eventually disappearing. The occurrence of gravitational cement features just above the paleo-water table, and not near the surface of subaerial exposure might be explained by the cause for cementation which is degassing of calcium carbonate rich saturated waters. Near the surface of subaerial exposure, the fluids filling the pore space degas quicker due to increased rates of evaporation, allowing for continual cementation of pore space, eventually completely filling oomolds. Moving down towards the water table, evaporation rates decrease, and degassing of fluids occurs slower, leaving porosity in some oomolds.

Logfacies B

Logfacies B extends over the entire field area. From the Raines #1 well southward, logfacies B occurs below logfacies A. From the RWD-2 #1 well northward, logfacies B encompasses the uppermost portion of the Bethany Falls Limestone (Figure App 2.5).

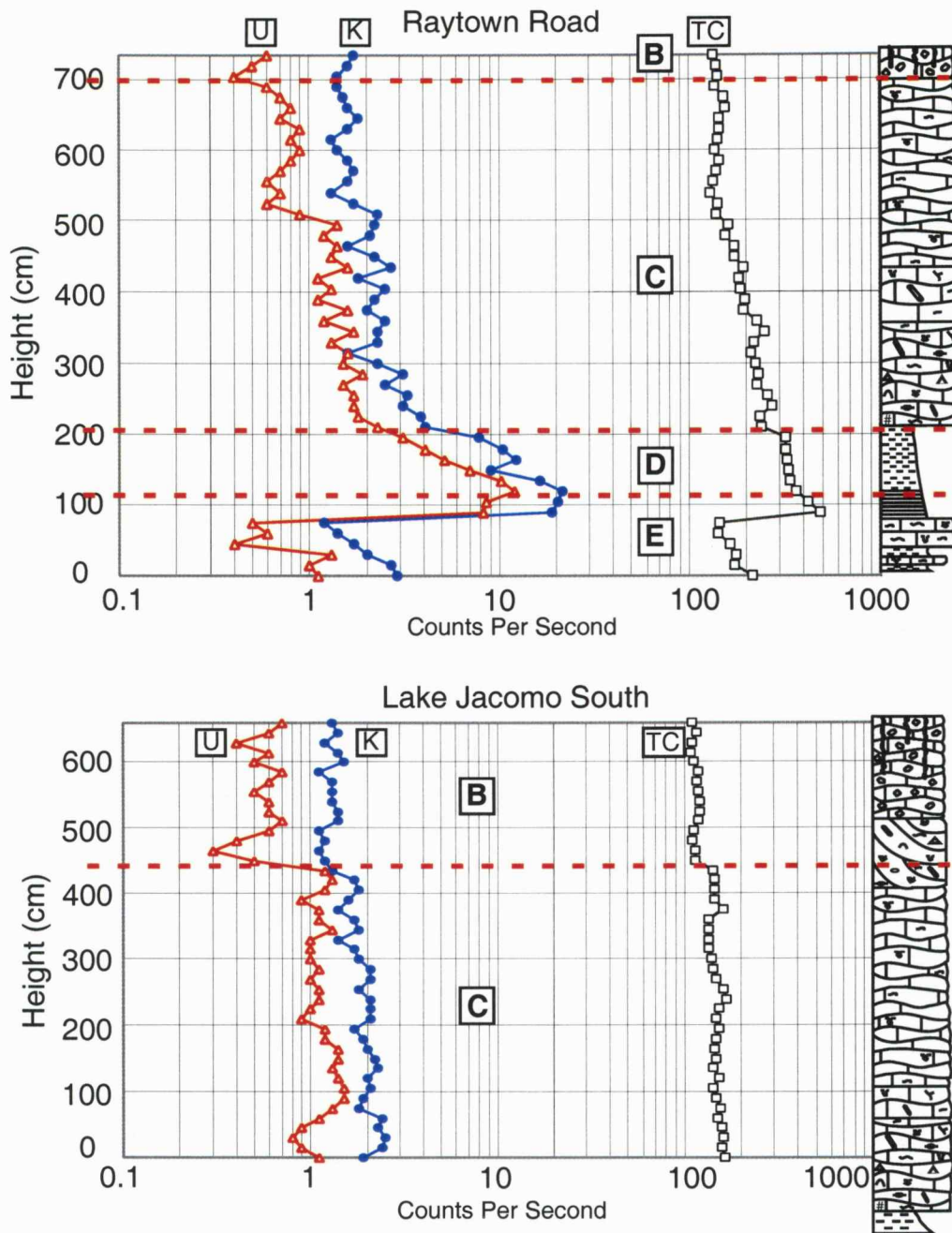


Figure App 2.5. Spectral gamma ray profiles of Raytown and Lake Jacomo South. Dashed red lines are the radioactive anomalies separating logfacies. Logfacies are marked B,C, D and E. The red profile is uranium, the blue profile is potassium, and the black profile is total count.

Logfacies B is characterized by a relatively clean, consistent gamma ray profile. The base of logfacies B is bounded by a radioactive anomaly. The uranium portion of the spectra shows a significant and consistent increase in counts per second at this anomaly (Figures App 2.1, App 2.5). Overall, there is a baseline shift in the uranium, potassium, and total count at this anomaly (Figures App 2.1, App 2.5).

Logfacies B does not seem to be related to any changes in depositional lithofacies. At most northern localities, however, the radioactive anomaly bounding the top of logfacies B coincides with the contact of the lime mudstone and the overlying pedogenically altered lime mudstone (Figure App 2.6).

Logfacies C

Logfacies C is recognized in the lower portion of the Bethany Falls Limestone over the entire field area. Logfacies C lies below logfacies B, and is characterized by having a higher relative gamma ray count than logfacies A and B. Logfacies C is also fairly consistent in character (Figure App 2.5). Logfacies C is bounded at the base by a large radioactive anomaly. This anomaly coincides with the boundary and change in lithofacies between the Bethany Falls Limestone and the upper portion of the Hushpuckney Shale (Figures App 2.1, App 2.5).

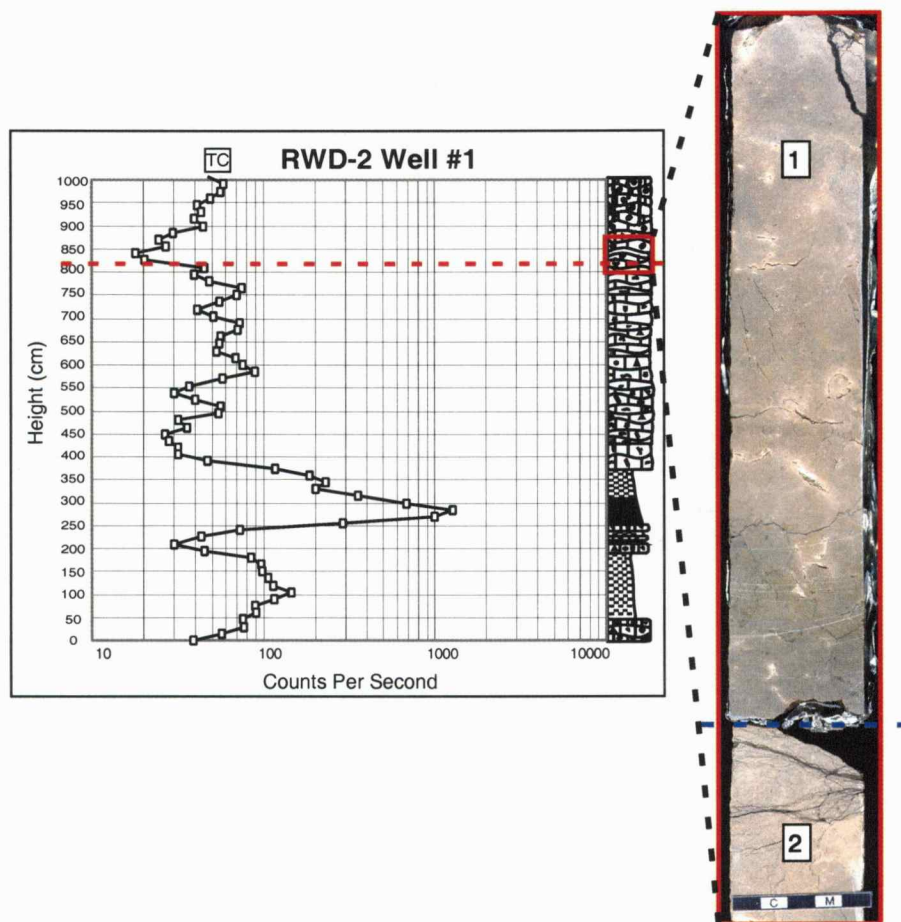


Figure App 2.6. Polished core section from the RWD-2 #1 well. The lithological contact between the 1) autobrecciated lime mudstone (interpreted as a paleosol), and the 2) unaltered lime mudstone (blue dashed line) is coincident with a radioactive anomaly. Note the color difference between 1 and 2, and the lack of shale filled rhizoliths in 2. The dashed blue line is the contact between logfacies B (1) and logfacies C (2).

Logfacies D

Logfacies D falls into the upper gray blocky portion of the Hushpuckney Shale. Logfacies D has high gamma ray values when compared to logfacies A, B and C. However, it has a lower total count than logfacies E. The gamma ray count shows a gradual, but persistent, increase down section toward the contact with Logfacies E (Figure App 2.7).

Logfacies E

Logfacies E represents the lower black laminated portion of the Hushpuckney Shale. Logfacies E is characterized by an extremely high gamma ray count, with total counts often over 1000 counts per second (Figure App 2.7). Logfacies E rapidly increases in gamma ray count upward (Figures App 2.5, App 2.7). The Middle Creek Limestone underlies this logfacies, and has a much cleaner gamma ray profile (Figure App 2.7). The extremely high gamma ray counts of the lower Hushpuckney Shale provides a correlation marker that is widely used in subsurface mapping (Watney et al., 1989).

Logfacies Interpretations

The radioactive anomalies within the Bethany Falls Limestone appear to be consistent with, but to a large degree independent of depositional lithofacies. Examination of the spectral gamma ray logs shows that a large increase in uranium is present at each radioactive anomaly within the Bethany Falls Limestone. Various workers have shown that in arid to semi-

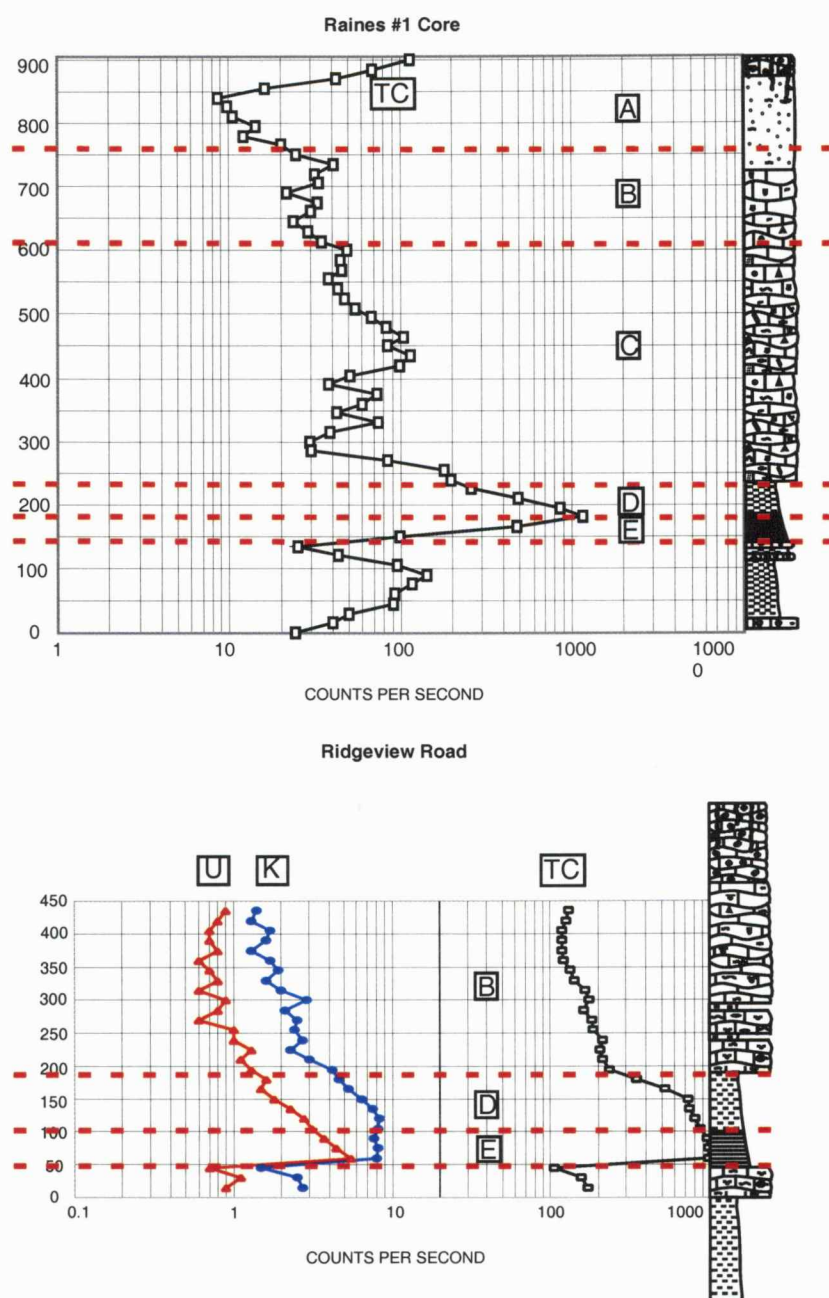


Figure App 2.7. Spectral gamma ray profiles of Raines #1 and Ridgeview Road. Dashed red lines are radioactive anomalies separating logfacies. Logfacies are marked A, B, C, D and E. The red profile is uranium, the blue profile is potassium, and the black profile is total count.

arid environments pedogenic and groundwater mechanisms increase uranium concentrations within the sediments (Mann and Horowitz, 1979; Arakel and McConchie, 1982; Carlisle, 1983). Chung and Stewart (1990) interpreted uranium enrichment as due to leaching and subsequent concentration of uranium in cements in the upper phreatic zone, in a calcrete, or in fractures in the weathered zone.

In the Bethany Falls Limestone, there is a clear surface of subaerial exposure at the contact with the Galesburg Shale. Calcrete, karst tubes, rhizoliths, and autoclastic brecciation, as discussed earlier in this chapter, characterize this surface. At Farlinville, the fenestral wackestone has been interpreted as being an additional surface of subaerial exposure (French et al., 1989; Stover, 1992; this study). The fenestral wackestone is interpreted as being eroded in a submarine environment, as evidenced by ripped up clasts of wackestone within the oolite facies. In exposures and core with oolite facies, there are two distinctive radioactive anomalies within the Bethany Falls Limestone. In exposures and core without oolite facies, there appears to be only one radioactive anomaly (Figures App 2.1, App 2.5).

Gamma-ray anomalies appear to be related to interpreted surfaces of subaerial exposure. Where there are two surfaces of subaerial exposure within the Bethany Falls Limestone, there are two gamma-ray anomalies. Where this is only one subaerial exposure surface, there is only one distinct radioactive anomaly (Figure App 2.8 *in packet*). The coincident relationship

of radioactive anomalies to surfaces of subaerial exposure supports the hypothesis that a surface of subaerial exposure exists below the oolite facies, as observed in the fenestral wackestone at the Farlinville Locality.

Correlation of the lower radioactive anomaly across the field area illustrates the widespread nature of this surface of subaerial exposure (Figure App 2.8)

The relationship of these anomalies to physical/diagenetic features within the Bethany Falls is important. Vertical tubes, interpreted to be rhizoliths, terminate in a horizontal root mat at the upper radioactive anomaly at Farlinville (Figure App 2.2). Oomoldic porosity occurs immediately below the radioactive anomaly cutting through and across the cross bedding of the ooid grainstone subfacies. Above the radioactive anomaly oomoldic porosity is not typically observed (Figures App 2.3, App 2.4a). In the northern portion of the field area, the top of the radioactive anomaly typically occurs at the boundary between the pedogenically altered lime mudstone, and the unaltered lime mudstone (Figure App 2.6). Pedogenic features are restricted to the logfacies above the uppermost radioactive anomaly.

Hoth et al. (1998) have shown that the uranium anomalies in the Bethany Falls Limestone result from selective inclusion of uranium and associated clays in cements. Hoth et al. (1998) interpreted these cements as occurring at the contact between a vadose and marine-phreatic environment. Field evidence observed in this study, along with previous work, strongly suggests that these radioactive anomalies are related to paleo-water tables.

Structures that occur within the Bethany Falls and interpreted as forming immediately after deposition appear related to these anomalies. Rhizoliths are observed only above the upper radioactive anomaly, in places terminating in a horizontal root mat at the gamma-ray anomaly. Formation of oomoldic porosity and pedogenic alteration appears coincident with or related to observed radioactive anomalies. This is evidence that anomalies were formed at the same time as these physical features.

Logfacies within the Hushpuckney Shale appear dependent on lithology. Logfacies E is tied to the black fissile shale in the lower portion. Logfacies D is found exclusively in the gray shale. The high gamma ray counts found in logfacies D and E have been attributed to high uranium concentrations (Watney et al, 1989). Within the profiles generated in this study, uranium is noticeably higher within the Hushpuckney Shale (Figure App 2.7). These uranium concentrations in the Hushpuckney Shale are probably related to combination of high TOC, wind blown dust derived from a granitic craton, and concentration by slow sedimentation rates.

Spectral Gamma Ray Log Legend

Uranium

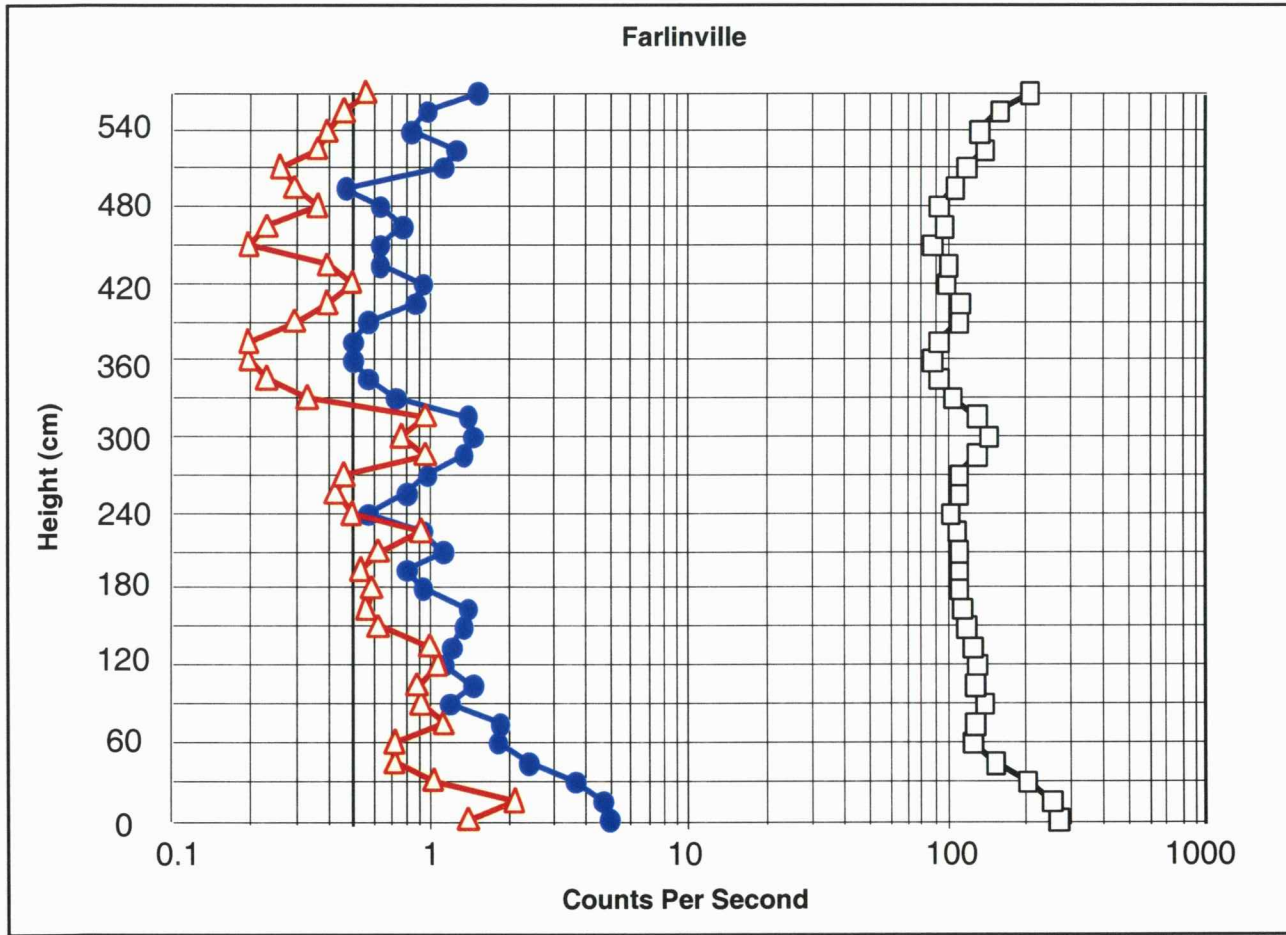


Postassium

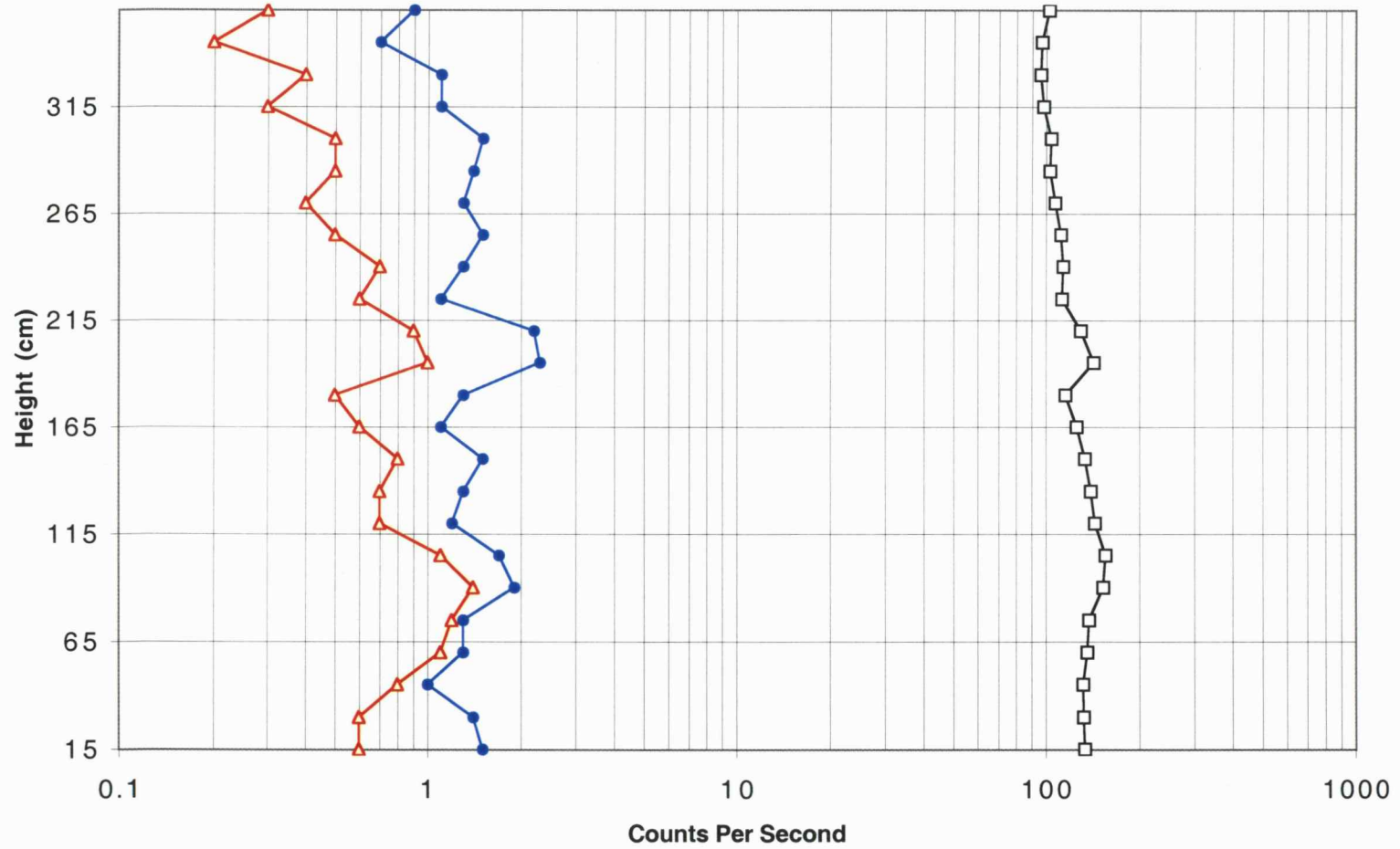


Total Count

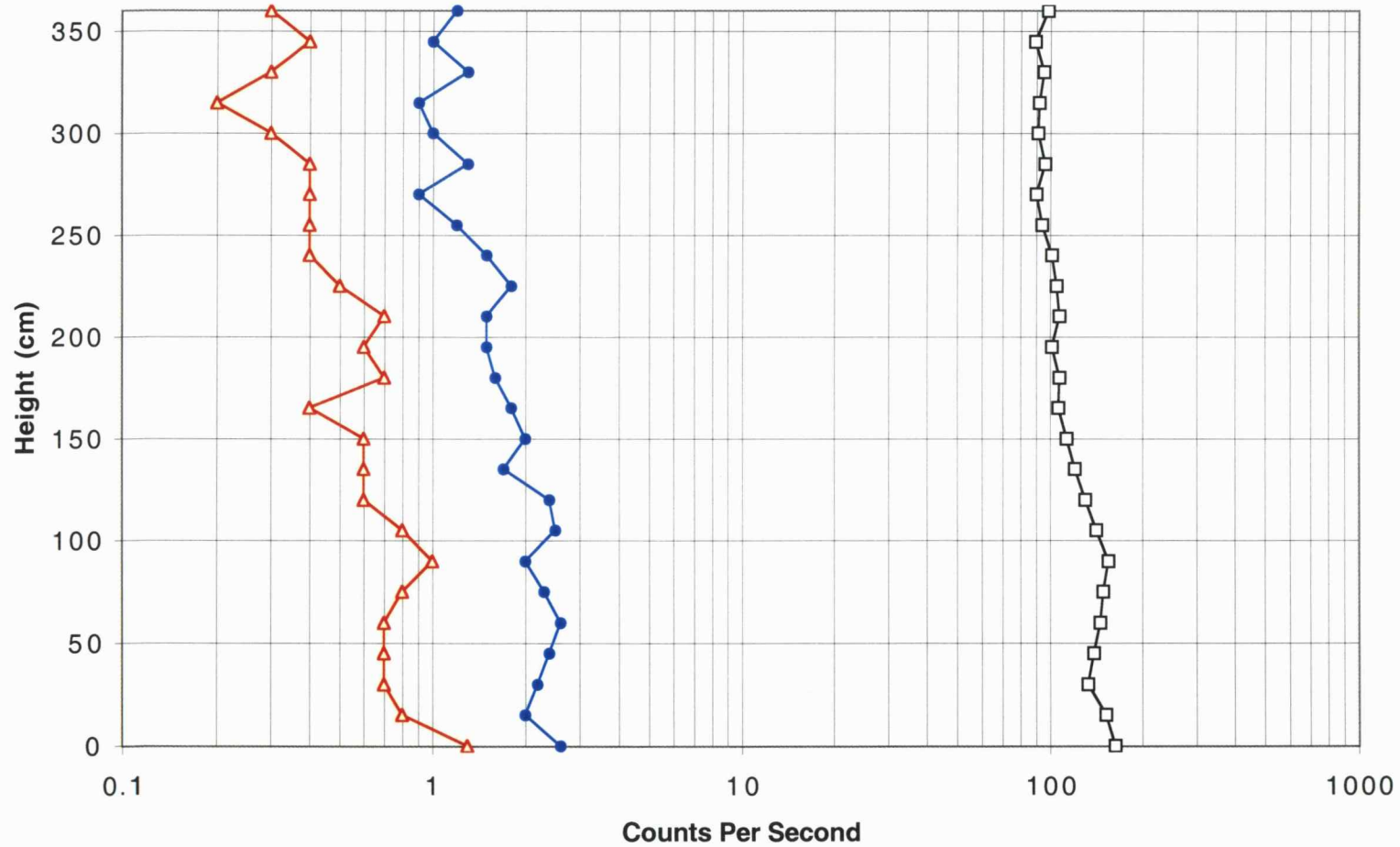


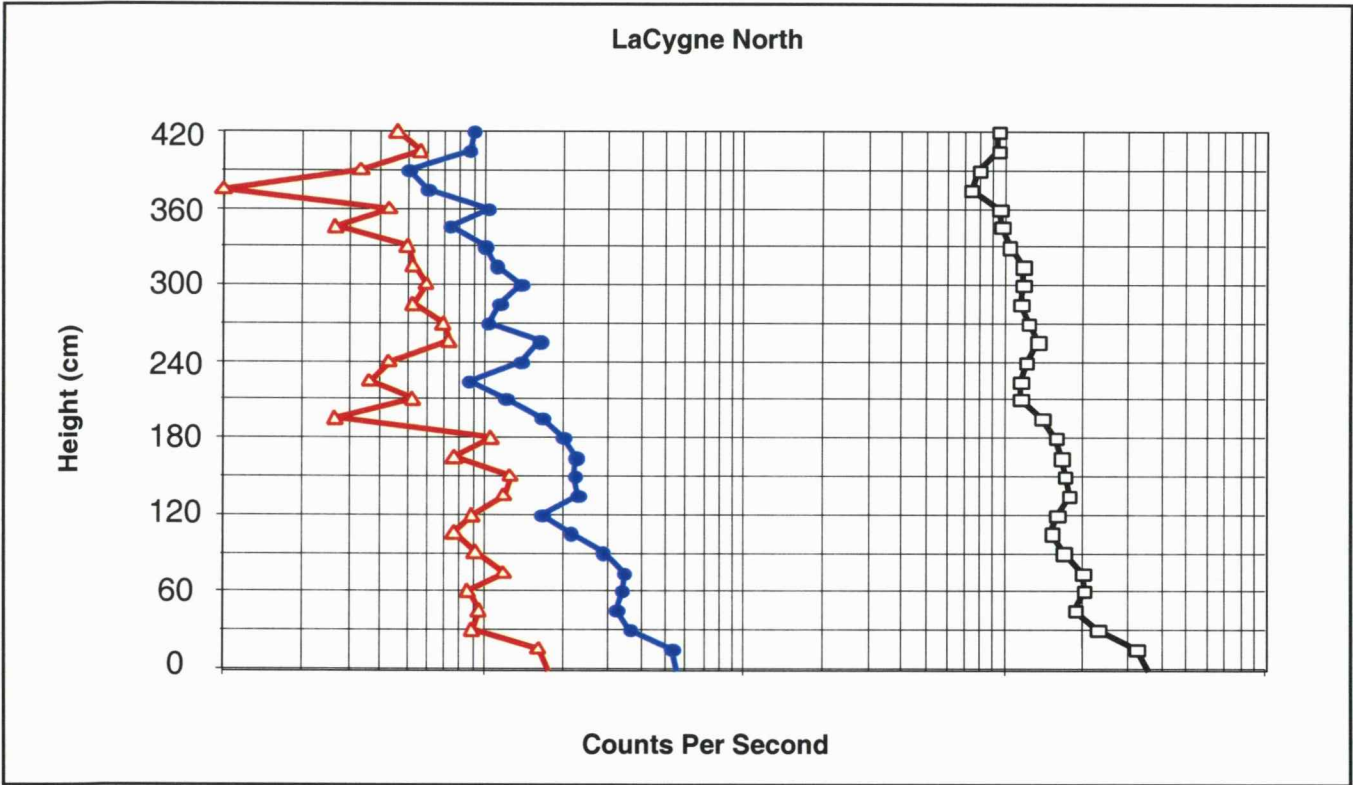


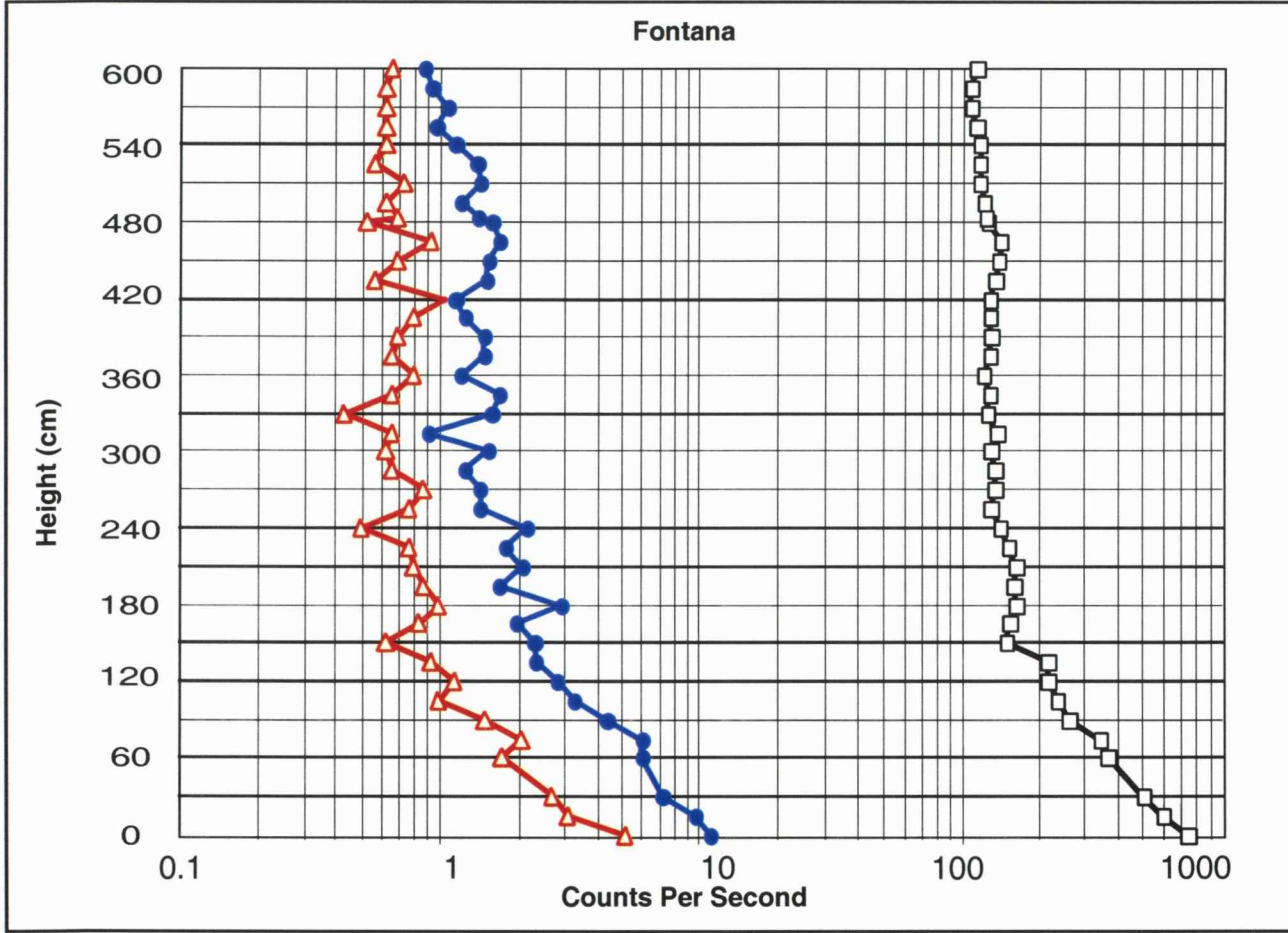
LaCygne West



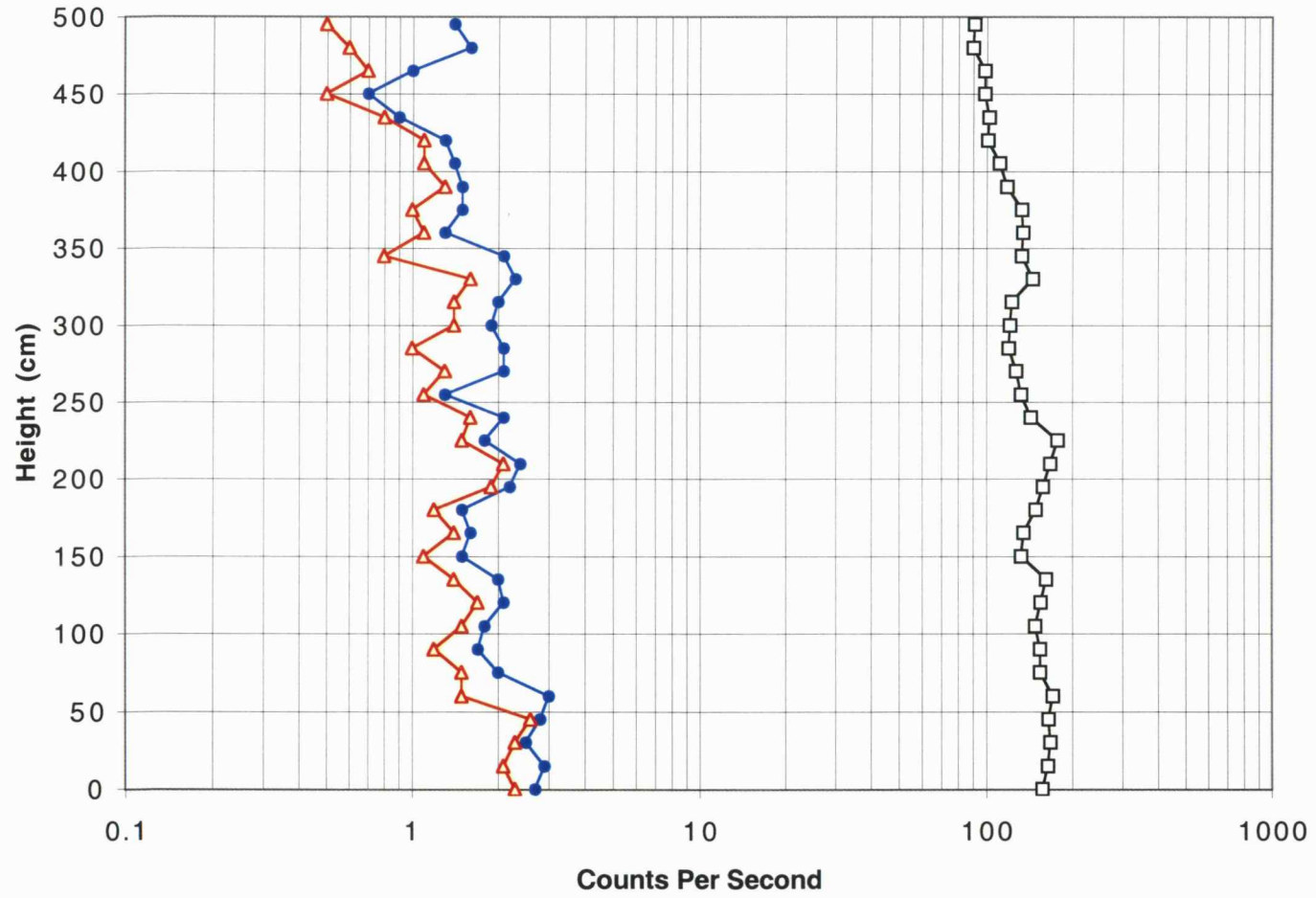
LaCygne East



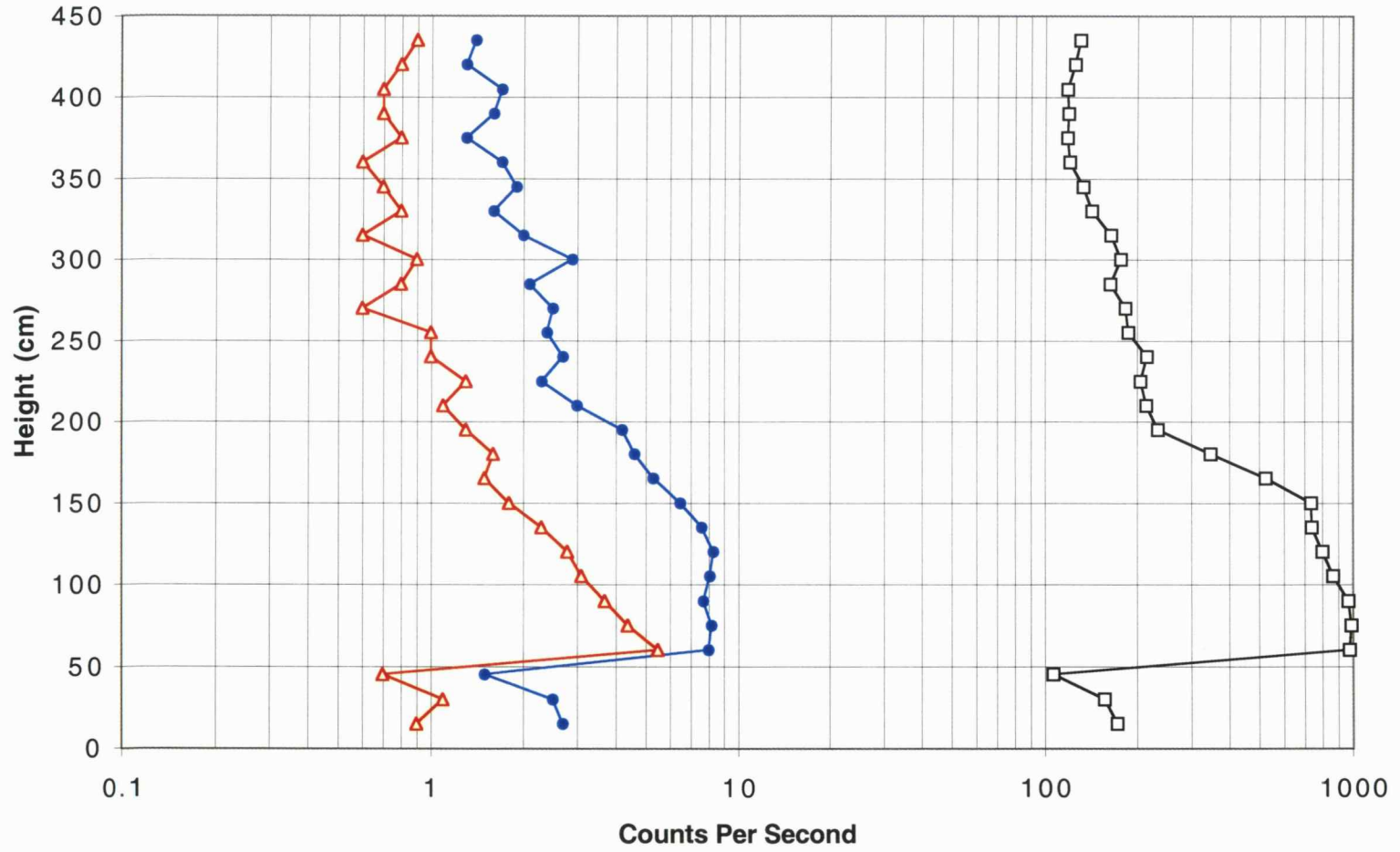




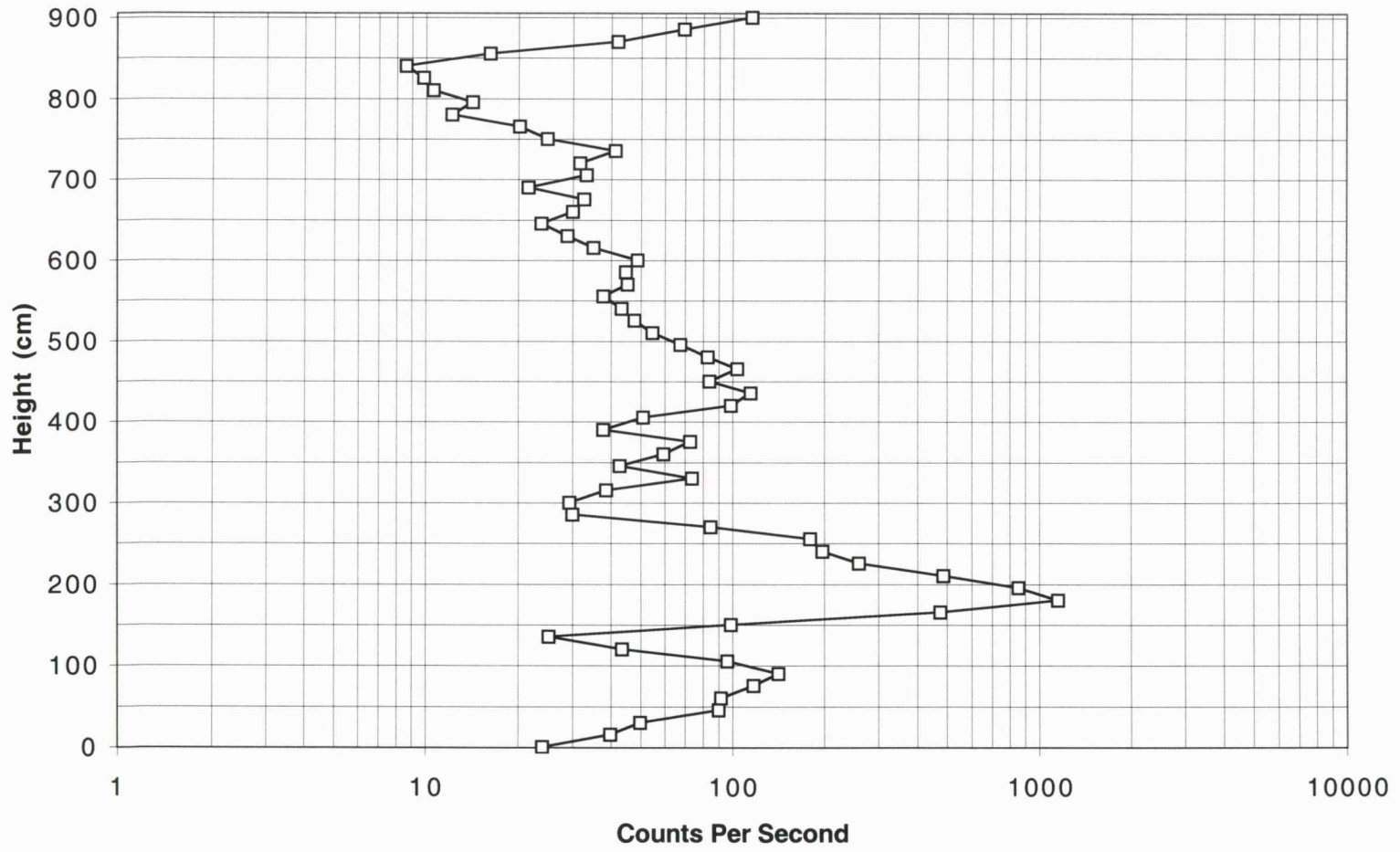
383rd Street



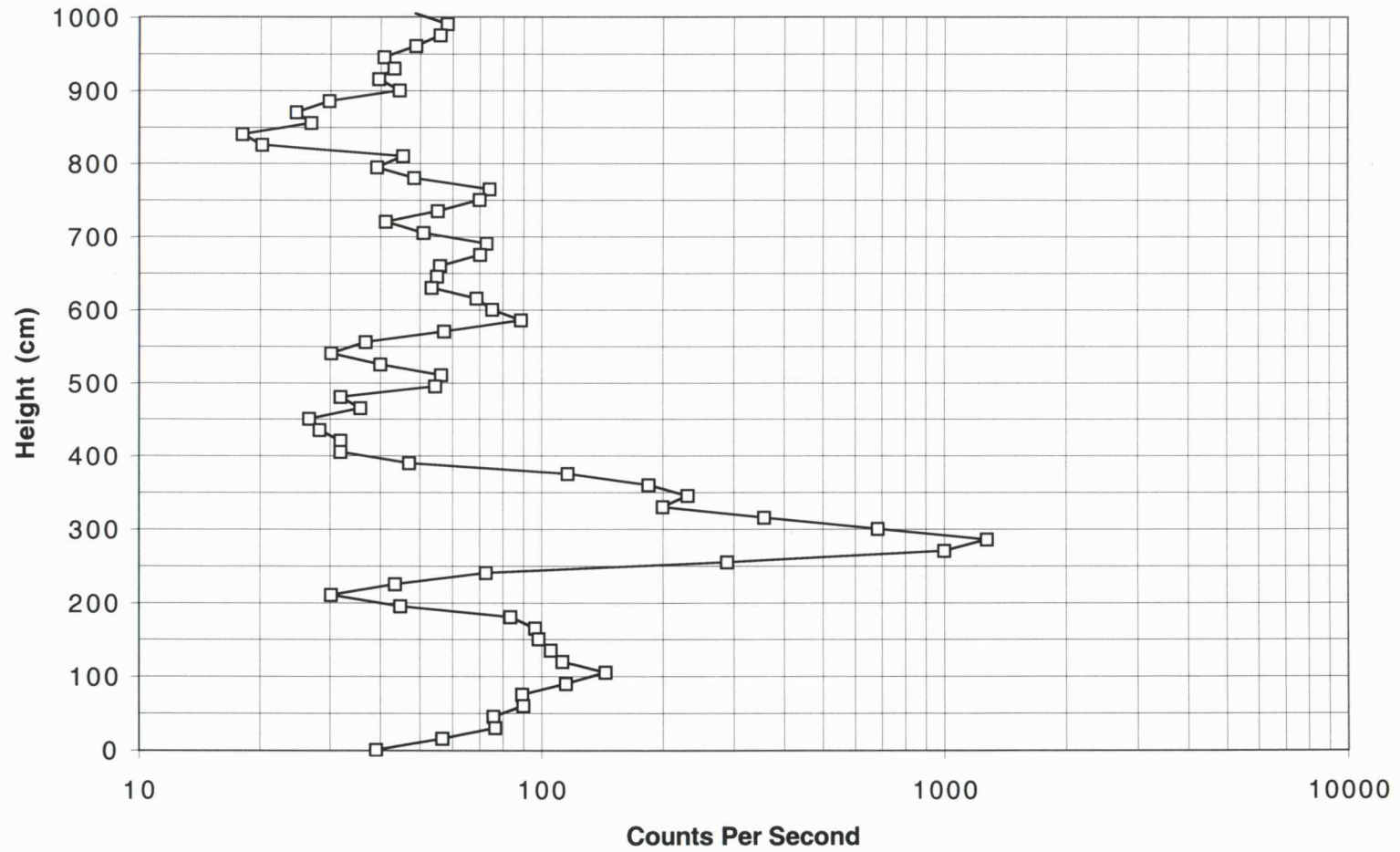
Ridgeview Road

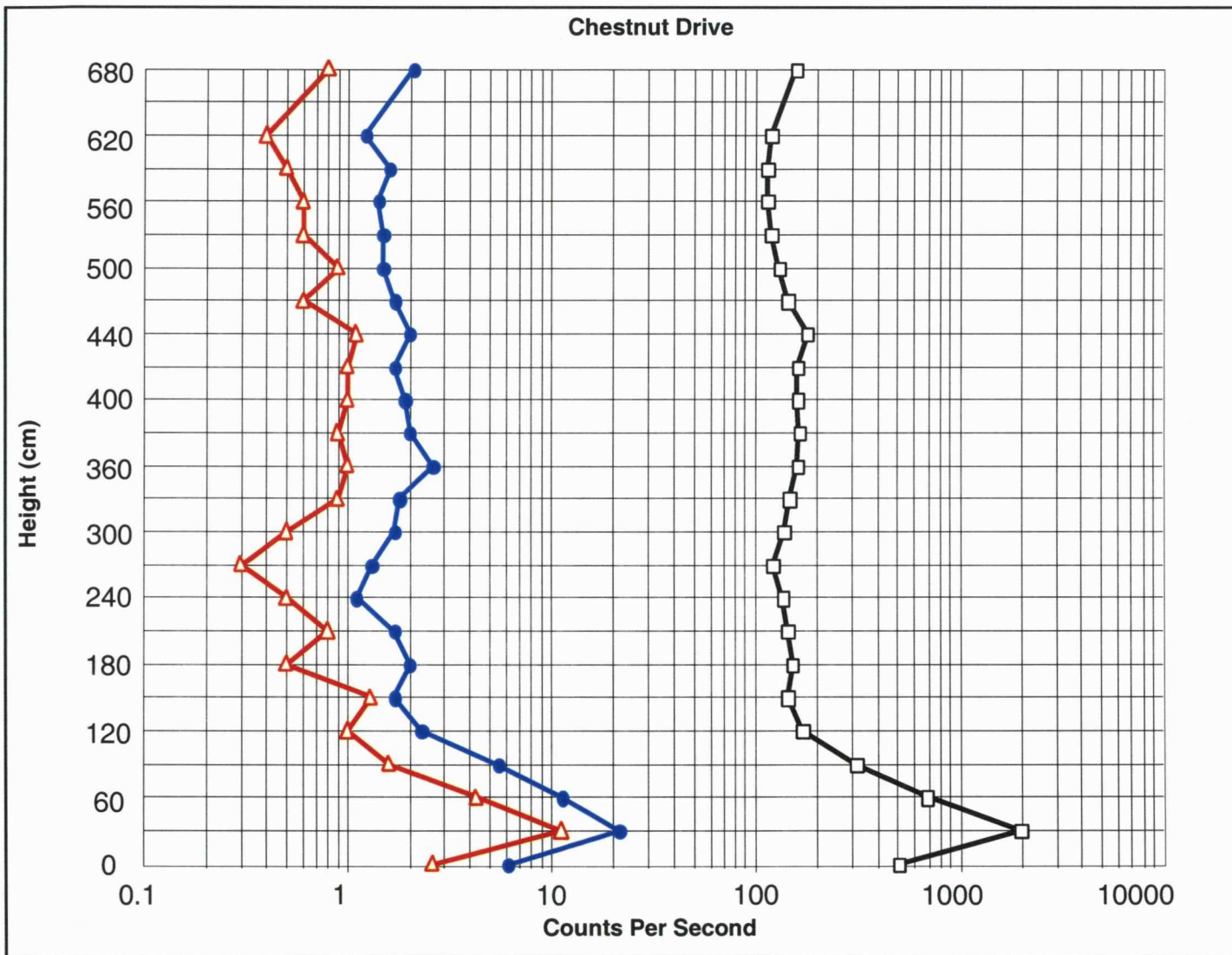


Raines #1



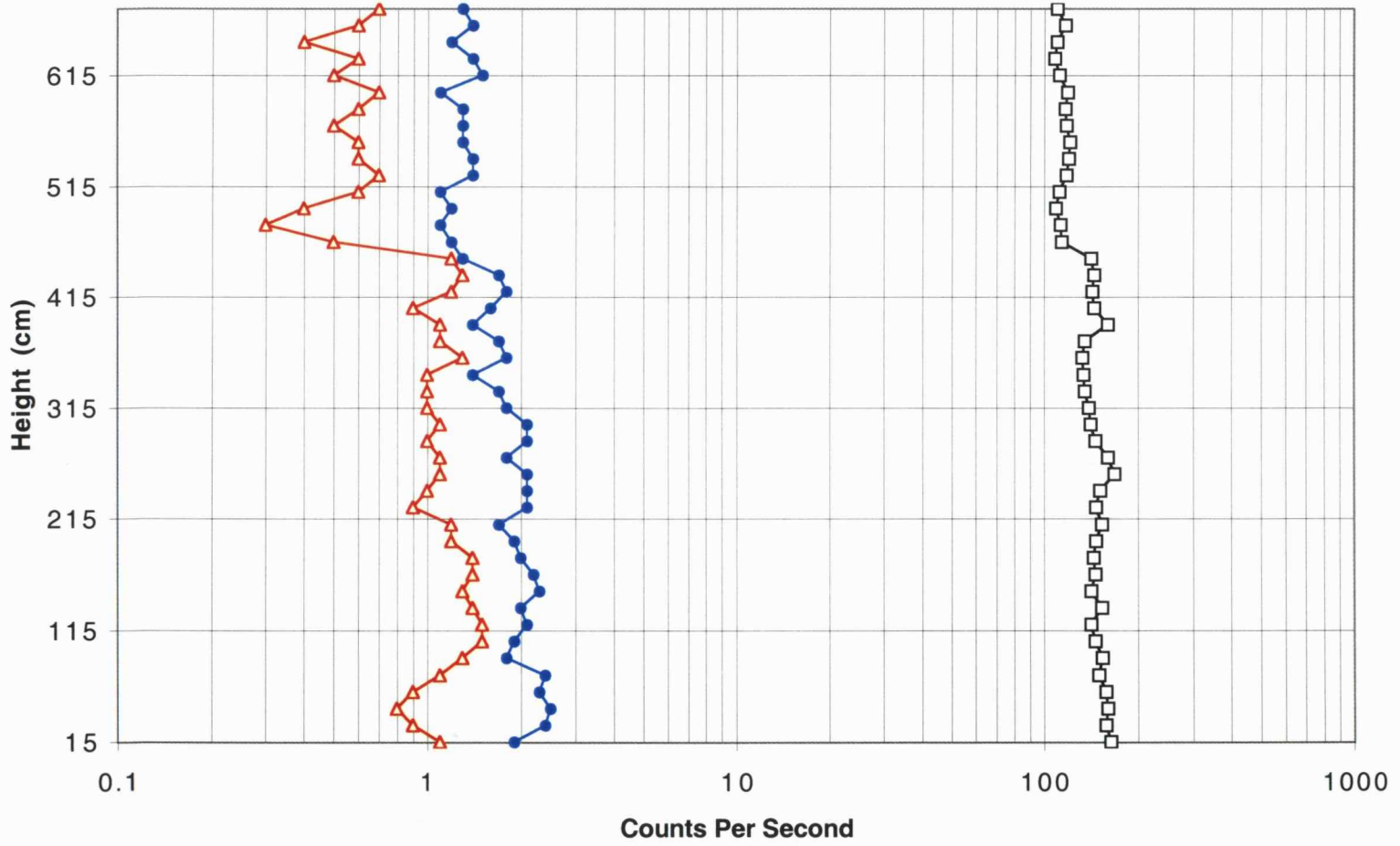
RWD-2 #1



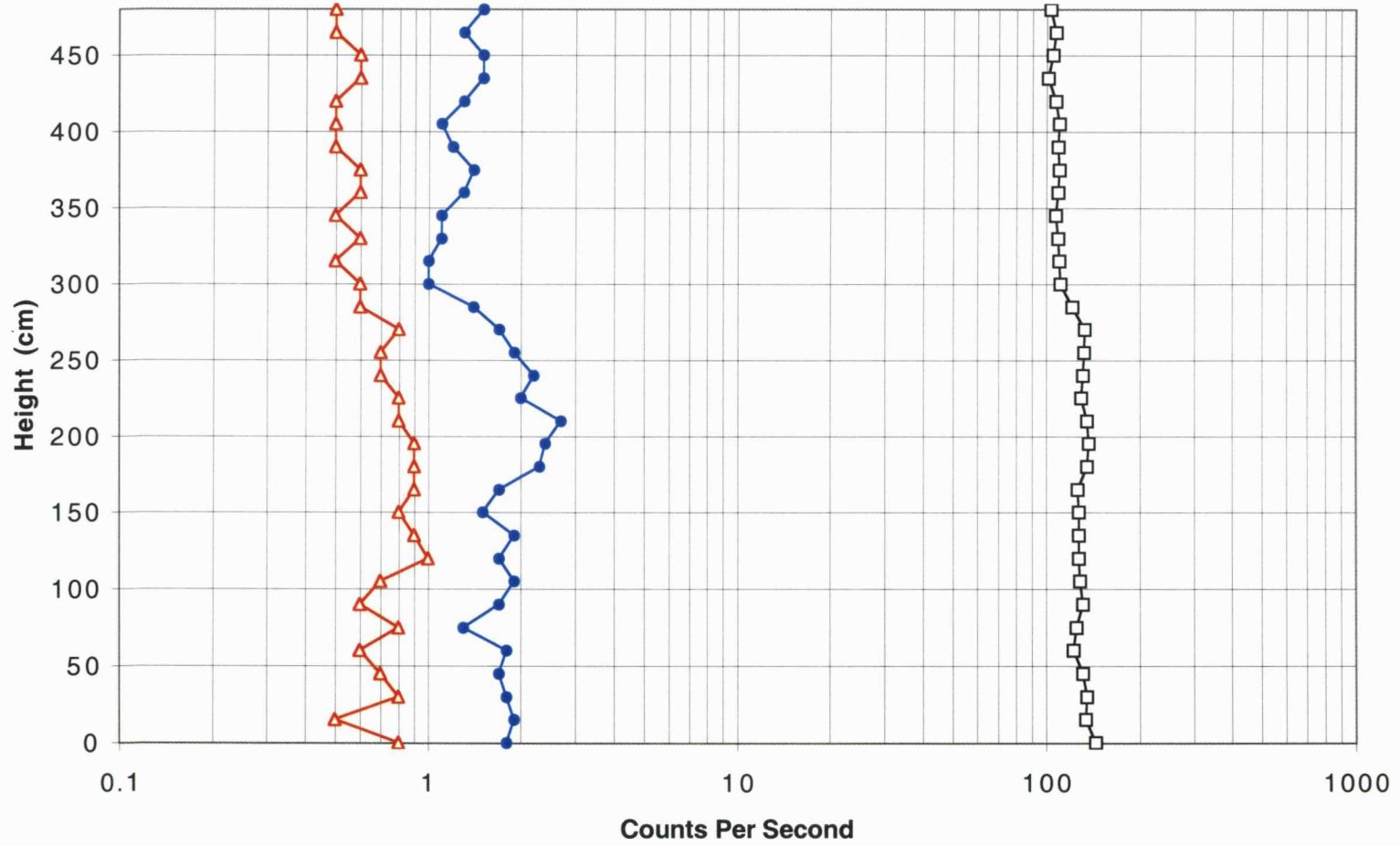




Lake Jacomo South



Lake Jacomo North



Raytown

